

HIGH ENERGY PHYSICS AT UCR

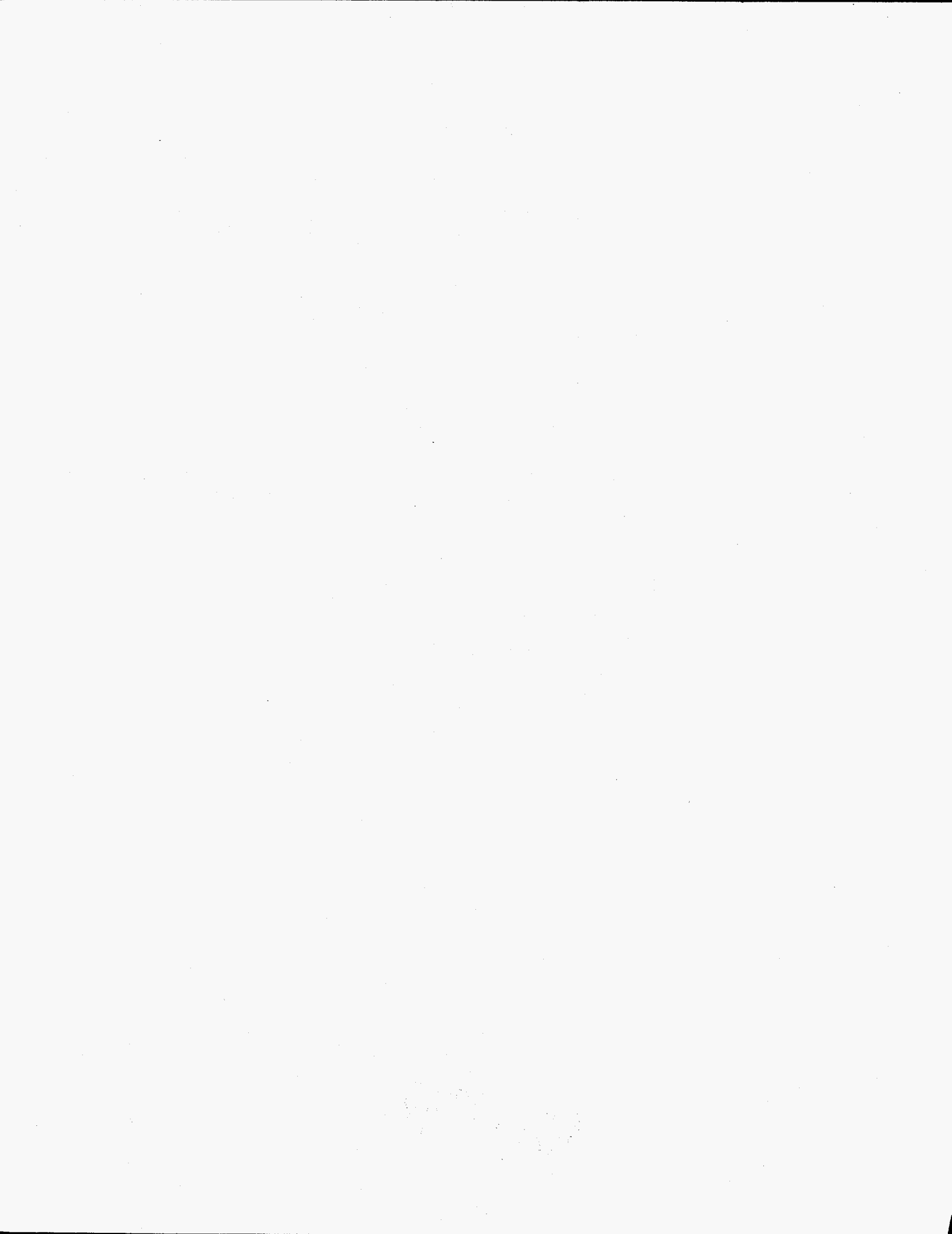
Table of Contents

| | |
|--|-----|
| I. PHYSICS RESEARCH | |
| A. Experimental High Energy Physics | 1 |
| 1. Hadron Collider Physics | 1 |
| a) Overview/Personnel/Talks/Publications | 1 |
| b) D-Zero : Proton-Antiproton Interactions at 2 TeV | 9 |
| c) SDC : Proton-Proton Interactions at 20 TeV | 40 |
| d) Nucleon Structure Functions | 44 |
| 2. e ⁺ e ⁻ Collider Physics and Neutrino Physics | 54 |
| a) Overview/Personnel/Talks/Publications | 54 |
| b) TPC/2γ at PEP | 69 |
| c) OPAL at LEP | 70 |
| d) Neutrino Physics at LAMPF | 114 |
| e) Muon Experiment at the SPS | 123 |
| B. Theory | 138 |
| a) Introduction | 138 |
| b) Research Program | 138 |
| c) Publications | 141 |
| d) Travel and Consultants | 144 |
| e) Personnel and needs | 145 |
| f) Future Research Plans | 145 |
| g) Vitae of H. Kikuchi | 146 |
| II. HIGH ENERGY PHYSICS COMPUTING AT UCR | 152 |
| III. BUDGET | 154 |
| IV. VITAE AND PUBLICATIONS | 172 |

DISTRIBUTION OF THIS DOCUMENT IS UNLIMITED

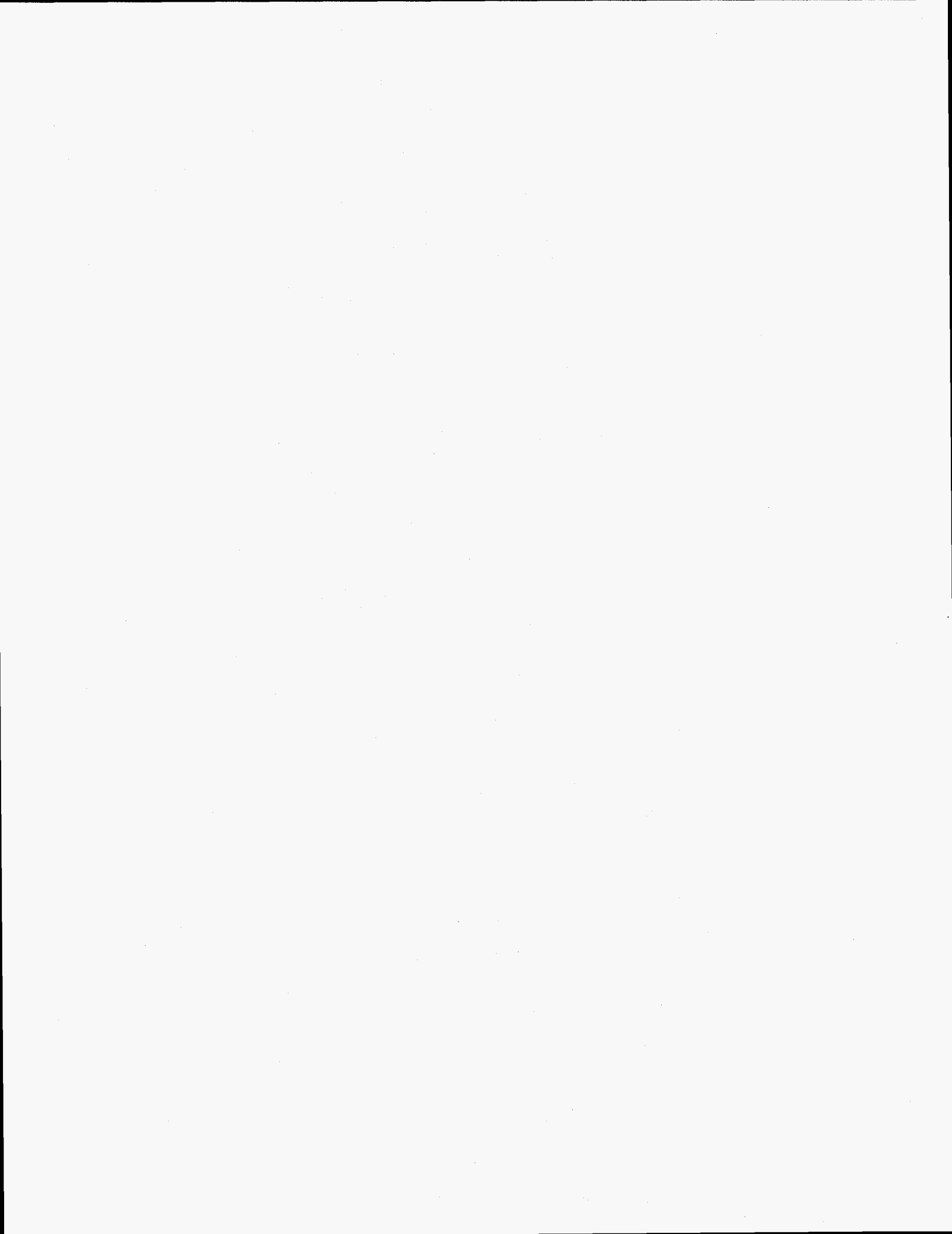
MASTER

29



DISCLAIMER

Portions of this document may be illegible in electronic image products. Images are produced from the best available original document.

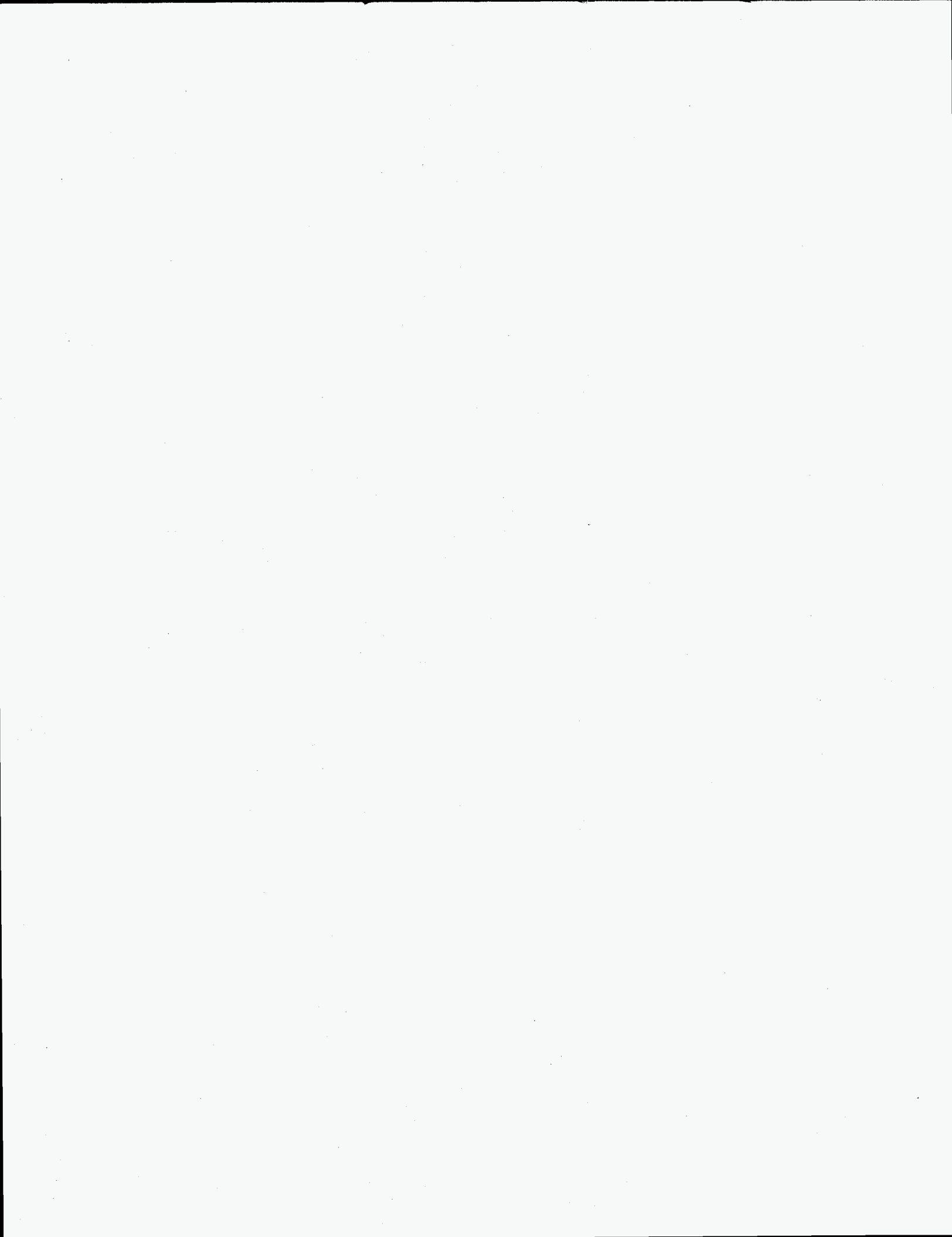


TASK A:

HADRON COLLIDER PHYSICS

DISCLAIMER

This report was prepared as an account of work sponsored by an agency of the United States Government. Neither the United States Government nor any agency thereof, nor any of their employees, makes any warranty, express or implied, or assumes any legal liability or responsibility for the accuracy, completeness, or usefulness of any information, apparatus, product, or process disclosed, or represents that its use would not infringe privately owned rights. Reference herein to any specific commercial product, process, or service by trade name, trademark, manufacturer, or otherwise does not necessarily constitute or imply its endorsement, recommendation, or favoring by the United States Government or any agency thereof. The views and opinions of authors expressed herein do not necessarily state or reflect those of the United States Government or any agency thereof.



1a.

HADRON COLLIDER PHYSICS OVERVIEW

The first run of D-Zero at the Fermilab Tevatron will start in early 1992. The central part of the detector is assembled (transition radiation detector, central tracking chambers, central calorimeters, and central muon chambers) and was commissioned in a cosmic ray run in Spring 1991. The North endcap (calorimeter plus muon spectrometer) will be commissioned in August, the South endcap in December. The current schedule calls for 'roll-in' of the completed detector in February 1992.

Our major effort in the coming year will be concentrated on muon detection in D-Zero. K. Bazizi is leading the effort to implement the muon trigger. A. Klatchko will be responsible for muon momentum analysis. T. Huehn will measure the inclusive $d\sigma/dp_T$ distribution as his Ph.D. thesis project. This measurement has several objectives: (i) to verify muon detection efficiency, (ii) to measure the b-quark production cross section and (iii) to account for known muon sources as a first step in searching for new phenomena involving leptons, in particular the top quark. R. Hall will search for strong production of the top quark for his Ph.D. thesis project. The search will be based on the decay $t\bar{t} \rightarrow W^+W^- b\bar{b}$ with the two W's decaying into $e\nu$ and $\mu\nu$ respectively.

Other D-Zero data analysis activities include continuation of the systematic study of Monte Carlo event generators with particular emphasis on the associated production of W's and jets: this reaction, in addition to its intrinsic interest, constitutes the major background to tt decaying to a single lepton plus jets. A search for $W + \gamma$ events in the D-Zero data will be initiated, with the goal of measuring the W magnetic moment.

Planning is well underway for an extensive upgrade of the D-Zero detector. This is necessitated by anticipated increases in luminosity and the associated reduction in beam crossing times from 3.4 μ s to 0.4 μ s. The major changes involve replacement of the central and forward tracking by a silicon microstrip detector covering the rapidity range $\eta < 2$ and surrounded by a scintillating fiber tracker. This tracking system will be enclosed in a 1.5 T

magnetic field. The UCR group (Ellison, Joyce, Wimpenny), in collaboration with LBL and Fermilab, are designing the silicon tracker. In particular UCR will be responsible for surveying the properties of commercially available silicon detectors in order to establish specifications for these elements.

We are also doing R&D for the SDC silicon tracker. Studies on radiation damage effects carried out in collaboration with UC Santa Cruz and Los Alamos, were presented by J. Ellison at the 2nd London Conference on Position Sensitive Detectors, Sept. 1990. Future efforts will be divided between the ongoing radiation damage studies and work on the SDC silicon tracker forward disks. Prototype wedge detectors will be acquired from vendors and we will evaluate their performance at UCR using a variety of signal generation techniques.

Work on the phenomenology of the nucleon structure functions is in progress. Preliminary results from studies of proton data were reported at the Workshop on Hadron Structure Functions and Parton Distributions at Fermilab in April 1990 and at 25th International Conference on High Energy Physics in Singapore, August 1990. Final results from this analysis and preliminary results from studies of the deuteron will be presented by S.J. Wimpenny at the Joint Lepton-Photon Symposium and European Physical Society High Energy Physics Conference in Geneva, July 1991. Future work will concentrate on the extraction of the neutron structure function and the determination of parton distribution functions.

The budget contains some increases compared to the 1992 budget estimate submitted a year ago. These reflect:

- 1.) New UC salary scales for RA's;
- 2.) Increased travel expenses associated with the 1992 collider run;
- 3.) Equipment expenses associated with development of the silicon microstrip detector for the D-Zero upgrade.

The center-of-gravity of the group is shifting from Riverside to Fermilab in preparation for the 1992 collider run. T. Huehn moved to Batavia in June to be followed by A. Klatchko in August. S.J. Wimpenny will be based at Fermilab for the second half of 1991; the university is paying his salary while he is on-site during the Fall quarter.

Postgraduate research associate D. Joyce replaces D. Smith who took a faculty position at Embry-Riddle University in August 1990. In early 1991 postgraduate researcher M.-J. Yang took a staff position at Fermilab and was replaced by K. Bazizi. Our three undergraduate lab helpers of the past two years have graduated and are planning to continue in particle physics: S. Jerger at MSU, T. Fahland at Brown and C. Lietzke at UCR; the latter two plan to continue working on D-Zero. Graduate student A. Khatchatourian will be joining our effort.

PERSONNEL - HADRON COLLIDER PHYSICS

Ph.D.'s

K. Bazizi : post graduate researcher
J. Ellison : assistant research physicist
D. Joyce : post graduate researcher
A. Kernan : professor
A. Klatchko : post graduate researcher
S.J. Wimpenny : associate professor

Graduate Students

R. Hall
T. Huehn
A. Khachatourian
C. Lietzke

Undergraduate Students

T. Reed
J. Fleming

INVITED TALKS - HADRON COLLIDER TASK

8 - 90 to 7 - 91

1. J. Ellison, "Radiation Hardness of AC-Coupled Silicon Microstrip Detector", 2nd London Conference on Position Sensitive Detectors, 4th-7th September, 1990.
2. S.J. Wimpenny, "High Energy Physics - An Experimentalist's Viewpoint", Harvey Mudd College, November 27, 1990.
3. A. Klatchko, "The Use of Kalman Filter in Muon Reconstruction", D-Zero Monte Carlo Physics Conference, LBL, Jan. 11-13, 1991.
4. J. Ellison, "Comparison of MC Generators on $p_T W$, $m_T W$, $p_T \mu$ and $p_T \nu$ ", D-Zero Monte Carlo Physics Conference, LBL, Jan. 11-13, 1991.
5. R. Hall, "Preliminary Results on Muon Isolation Studies in the D-Zero Detector", D-Zero Collaboration Meeting, Fermilab, May 22-24, 1991.
6. A. Kernan, "Results on Double Pomeron Exchange in the UA1 Experiment", UA1 Final Physics Meeting, CERN, Dec. 8, 1990.

PUBLICATIONS - HADRON COLLIDER TASK

8 - 90 to 7 - 91

1. "Heavy Quark Production at the CERN $p\bar{p}$ Collider", N. Ellis, A. Kernan, Phys. Reports, 195, Nos. 2 & 3, 23-125 (1990).
2. "Study of the D^* Content of Jets at the CERN $p\bar{p}$ Collider", (UA1 Collaboration), UCR authors: M. Ikeda, D. Joyce, A. Kernan, M. Lindgren, S.J. Wimpenny. Phys. Lett. B244, 566-572 (1990).
3. "Measurement of the Strong Coupling Constant α_s from Jet Production in $W \rightarrow e\nu$ Events", M. Lindgren, Ph.D. Thesis, University of California, Riverside, Dec. 1990, UCR/UA1/90-03 (1990).
4. "An Investigation of Double Pomeron Exchange in $p\bar{p}$ Interactions at a CM Energy of 630 GeV", D. Joyce, Ph.D. Thesis, University of California, Riverside, Dec. 1990, UCR/UA1/90-04 (1990).
5. "The D-Zero High Voltage System", (D0 Collaboration), M.J. Yang. Talk presented at 2nd Int. Conf. on Adv. Tech. and Particle Physics, Como, Italy, June 1990, Nucl. Instrum. Methods (in press).
6. "Study of Radiation Effects on AC-Coupled Silicon Strip Detectors", J. Ellison, S.J. Wimpenny. Proceedings of the 2nd Int. Conf. on Advanced Technology and Particle Physics, Como, Italy, June 1990, 16 pp., Nucl. Phys. B (in press).
7. "Simulation of a Silicon Vertex Detector in the D0 Experiment", J. Ellison, A. Kernan and D. Smith. Proceedings of the 1990 Summer Study on High Energy Physics - Research Directions for the Decade, Snowmass, CO, July 1990, 8 pp. (in press).
8. "Simulation of B-Jet Identification in a Non-Magnetic Detector", J. Ellison, A. Kernan, D. Smith, Nucl. Instrum. Methods, A302, 227-240 (1991).
9. "Comparison of Structure Function Measurements from Hydrogen and Deuterium", K. Bazizi, T. Sloan, S.J. Wimpenny. Proceedings of 25th International Conference on High Energy Physics, Singapore, August 1990, 8 pp., (in press).
10. "Tests of the Radiation Hardness of VLSI Integrated Circuits and Silicon Strip Detectors for the SSC under Neutron, Proton, and Gamma Irradiation". UCR authors: J. Ellison, S. Jerger, C. Lietzke, and S.J. Wimpenny. IEEE Trans. Nucl. Sci. 38, 269-276 (1991).
11. "The VME-Based D0 Muon Trigger Electronics", (D0 Muon Group), UCR authors: K. Bazizi, T. Fahland, R. Hall, S. Jerger, C. Lietzke, D. Smith. IEEE Trans. on Nucl. Science, 38, No. 2, Part 1, 480- (1991).

12. "Forward Produced Hadrons in μp and μd Scattering and Investigation of the Charge Structure of the Nucleon", (European Muon Collaboration), UCR author: S.J. Wimpenny, 51 pp., to appear in Z. Phys. C., (in press).
13. "Comparison of Forward Hadrons Produced in Muon Interactions on Nuclear Targets and Deuterium", (European Muon Collaboration), UCR author: S.J. Wimpenny, 35 pp., Z. Phys. C, (in press).
14. "A QCD Analysis of the Proton Structure Function $F_2(x, Q^2)$ ", K. Bazizi, Ph.D. Thesis, University of California, Riverside, March, 1991, UCR/DIS/91-01 (1991).
15. "A Measurement of the Strong Coupling Constant α_s at the CERN SPS Collider", M. Lindgren, M. Ikeda, D. Joyce, A. Kernan, J-P. Merlo, D. Smith, S.J. Wimpenny. Submitted to Phys. Rev. D, (1991).
16. "A Comparative Study of Structure Function Measurements from Hydrogen and Deuterium", K. Bazizi, S. Wimpenny, UCR/DIS/91-02. Submitted to LP-HEP 91 Conference, Geneva, 25th July - 1st August, 1991.
17. "A QCD Analysis of the Proton Structure Function $F_2(x, Q^2)$ ", K. Bazizi, S. Wimpenny, UCR/DIS/91-03. Submitted to LP-HEP 91 Conference, Geneva, 25th July - 1st August, 1991.

TECHNICAL NOTES - HADRON COLLIDER TASK

D-Zero Notes

1. "Description of the MAC Test Board and Supporting Software Code", R. Hall, (UC Riverside), R. Zazula, R. Morphis, R. Korte, (Northern IL, Univ.), D0 Note 1047, (1990).
2. "Description of Software Tests for the Module Address Card", T. Fahland, D0 Note 1048, (1990).
3. "Muon Reconstruction with a Parabolic Interpolation", D. Franks, A. Kernan, A. Klatchko, D0 Note 1101, (1990).
4. "Muon Reconstruction with a 3D Kalman Filter and Chebychev Interpolation", D. Franks, A. Kernan, A. Klatchko, D0 Note 1102, (1991).
5. "Installing the Magnetic Field Map into the D-Zero Software", T. Fahland, A. Klatchko, D0 Note 1103, (1991).

6. "Muon Module Address Card (MAC) Description (Specification Version 3.0)", UCR authors: K. Bazizi and R. Hall, A. Taketani (Fermilab), D0 Note 1143, (1991).
7. "Tests of the Level 1.0 Muon Trigger at the D-Zero Cosmic Ray Commissioning", D0 Note No. 1145, June 1991. UCR author: K. Bazizi, C. Yoshikawa - Univ. of Hawaii.
8. "Hardware Modifications to the Version 4.01 Module Address Card", UCR authors: K. Bazizi and R. Hall, T.R. Knol (Northern Illinois Univ.), S. Hansen, C.S. Gao, A. Taketani (Fermilab), D0 Note 1137, (1991).

UCR Notes

1. "Report on Progress in the Muon Reconstruction", D. Franks, A. Kernan, A. Klatchko, UCR/D0/90-05, (1990).
2. "UC Riverside Proposal for Work on D0 Silicon Tracker Upgrade", J. Ellison, D. Joyce, and S. Wimpenny, UCR/D0/90-06, (1990).
3. "Comparison of Structure Function Measurements from Hydrogen and Deuterium", S.J. Wimpenny and K. Bazizi, (UCR), T. Sloan, (Univ. of Lancaster, UK), UCR/DIS/90-06, November (1990).
4. "Radiation Effects on Silicon Microstrip Particle Detectors", C. Lietzke, UCR/SSC/91-03 (1991).

1b. D-ZERO : PROTON-ANTIPROTON INTERACTIONS AT 2 TeV

1. Introduction

Riverside joined the D-Zero collaboration at Fermilab in late 1986. Our work to date spans four main areas: the implementation of the high voltage system, R&D studies for a silicon microstrip detector for the D-Zero upgrade and hardware/software development for the D-Zero muon system.

Work on the high voltage system and the hardware development for the muon trigger system is approaching completion and we are in the process of changing our focus onto data analysis with initial emphasis on the search for the top quark. We have also assumed responsibility for pattern recognition and momentum reconstruction software for the D-Zero muon system. R&D studies for a silicon microstrip detector for the D0 tracking system upgrade are also in progress and are being done in conjunction with similar work for the SSC.

In section 2 we discuss the physics goals and general features of the D-Zero detector. Section 3 describes in detail the activities of the Riverside group.

2. Physics and detector

D-Zero is a 4π non-magnetic hermetic detector designed for the Tevatron Collider at Fermilab. The evolution of the D-Zero design has benefitted substantially from the experience with the UA1 and UA2 detectors at CERN and the CDF detector at Fermilab. Additional input from the ongoing SSC R&D program has also proved valuable especially in the areas of readout and tracking designs for the projected Tevatron upgrades. In overall concept D-Zero has been designed to complement the strengths of the existing CDF detector.

The dominant emerging areas for new physics at the Tevatron are the search for the top quark and exploration of the B-physics sector. In addition the general themes of the Tevatron program include: (i) precision measurements of W and Z properties (mass differences, decay widths, production mechanisms, rare decays, decay asymmetries, study of trilinear boson couplings); (ii) tests of QCD at very large Q^2 (jet topological cross sections, searches for parton compositeness, direct photon studies, searches for quark-gluon phase transitions, measurement of fragmentation functions); (iii) searches for new states which could direct the extension and evolution of the standard model (manifestations of supersymmetry - squarks, gluinos, winos, zinos, sleptons), technicolor particles, heavy leptons, additional gauge bosons, or massive quasistable objects; (iv) measurement of the characteristics of the large cross-section, low p_T processes (multiplicity distributions, multiparton collisions, emergences of some new phenomena glimpsed in cosmic ray experiments); and (v) sensitivity to qualitatively new phenomena in the heretofore unexplored high energy, large Q^2 domain.

These physics issues dictated the basic design choices for D-Zero :

i.) No central magnetic field is provided. Since the relevant particles to be detected are jets (partons), leptons and non-interacting secondaries (neutrinos, photinos etc.) at large momentum, calorimetric measurement of energies are superior to momentum determination by track curvature. Moreover, a non-magnetic tracking system can be compressed, giving the opportunity for enhanced calorimetry and muon detection.

ii.) Lepton identification is of fundamental importance in searching for most high mass states, due to the relative cleanliness of leptonic decay modes of W,Z and heavy quarks. Measurement of both electrons and muons over the fullest possible solid angle is highly desirable; electron and muon measurements have quite different systematics so confirmation of new effects in both channels is highly beneficial. Electron channels are superior for precision mass measurements, while muons offer the possibility of seeing a lepton within a jet.

iii.) Measurement of the missing transverse energy in an event is crucial for many studies, and achievement of the best possible E_T resolution is a dominant goal. It is of particular importance to prevent unknown large fluctuations in measured event E_T , particularly far out in the tails of the distribution, in order to avoid having common event types simulate new physics. Good missing E_T resolution involves optimization of several features of the detector. Calorimeter coverage should cover the full solid angle with minimal cracks or hot spots. Holes for beam entrance and exit should be limited to $\theta < 1^\circ$ ($\eta \geq 5$). Good energy resolution helps control the rms width of the E_T distribution; of more importance here is the near equality of response to electrons and hadrons so that fluctuations in hadron shower composition are of minimal importance. Fig 1 is a schematic of the D-Zero detector.

The first run with the completed Detector will commence in the Spring of 1992. The central part of the detector has been completed (Central Calorimeter, Central Tracking Chambers and Central Toroid Muon Chambers) and was commissioned during a Cosmic Ray run in the spring of this year. No major problems were found in either the detector elements or the data-acquisition system and the run provided the first substantive test of the integrated detector control system. The next major milestone will be the second Cosmic Ray Run which is scheduled to start in August for which the first of the two End-cap Calorimeters and the North Muon Toroid will be commissioned. The second and last End-cap is scheduled for completion in November and will be moved into position in early December. The exact date of the 'roll-in' to the collision hall is still uncertain because of delays in the fixed target program scheduled prior to the next collider run. Current estimates place this in mid February 1992 by which time the detector will be complete and ready for physics.

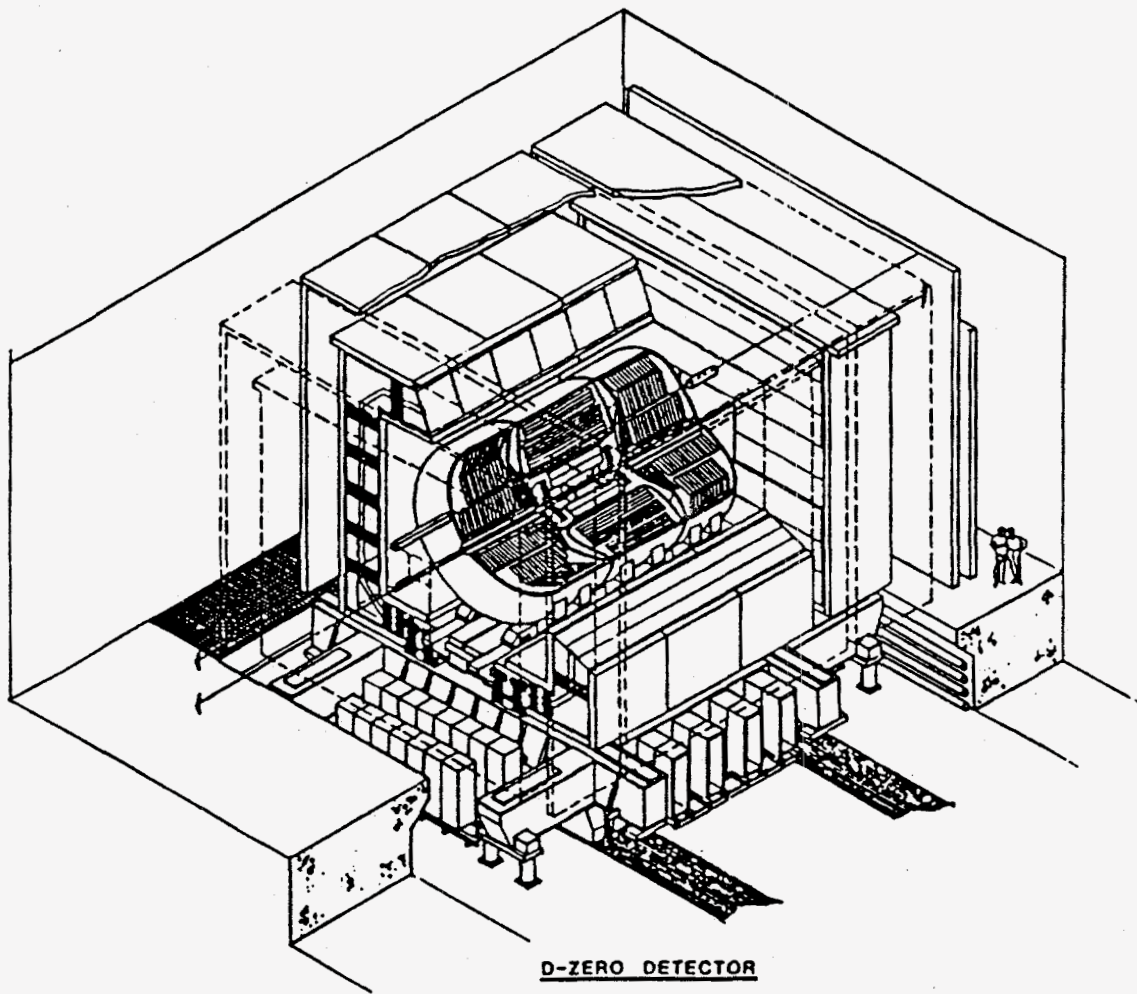


Fig.1 Schematic View of the D-Zero Detector

3. Riverside Activities

The expected date for D-Zero 'roll-in' is February 1992. Our major responsibility during the subsequent run will be for the operation of the muon detector and the reconstruction of muon data (section 3.1). This responsibility is shared with groups at Arizona, Fermilab and Northern Illinois University. Work on the design and implementation of the D-Zero high voltage system for which S.J. Wimpenny was largely responsible is close to completion with the final modules being installed throughout the detector (section 3.2). Physics analysis interests include i.) a systematic study of Monte Carlo generators, emphasizing background to top (section 3.3.1) , ii.) a search for associated $W + \gamma$ production (section 3.3.2) , iii.) the measurement of the inclusive muon cross section (section 3.3.3) and iv.) the search for the top quark (section 3.3.4). If the D-Zero upgrade proposal for the 1995 run is approved then we will begin working with Fermilab and LBL groups on the construction of the central silicon tracker (section 3.4).

3.1 The D-Zero Muon System

In D-Zero the muon detection system covers the entire solid angle to within 2.5° of the circulating beams. It consists of two toroidal magnetic spectrometer systems: WAMUS AND SAMUS. WAMUS, the Wide Angle Muon Spectrometer, consists of one central and two endcap iron toroids instrumented with planes of proportional drift tube (PDT) for tracking; angular coverage extends from within 10° to 170° of each beam. The Small Angle Muon Spectrometer extends coverage down to 2.5° using two iron toroids and PDT planes. An elevation view of the combined system is shown in Fig. 2.

The expected date for D-Zero 'roll-in' is Feb 1992 and commissioning of the muon detector is well underway. About 80% of large-angle PDT's were commissioned during the Spring 1991 cosmic ray run; the remaining chambers are installed and will be checked out using cosmic rays in the Fall. The muon system was successfully integrated with the

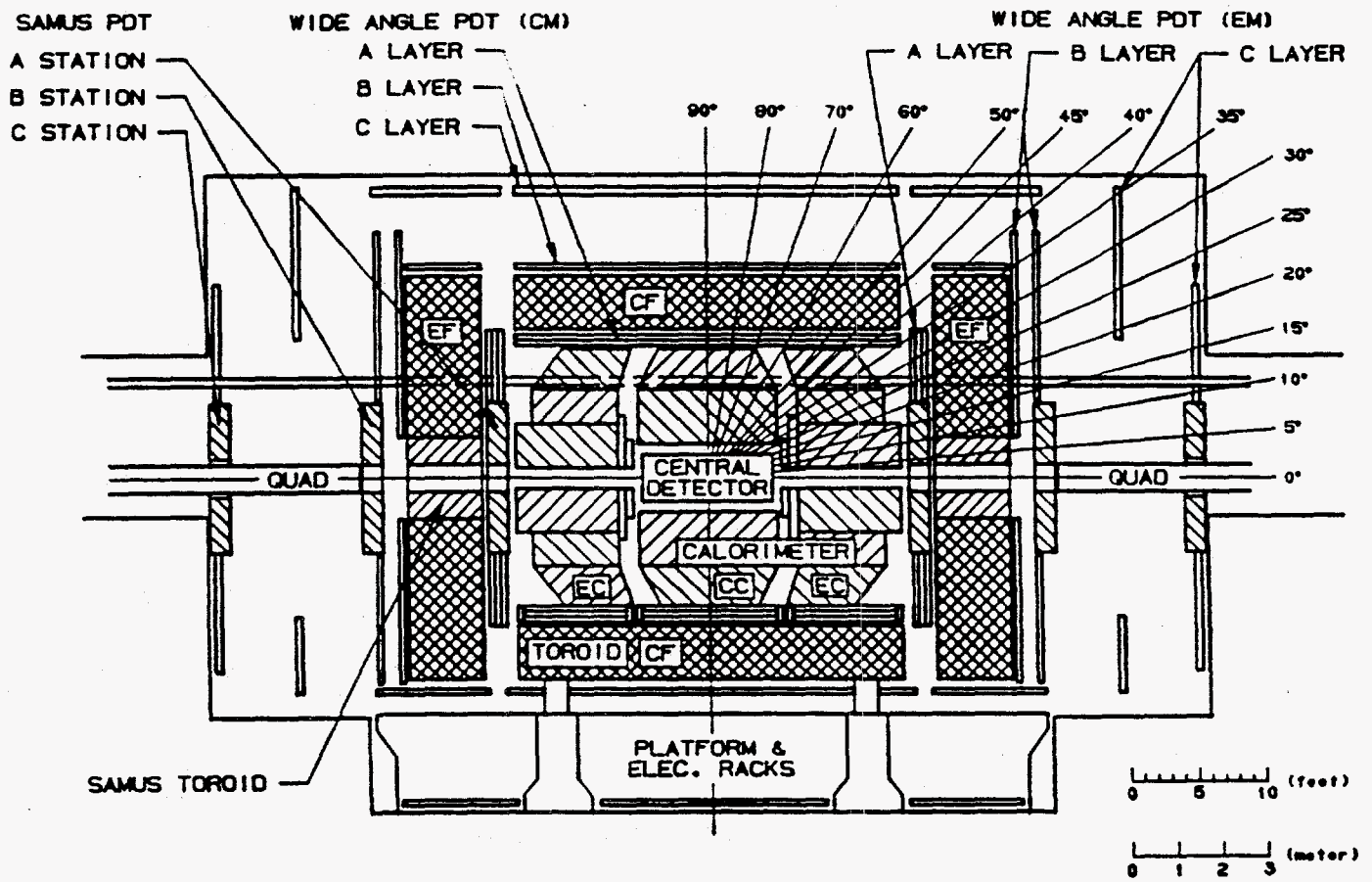


Fig.2 Side Elevation of the D-Zero Muon System

D-Zero central tracking and calorimeters in the Spring test. Figure 3 shows a cosmic ray muon traversing the various sub-systems.

At present and throughout most of the coming year the major UCR effort will be devoted to commissioning and running the D-zero muon system. Four UCR people are currently working fulltime on this project: post-doc K. Bazizi and grad students R. Hall and T. Huehn at Fermilab, and post-doc A. Klatchko at UCR. A. Klatchko will move to Fermilab in August 1991. We also have a strong involvement of undergraduate students in this work. As outlined below we are concerned with both hardware and software aspects of the muon system.

3.1.1 Hardware

(i.) Electronics

We began working on the electronics in 1988. Our first task was the testing of the Module Address Cards (MAC). The MAC resides in a 9Ux280 mm crate equipped with a custom VME backplane. The primary role of the MAC is the performance of zero suppression for data acquisition, and generation of trigger patterns ("centroids"). The testing, carried out mostly at UCR, is now almost completed, having gone through several iterations of software development, debugging boards and hardware modifications. We have recently documented the final version of the MAC [1] together with an account of the hardware changes implemented in the MAC since the original design [2].

(ii.) Installation and Trigger

K. Bazizi is leading the effort to implement the muon trigger. During the recent cosmic ray run he set up the level one muon trigger, (requiring a track candidate in the muon detector), and integrated it into the overall trigger framework. He is in the process of writing a document describing the level one muon trigger and its operation [3]. Work in progress includes the design a system to test the muon trigger independently of the D-Zero

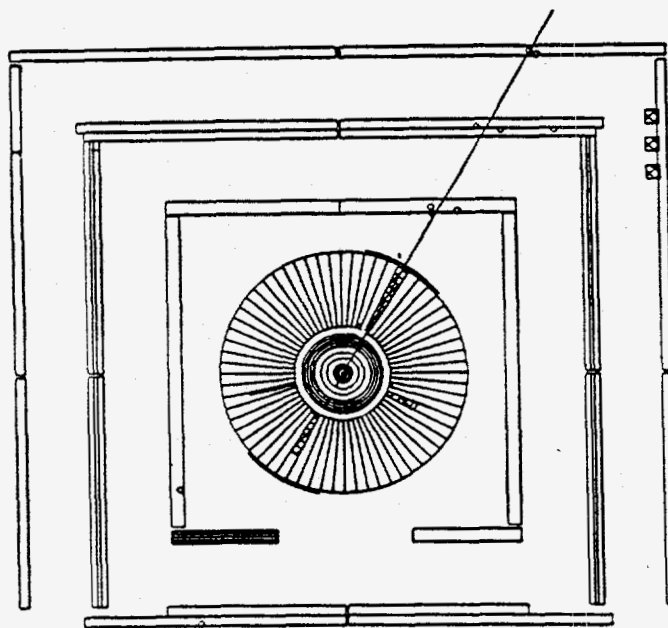
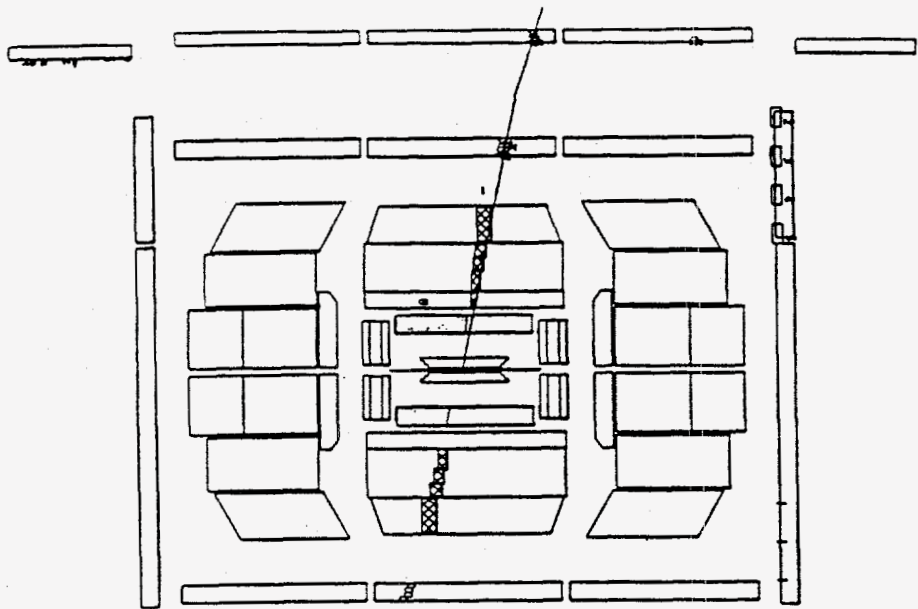


Fig.3 A Cosmic Ray Event from the Spring Run

data acquisition system : large numbers of VME trigger patterns will be downloaded and compared to the corresponding muon triggers.

Both Bazizi and Hall are checking out the muon chambers as they are mounted on the detector. This involves installing and debugging front-end electronics and setting up data acquisition crates in the counting house. This process will continue through the next few months. The plan is to have all muon chambers in place and certified, all data acquisition crates filled and tested, and both trigger levels 1 and 1.5 operational for the collider run beginning early 1992.

3.1.2 Software

As shown in Fig. 4 muon track is registered by the A layer (4 space points) of PDT's before the toroid, and by the B and C layers (3 space points each) after the toroid. The expected spatial resolution is 2.0 mm along the wire and 0.5 mm perpendicular to the wire. Momentum resolution is limited to 18% by multiple Coulomb scattering in the toroid.

A. Klatchko and T. Huehn are developing the software for off-line track-finding and fitting. This will replace the current simple algorithm which ignores multiple scattering and assumes a constant magnetic field everywhere. Initial work is described in the D-Zero notes below [4,6]. A program for muon momentum measurement is now working for all regions of the LAMUS detector, and is in process of integration into the D-Zero reconstruction package. It works as follows :

- straight-line segments in the A and BC layers are independently fitted.
- the A and BC track parameters are matched at the toroid surfaces with a third order Chebychev Polynomial expansion. The Chebychev expansion has the advantage of minimizing truncation error.
- Bdl is integrated along the resulting toroid trajectory, using the magnetic field map [6].

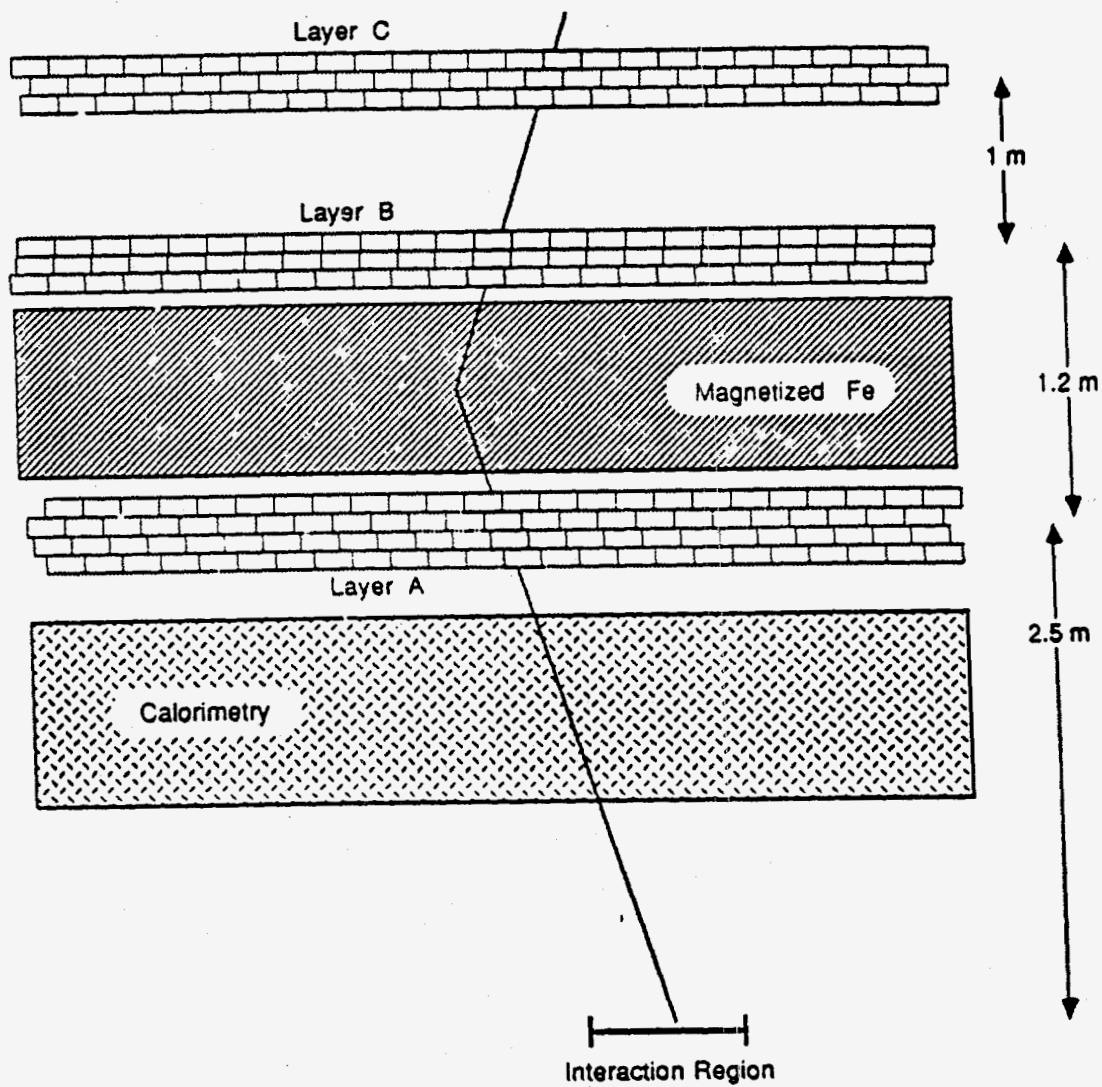


Fig.4 Schematic View of a Muon traversing the PDT Chambers

This gives $p = \int B dl / \delta\phi$. Figure 5 shows that the program has achieved the limiting momentum resolution, $\Delta p/p = 18\%$, on Monte Carlo data.

The Kalman filter method [7] is used for track fitting in the A and BC modules; this is currently done separately in the bend and non-bend planes. The Kalman technique has several advantages over the more conventional Winer-Hopf "global estimator" method :

- it is very sensitive to bad hits.
- the global method gives the track parameters at a single point whereas the Kalman filter yields optimal estimates of the parameters everywhere along the track. This permits more precise extrapolation to other detectors.

- when multiple scattering is taken into account globally a large non-diagonal covariance matrix must be inverted. In the Kalman filter approach multiple scattering is treated locally, so that only small matrices (2x2 for 2-D fits) are involved.

The next step is to incorporate multiple scattering in the toroid. This will be done as follows :

- starting with the the estimated momentum and the track measured in the A layer, propagate the track through the toroid, folding in multiple scattering and dE/dx at each step.
- fit the BC points to the propagated track.
- repeat the process for different momenta until the chisq for the BC track fit is minimized.

This procedure will be implemented first for a helical track model and then more generally with Runge-Kutta track following.

The measurement of the muon direction is improved by extrapolating from the muon detector back to the central tracker. For very high momentum tracks, $p > 100 \text{ GeV}/c$, for which multiple scattering in the intervening calorimeters is minimized, the central tracking information will also be used to improve the momentum estimate.

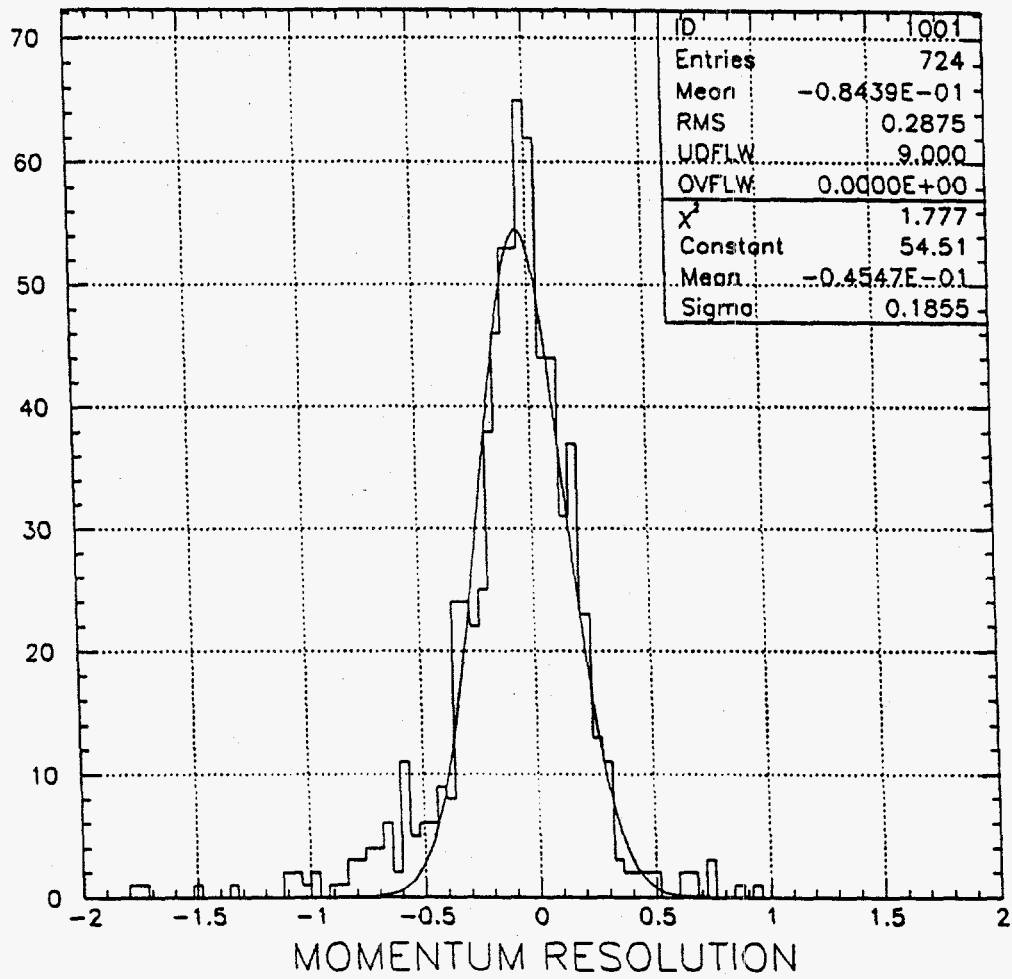


Fig.5 Muon Momentum Resolution for Monte Carlo Data

References

- [1.] "Muon Module Address Card (MAC) Description (Specification Version 3.0)", D0 Note No. 1143, June 1991, R. Hall, K. Bazizi - UC Riverside, A. Taketani - Fermilab.
- [2.] "Hardware Modifications to the Version 4.01 Module Address Card", D0 Note No. 1147, May 1991, K. Bazizi, R. Hall - UC Riverside, T. Knol - N. Illinois U., S. Hansen, C. Gao, A. Takatani - Fermilab.
- [3.] "Tests of the Level 1.0 Muon Trigger at the D-Zero Cosmic Ray Commissioning", D0 Note No. 1145, June 1991, K. Bazizi - UC Riverside, C. Yoshikawa - U. of Hawaii.
- [4.] "Muon Reconstruction with a Parabolic Interpolation", D0 Note No. 1101, November 1990, D. Franks, A. Kernan, A. Klatchko.
- [5.] "Muon Reconstruction with a 3D Kalman Filter and Chebychev Interpolation", D0 Note No. 1102, March 1991, D. Franks, A. Kernan, A. Klatchko.
- [6.] "Installing the Magnetic Field Map into the D0 Software", D0 Note No. 1103, March 1991, T. Fahland and A. Klatchko.
- [7.] R.E. Kalman, J. Basic Eng. 82 (1961) 34.

3.2 D-Zero High Voltage System

The D-Zero high voltage system is a computer controlled power system which provides high voltage power to all of the parts of the detector. It consists of a VME power supply and control system which are mounted in the moveable counting house, a remote control system which operates from the main control room and a passive splitter and distribution system. Each of these items has been custom designed for D-Zero by a joint UCR and Fermilab team.

The R&D work is completed and the majority of the components have been fabricated and installed in the experimental hall. A large fraction of the distribution system was commissioned during the Spring 1991 cosmic ray run using manual controlled power supplies. UCR effort over the coming year will be devoted to completion of the commissioning in time for the first data-taking run in February 1992. At present one UCR

person is working on this project : S.J. Wimpenny who will be based at Fermilab for the second half of 1991.

3.2.1 Hardware

We have coordinated work on the design of the D-Zero high voltage system since early 1987. The system is built around an 6U x 160 mm VME module which contains 8 independent high voltage power supplies (Fig.6). These can be run as either 0 to ± 5.6 kV at 1mA (for the central tracking chambers, muon system and calorimeters) and or 0 to ± 2 kV at 3mA (for the Level 0 trigger and Inter Cryostat Detector scintillation counters). Apart from the wide dynamic range these units are also required to be low noise and to have fast response for current and trip monitoring[1]. We have recently completed the design and testing and are in the process of producing final user documentation [2].

Work on the distribution system is essentially completed and most of the cabling, and splitter systems have been installed and tested in the experimental hall. The cabling and connector system are now available as off-the-shelf commercial products.

3.2.2 Software

Control of the power system is provided either locally via a PC or remotely from a VaxStation in the D0 Control Room (Fig.7). The microprocessor and PC software have been implemented by S.J. Wimpenny and M-J. Yang and will be commissioned during the Fall cosmic ray run [2]. In addition to the basic control functions the system has a suite of diagnostic routines for use in studying time stability and noise levels (eg. Fig.8). The Vax system is an on-going project and it is planned to have this operational in time for the collider run in early 1992.

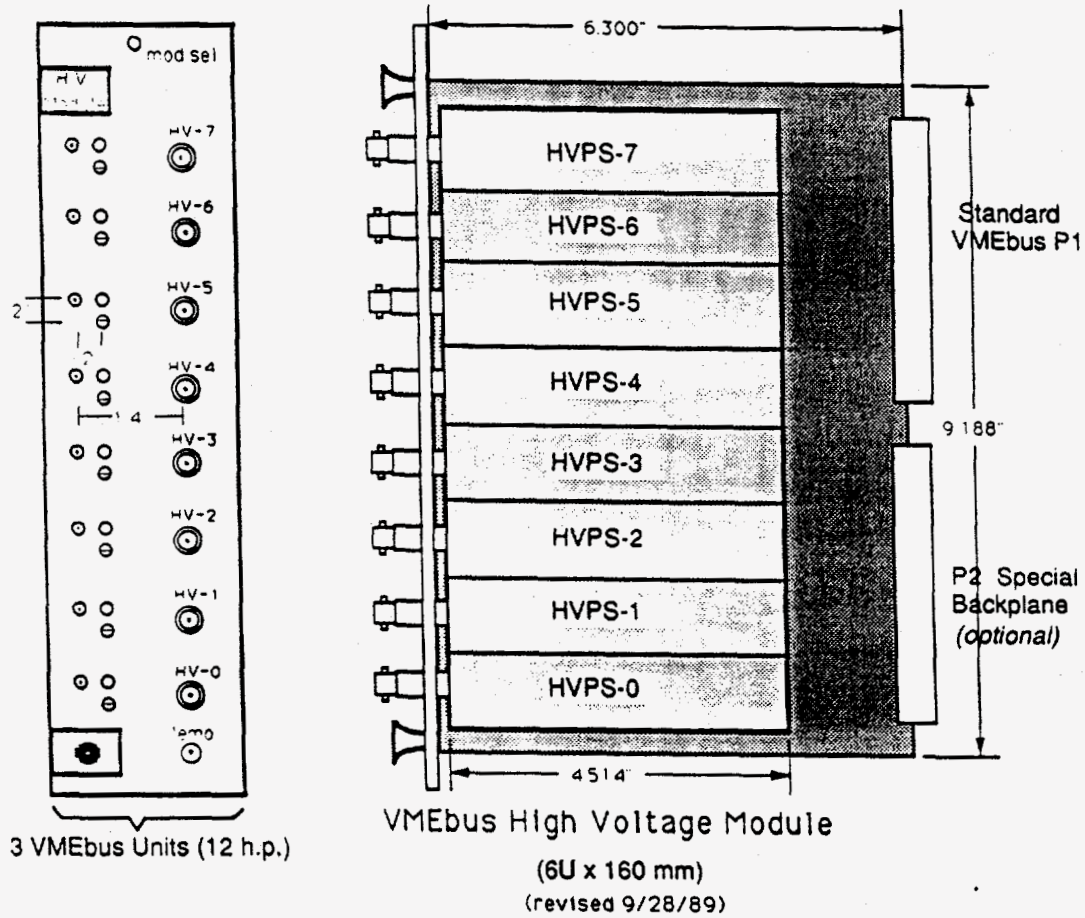


Fig.6 Schematic of the D-Zero VMEbus High Voltage Power Supply

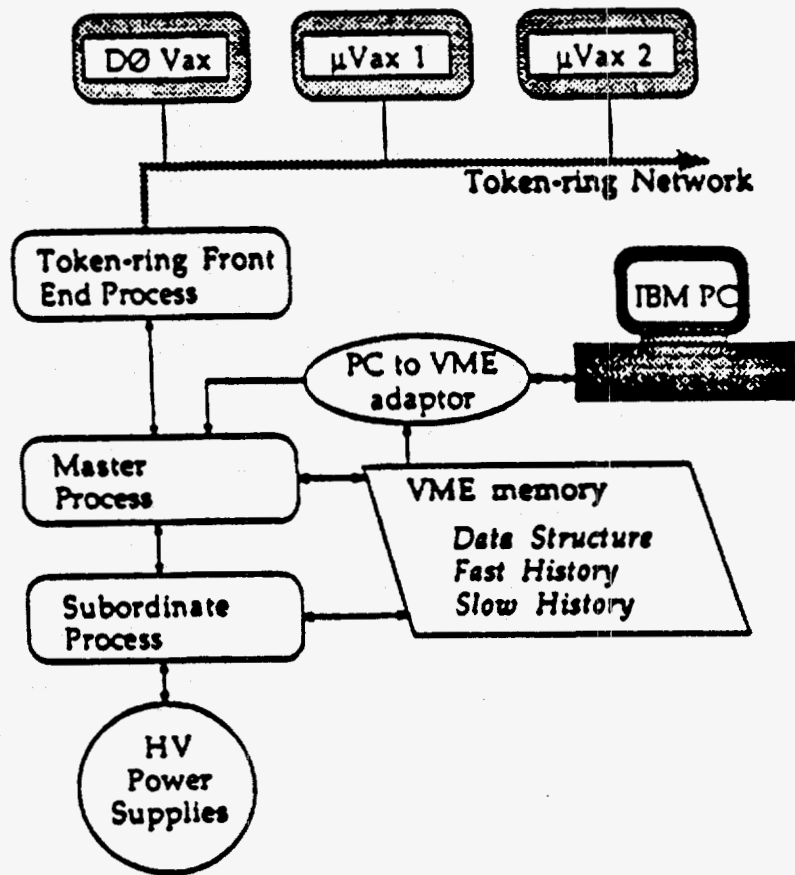


Fig.7 Software Configuration of the High Voltage Control System

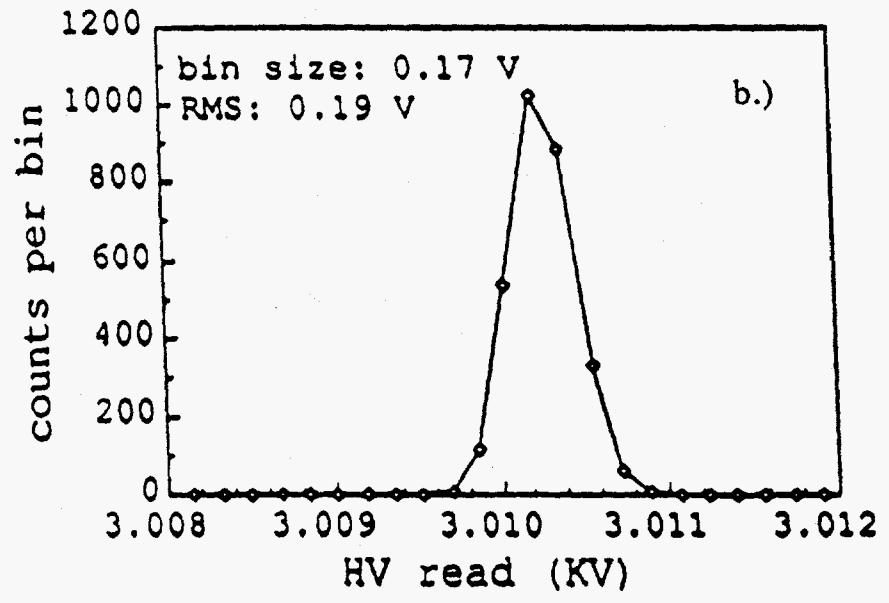
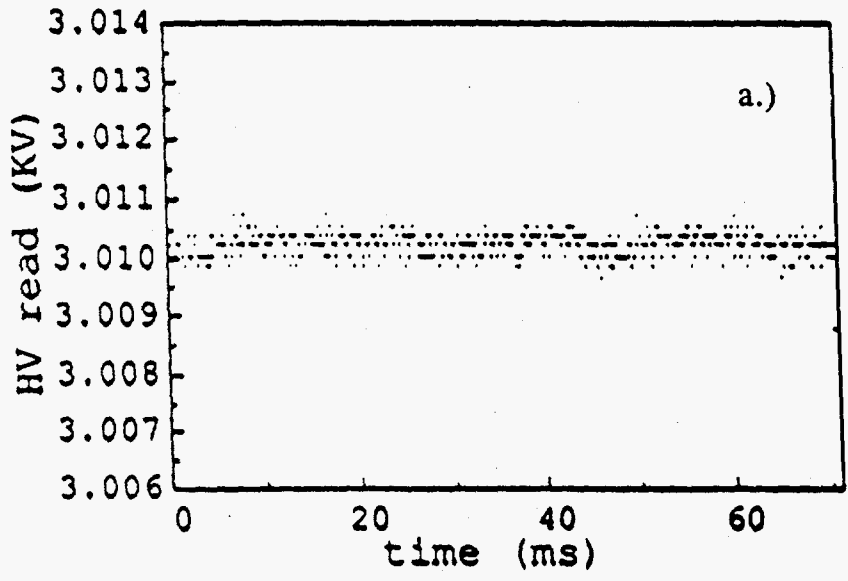


Fig.8 Displays of the ADC Readback of High Voltage Output Signal
 a.) Time Stability
 b.) Resolution Histogram

References

- [1.] "The D-Zero High Voltage System", M-J. Yang, talk presented at 2nd International Conference on Advanced Technology and Particle Physics, Como, UCR Report No. UCR/D0/90-10, Nucl. Inst. Meth. (in press), 1990.
T.F. Droege et al., Nucl. Inst. Meth. A279 (1989) 359.
- [2.] "The D-Zero High Voltage System Users Guide", M-J. Yang, S.J. Wimpenny - in preparation.

3.3 Physics Analysis

With the approach of the first collider run next year we have initiated a series of studies in preparation for physics analysis. As a group we are concentrating our efforts on the search for the top quark and some aspects of W/Z physics. The studies in progress are summarized in sections 3.3.1 to 3.3.4 .

3.3.1 Study of Different Monte-Carlo Generators

An essential question in the search for new physics such as the top quark and the search for SUSY particles is how well do we understand the conventional physics background processes and how well can we model them. This relies on two things : the Monte Carlo generator used to simulate the process and the simulation of the detector response. To correctly estimate the systematic uncertainties in any calculation both need to be considered carefully.

There are several generators available for hadron collider physics each of which treat differing numbers of Feynman graphs and use different approaches in event generation. To investigate the uncertainties due to the choice of a particular generator we have begun a comparative study of the different generators. The generators being considered are ISAJET[1], PAPAGENO[2], PYTHIA[3] and HERWIG[4].

For the moment we are concentrating on the production of W bosons in association with one or more jets. This process is important as it forms the primary background to the search for the top quark in the W + jets decay mode and is also important in the study of W γ physics and QCD.

As a first study we have made a comparison of the W transverse momentum distribution at the parton level using each of the programs. As a reference we have taken the theoretical calculation of Arnold and Kaufman which is in good agreement with the experimental data from the CDF Collaboration [5]. Fig 9 shows the comparison with the p_T distributions from ISAJET for the region $p_T \leq 25$ GeV/c. There is good agreement between the calculations at small p_T but at larger values of p_T ISAJET systematically underestimates the cross-section. This is further exemplified by Fig 10a which shows the same comparison for the extended range $p_T \leq 100$ GeV/c. Figs 10b-d show the same distribution for PAPAGENO, PYTHIA and HERWIG respectively. Note that cuts applied in the event generation are responsible for the differences for $p_T < 10$ GeV/c in the cases of PAPAGENO and PYTHIA so that these are not significant.

At the parton level this preliminary study suggests that PAPAGENO is the best estimator of true shape of the W p_T spectrum. Unlike the other programs this includes diagrams up to 3rd order in α_s . Our future program will be to study other variables and to implement parton fragmentation for PAPAGENO and interface it to DOGEANT, the D-Zero detector simulation package.

We also note that PAPAGENO also has the advantage that both the "production" and "decay" events in W γ production can be generated and the anomalous magnetic moment of the W can be varied (see next section).

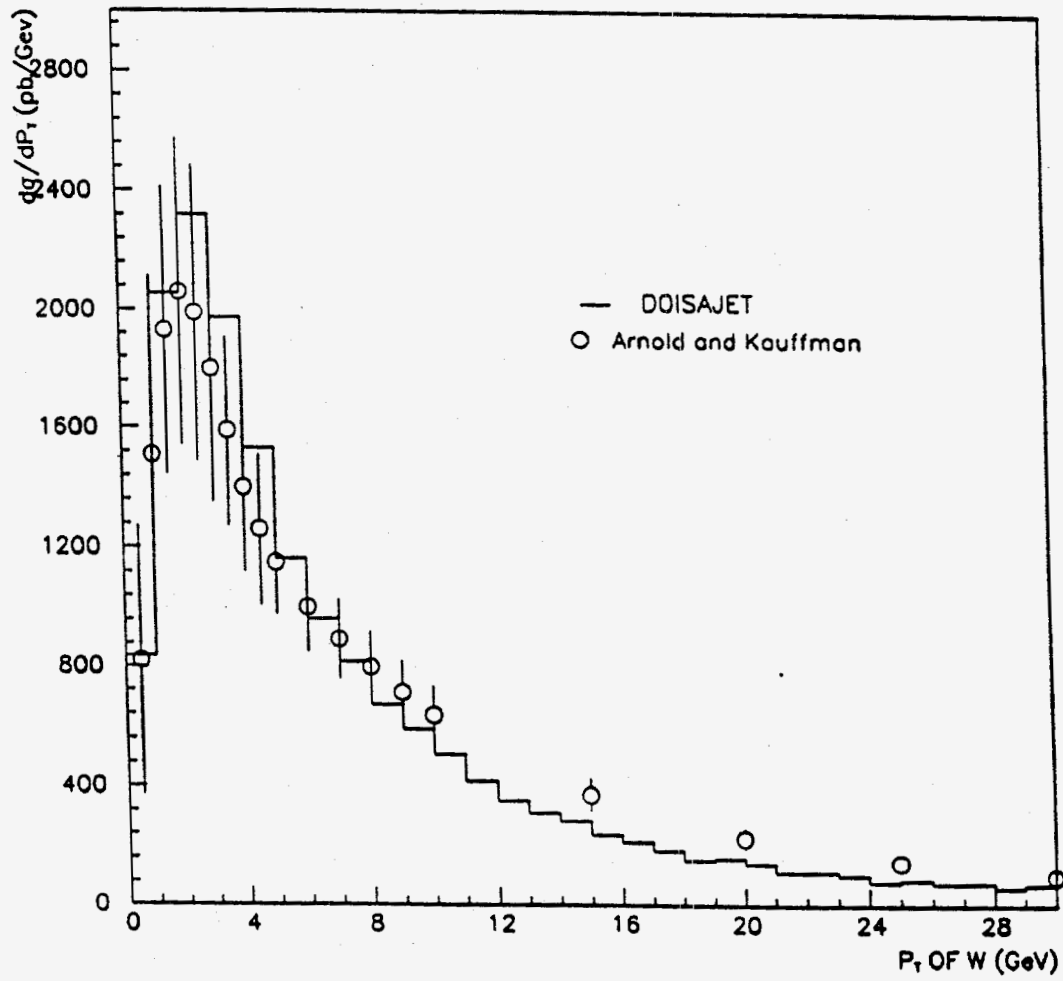


Fig.9 Comparison of W p_T Distributions from ISAJET and [5] in the region $p_T < 25$ GeV/c.

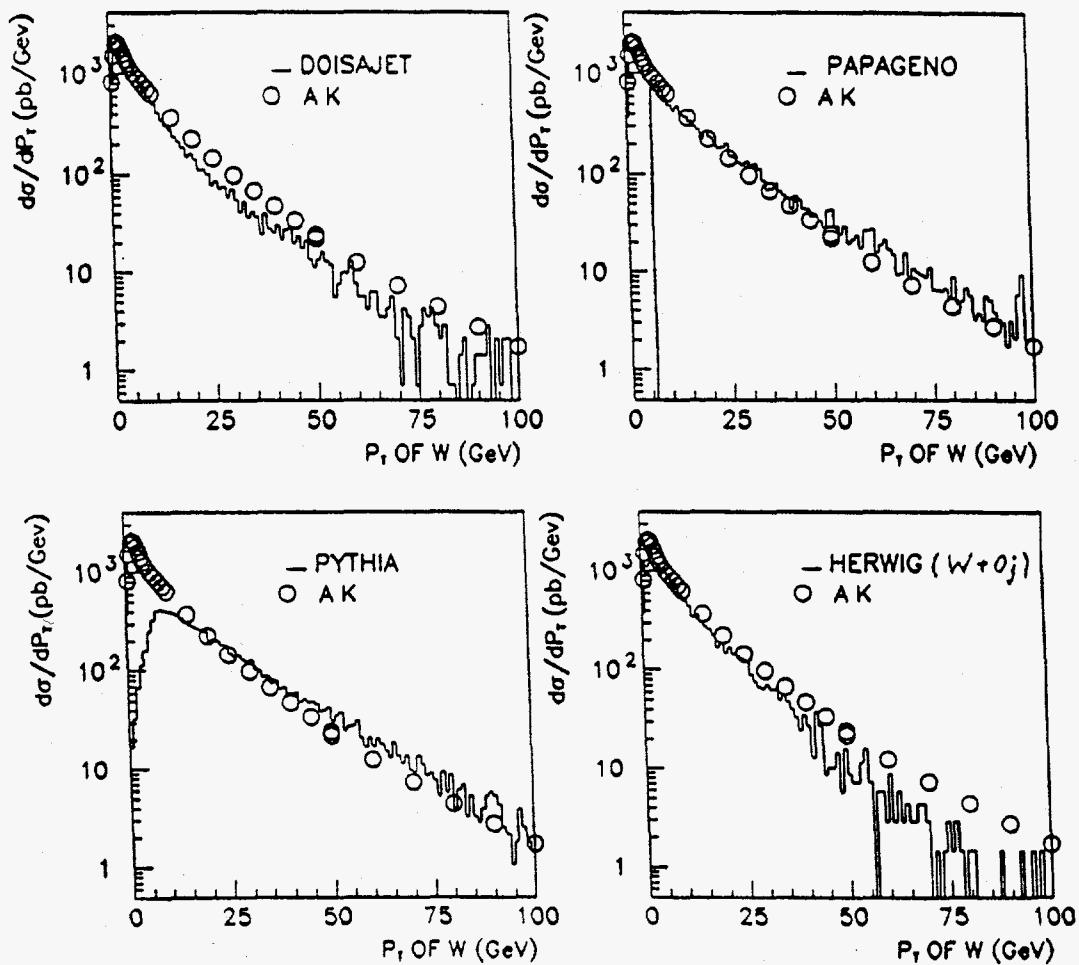


Fig.10 Comparison of Calculations of [5] and those of a.)ISAJET, b.)PAPAGENO, c.)PYTHIA and d.)HERWIG for $p_T < 100$ GeV/c.

References

- [1] F.E. Paige and S.D. Protopopescu, ISAJET Version 6.25, "A Monte Carlo event generator for proton-antiproton and proton-proton interactions", Brookhaven National Laboratory, 1986.
- [2] I. Hinchliffe, PAPAGENO Version 3.30, Lawrence Berkely Laboratory.
- [3] H-U. Bengtsson, T. Sjostrand, PYTHIA Version 5.4, "The Lund Monte Carlo for Hadronic Processes", CERN Program Library.
- [4] G. Marchesini, I.G. Knowles, B.R. Webber, "HERWIG, A Monte Carlo event generator for simulating hadron emission reactions with interfering gluons", CERN Program Library.
- [5] P.B. Arnold and R.P. Kauffman, Argonne report no. ANL-HEP-PR-90-70, (1990).

3.3.2 Search for $W + \gamma$ Associated Production

Testing gauge theories can be done either by comparing the Renormalizability of the theory with the experiment (higher order corrections), or by checking observables sensitive to the couplings which are restricted by gauge invariance. The magnetic moment of the W-boson, μ_w :

$$\mu_w = \frac{e}{2M_w} (1 + \kappa)$$

is such an observable. The non-abelian gauge invariance of the theory constrains the self-couplings of the gauge bosons, thereby restricting the value of κ to unity at tree level (higher order corrections are of the order of α). Note however that in non-gauge theories the value of κ is not restricted by any fundamental principle.

At $p\bar{p}$ colliders processes involving the $W\gamma$ coupling are sensitive to the value of κ . On the quark level the principal processes are :

$$\text{"production"} \quad d + \bar{u} \rightarrow \gamma + W^- (W^- \rightarrow l^- + \bar{\nu})$$

and

$$\text{"decay"} \quad d + \bar{u} \rightarrow W^- \rightarrow \gamma + l^- + \bar{\nu}$$

and their charge conjugate processes. It is known that in non-abelian gauge theories the "production" amplitude vanishes at $\cos\theta^*_{d\gamma} = \frac{1}{3}$, while the "decay" amplitude vanishes at $\cos\theta^*_{l\gamma} = -1$ suggesting a remarkable test of the theory [1].

To investigate this we have generated "production" type events using the standard PAPGENO generator [2] applying cuts of 10 GeV/c on the W transverse momentum, p_T^W and the transverse momentum of the photon, p_T^γ . Fig 11 shows the angular dependence of these events showing the expected minimum around 1/3. The corresponding total cross section is around 3.1 pb which will lead to 30 events (both μ and e) for an integrated luminosity of 10 pb^{-1} .

In addition to this sample we expect a factor of about 5 times more events coming from the "decay" process. The latest version of PAPGENO [3] includes the decay events and we plan to generate a corresponding sample of Monte Carlo events for further study. Both processes give rise to events containing both a high p_T charged lepton and photon which are isolated from each other.

The principal experimental background comes from high p_T gluon jets in which a π^0 has been misidentified as a γ . This is of the order of α_s/α and can probably be suppressed using isolation cuts.

Since the amplitude for each channel vanishes at different system at different values of $\cos\theta^*$, one has to distinguish between the two. This can be done with a cut on the cluster transverse mass, m_T where :

$$m_T^2(\gamma, l, \nu) = \left(\sqrt{m_\pi^2} + |p_T^\gamma + p_T^l|^2 + |p_T^\nu|^2 \right)^2 - |p_T^\gamma + p_T^l + p_T^\nu|^2$$

which for "decay" type events is bounded by M_W .

Following this preliminary work we intend to pursue the study with the inclusion of the decay events and using the full D-Zero detector simulation, DOGEANT, especially studying the issue of π^0/γ separation.

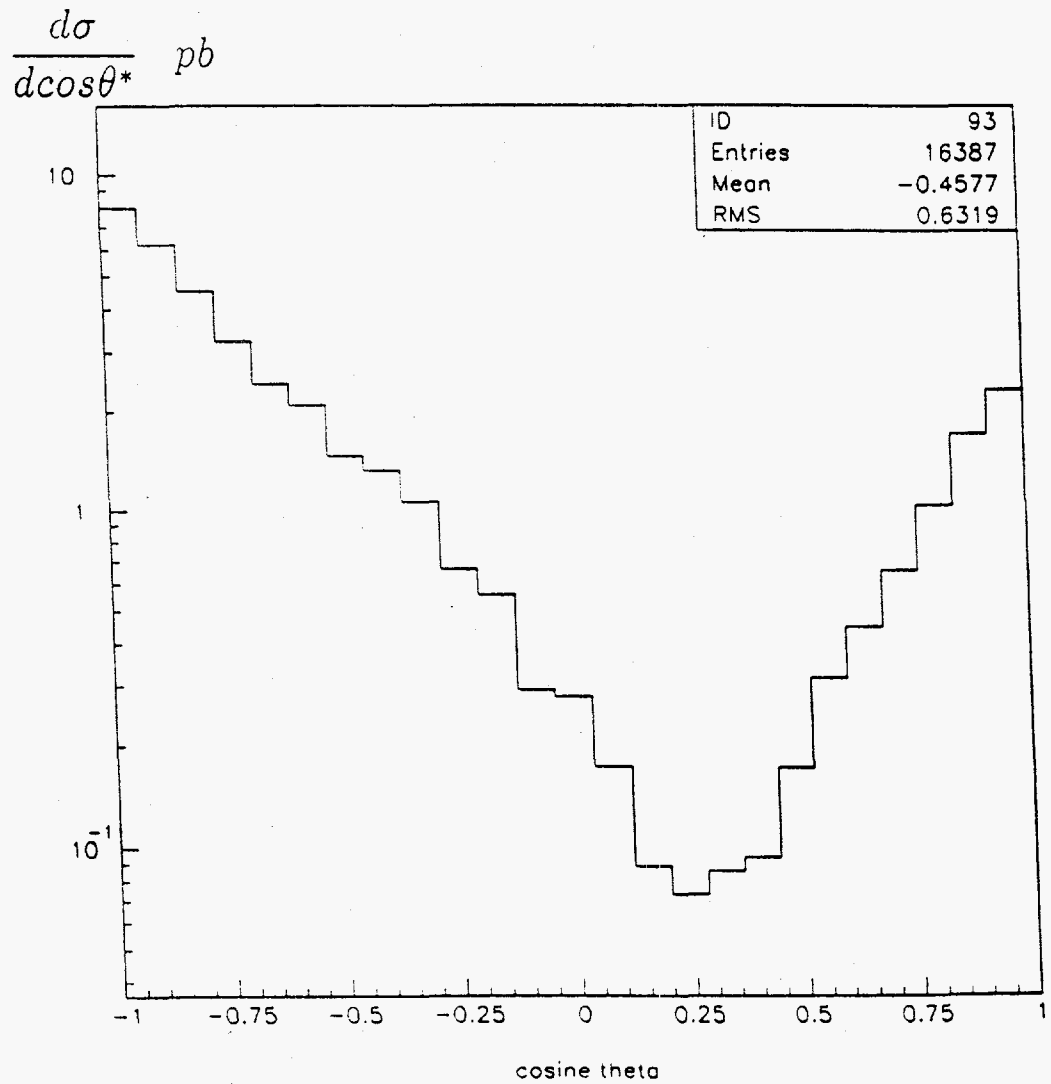


Fig.11 $\cos \theta^*$ Distribution for $W\gamma$ "production" Events showing the expected minimum around $1/3$.

References

- [1] Dongpei, Phys. Rev. D22 (1980) 2266.
- [2] Version 3.30 of PAPAGENO only includes the production diagrams.
- [3] I. Hinchliffe, PAPAGENO Version 3.41, Lawrence Berkely Laboratory.

3.3.3 The Inclusive Muon Cross-Section

Many processes contribute to muon production in hadron-hadron collisions at high energy. These include Drell-Yan, J/ψ and Υ production, W and Z^0 decays into muons and the semi-leptonic decays of C and B hadrons. All these processes give rise to "prompt" muon production. In addition non-prompt muons from pion and kaon decay-in-flight are expected to contribute strongly at low p_T .

The measurement and analysis of the inclusive muon cross section in proton-antiproton interactions at 1.8 TeV is an important goal of the first run of the D-Zero detector for the following reasons :

- it will be the first such measurement at the Fermilab Collider.
- it will be important to verify Monte Carlo calculations of the decay-in-flight background to prompt muons and our understanding of muon detection efficiency.
- since the prompt muon p_T spectrum below 15 GeV/c is dominated by b-quark production it will provide a measurement of the total b-quark cross section.
- the b-quark differential cross section can be measured out to large values of p_T since the B decay muon, being in a jet, can be readily separated from the isolated muons from W and Z^0 decay.
- the $c\bar{c} / b\bar{b}$ cross section ratio can be estimated from the structure of the transverse momentum of muons relative to the axis of the accompanying jet.

Finally it is essential to account for all known muon sources before we can search for new phenomena involving leptons, in particular the top quark.

This study will constitute the thesis project of graduate student T. Huehn. He has made a start by using ISAJET to generate the prompt muon p_T spectrum. He is also contributing to the development of the the muon reconstruction software (section 3.2.2). In the coming year he will start processing the muon data and will continue the Monte Carlo generation (including detector simulation) of known muon sources.

3.3.4 The Search for the Top Quark

One of the primary objectives for D-Zero is detection and study of the top quark. The CDF Collaboration has established that the top quark mass exceeds $89 \text{ GeV}/c^2$, while theoretical considerations set an upper bound around $200 \text{ GeV}/c^2$. Thus top will decay to a real W and a b quark :

$$\begin{array}{l}
 t \rightarrow W + b \\
 \quad | \\
 \quad \rightarrow l \nu \\
 \quad \rightarrow q \bar{q}
 \end{array}$$

and $t\bar{t}$ final states will be characterized by multiple leptons and/or jets. D-Zero is an ideally suited for such studies since it is hermetic and has precise and uniform muon, electron and jet capability covering almost 4π in solid angle.

To date no group has been able to reliably tag W boson decays into quark final states. Also the $t\nu$ decay has been observed but is difficult to tag with any efficiency so that the most promising decay channels will be $e\nu$ and $\mu\nu$. Thus a $t\bar{t}$ event will be tagged using either one or both of the daughter W decays into a high p_T lepton and missing energy, and the experimental signatures will be :

- two high p_T leptons (e^+e^- , $\mu^+\mu^-$, $e^+\mu^-$, $e^-\mu^+$), missing energy and two quark jets ;
- one high p_T lepton (e or μ), missing energy and four quark jets .

Each channel has a different admixture of conventional backgrounds and to establish a top signal it will be necessary to understand each of these in detail and to find a signal in at least two decay channels.

As a group we plan to concentrate our efforts onto the $e\mu + \text{jets} + \text{missing energy}$ and $\mu + \text{jets} + \text{missing energy}$ channels for the first collider run. The Monte Carlo (section 3.2.1) and Inclusive Muon Cross-Section (section 3.2.3) studies will each contribute to this.

An additional tool in the discrimination of prompt and non-prompt leptons is the isolation of the lepton from additional hadronic activity. R. Hall is studying different isolation algorithms to determine which is optimal for background rejection. The search for top via the $e\mu$ decay channel will constitute his thesis project. He is also working on the muon trigger electronics (section 3.1.1).

3.4 D-Zero Upgrade R&D

A major upgrade of the D-Zero detector is required for running with the increased luminosity ($5 \times 10^{31} \text{ cm}^{-2} \text{ s}^{-1}$) and decreased bunch crossing time (400 ns) projected for the Tevatron collider runs beyond 1995. To meet these requirements it is proposed to replace all of the present central and forward tracking chambers with a new system consisting of silicon microstrip detector covering the pseudorapidity range $|\eta| \leq 2.3$ surrounded by a scintillating fiber outer tracker. The new tracker will be enclosed in a 1.5 T solenoidal magnetic field.

The silicon tracker is a hybrid consisting of a mixture of 'conventional barrel' and 'forward disk' topology and using a mixture of single and double sided silicon detector technology. The UCR group (Ellison, Joyce and Wimpenny) is playing a major role in the design and, together with LBL and Fermilab, will be responsible for its construction. Initial Monte Carlo studies of the detector geometry are approaching completion and the next

phase of the project is to establish details of the R&D work needed and to set realistic milestones for the construction of the final detector.

If we take as a target to have a significant fraction of the final detector ready in time to be tested during the 1995 collider run then the R&D timescale shown in Fig 12 results. Within this effort the UCR contribution would be (i.) to develop realistic radiation hardness and detector geometry specifications in collaboration with potential vendors (Fig 13) and (ii.) use our on-campus facilities to evaluate detector prototypes.

Using modelling developed for the SSC we have estimated the effects of the radiation levels to which a nominal detector would be subjected for the conditions projected for collider runs 1(1992) through 3 (1997) and have studied the effects on detector noise and bulk damage to the silicon doping [1]. Test beam studies at Los Alamos National Lab scheduled during July and September will be used to confirm these conclusions. The next phase will then be to apply the modelling to the D-Zero geometry and work with industry to produce prototypes.

Although the radiation levels do not seem to be a problem for the strip detectors themselves they are problematic for the current generation of VLSI readout electronics and it will be necessary to develop new radiation hard readout electronics. Further, since the time between bunch crossings will ultimately be 400 ns, it will be necessary to develop a readout chip which can handle such a rate. Work on chip development is presently in progress for the CDF Collaboration who are developing a radiation hard version of the Berkeley SVX chip. This may be suitable for D-Zero use although some additional development work will be needed to meet the D-Zero design specifications.

The UCR silicon test lab has been developed around our program of R&D studies for the SDC detector at the SSC (section 1c). Although many of the issues are in common between SDC and D-Zero differences in configuration and readout electronics will necessitate some additions to our setup at UCR. These are principally modifications to our

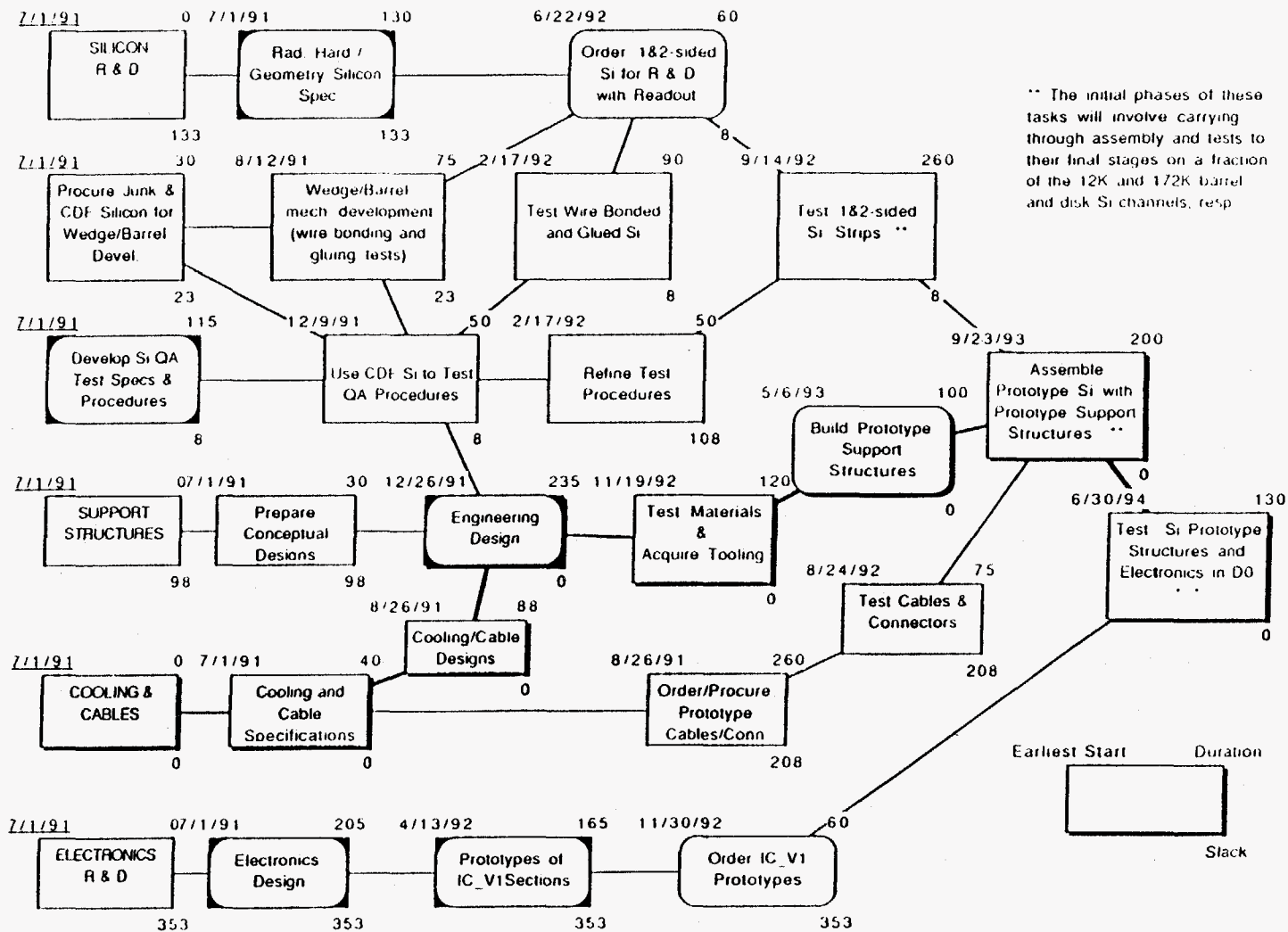
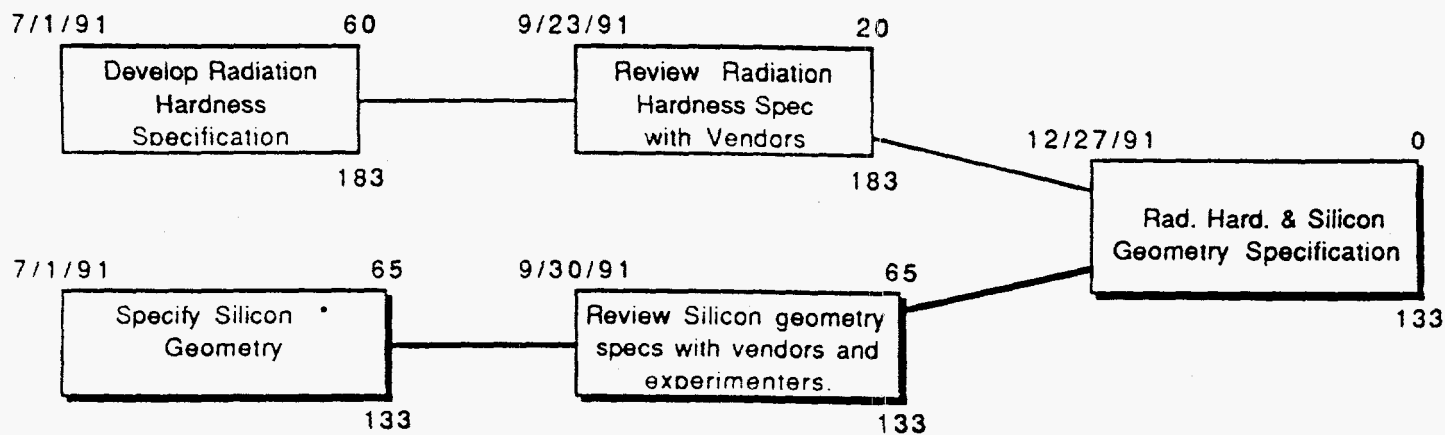


Fig.12 Preliminary Schedule for the D-Zero Silicon Vertex Detector Project.

Radiation Hardness & Si Geometry Specification



- Specify bias current, depletion voltage limits, thickness, double sided/ single sided, etc. Understand channel counts, costs, bulk structural properties, etc.

Fig.13 Preliminary Schedule for Radiation Hardness and Geometry Specification.

probe station and for the purchase additional electronics for the study of detector / amplifier noise. A detailed breakout of the necessary equipment is given in task A1 budget section.

References

- [1] "Radiation Levels in D-Zero and Effects on Silicon Detectors", D0 Note - in preparation, June 1991, J. Ellison.

1. Introduction

The Solenoidal Detector Collaboration or SDC will be the first of the two major detectors to be constructed for the 20 TeV Superconducting Super Collider in Texas. Taking the view that SDC provided the logical next step in the development of our Hadron Collider Research Program UC Riverside joined the SDC Collaboration in mid 1989. Our work is concentrated on the development of the detector design with particular emphasis on the inner silicon tracking system.

2. The SDC Silicon Tracker

The design of the SDC Collaboration detector for the SSC[1] calls for a very large silicon tracking system which will form the basis of the charged particle tracking at radii between 15 and 60 cm from the beam (Fig 14). This covers an area of about 32 m^2 and the system will contain about 10 million readout channels. The design represents a significant step beyond any of the present generation of vertex detectors proposed for hadron colliders.

The tracker consists of $300 \mu\text{m}$ thick double sided detectors with axial strips on one side and stereo strips on the other side. Pairs of such detectors with opposite stereo pitch are arranged in superlayers in a cylindrical barrel section and also in planar endcaps. The superlayers allow local hit association into segments that are then further associated into tracks. The transition from barrel to intermediate angle geometry is near 45 degrees to minimize the thickness of material traversed by particles. The intermediate angle detectors are spaced along the beam at a distance of nearly 3 m from the interaction point to allow good momentum measurement at large rapidities.

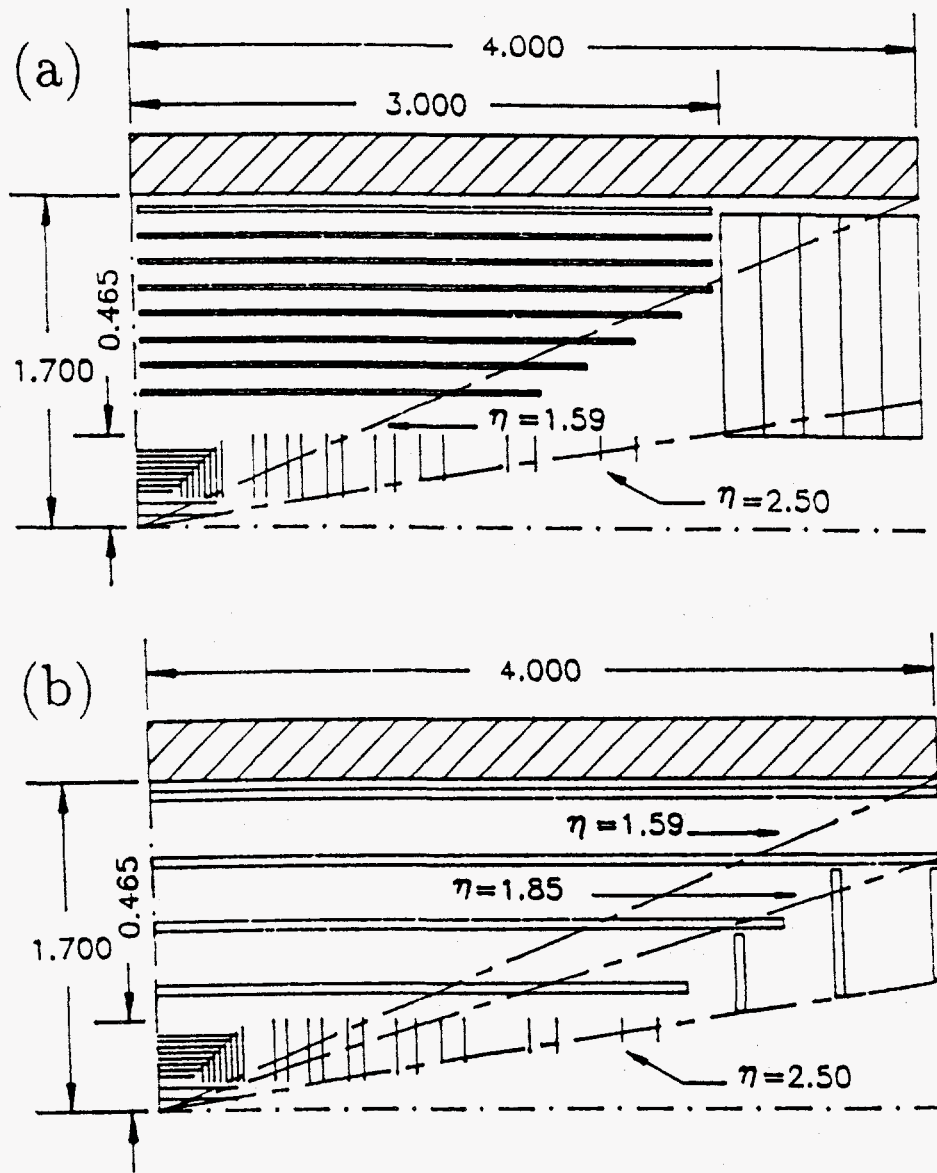


Fig.14 Schematic Diagrams of the SDC Inner Tracking System
 a.) silicon pixels, strips, straw tubes and radial wire chambers
 b.) silicon pixels, strips scintillating fibers

3. Detector R&D at UCR

The silicon detector laboratory at Riverside was set up in 1989 using UCR funding with the purpose of studying silicon detector and readout for trackers in the hadron collider environment. Since this time the facility has been continually evolving and is currently tailored to the R&D program of SDC. At the present time it is equipped with a semiconductor probe station for wafer characterization, an ultrasonic wire bonder for the study of double sided bonding and a laser/infra red light source for studying detector response.

Complimentary to our silicon microvertex detector studies for D-Zero we have been participating in the SSC Silicon Tracking subsystem R&D work [2]. Although many of the areas of study are common to both projects, the SSC poses additional problems due to the very high rates, the harsh radiation environment and the very large area of silicon required for the proposed tracking system.

We have studied the effects of proton and neutron radiation damage on silicon detectors using the LAMPF and LASREF facilities at Los Alamos National Laboratory. The aim of this work has been to determine the limit on the lifetime of the silicon tracker due to detector radiation damage effects and to study the effects on AC-coupled microstrip detectors. Our results [3,4] show that, over a nominal 10 SSC year running period, there is no serious degradation in the coupling capacitors on AC-coupled detectors and that polysilicon bias resistors are stable under a similar radiation exposure. Additional studies of bulk silicon effects using 1 cm^2 PIN diodes predict SSC detector lifetimes of around 10 years [4].

Our future efforts will be divided between ongoing radiation damage studies and R&D work on the SDC silicon tracker forward disks. Further proton runs are planned at LAMPF during July and September 1991. We plan to study the effects of radiation on detector pulse height, interstrip resistance/capacitance, leakage currents and changes in the silicon doping concentration.

Work on the SDC forward silicon disks is also planned. We will develop layouts of the silicon disk detectors. Several designs will be considered such as different stereo angles and different readout chip placement. The possibility of supplying mask artwork to detector vendors may allow us to gain greater flexibility in specifying our needs. Prototype wedge detectors will be acquired from vendors and we will evaluate their performance in the silicon lab at UCR, emphasizing issues unique to particular wedge detectors geometries. This evaluation will use various means of signal generation in the silicon (IR photons, charged particles), and already-developed readout electronics (SVXH readout chip).

References

- [1] J. Ellison, S.J. Wimpenny et al., "Solenoidal Detector Collaboration Expression of Interest to Construct and Operate a Detector at the Superconducting Super Collider", May 24th 1990.
J. Ellison, S.J. Wimpenny et al., "Letter of Intent by the Solenoidal Detector Collaboration to Construct and Operate a Detector at the Superconducting Super Collider", November 30th 1990.
- [2] J. Ellison, S.J. Wimpenny et al., "SSC Detector Subsystem Proposal: Subsystem R&D Proposal to Develop a Silicon Tracking System", 1989.
J. Ellison, S.J. Wimpenny et al. "Subsystem R&D Proposal to Develop a Silicon Tracking System 1990-1991", 1990.
- [3] J. Ellison, S.J. Wimpenny et al., "Study of Radiation Effects on AC-Coupled Silicon Strip Detectors", Proceedings of 2nd Conference on Advanced Technology and Particle Physics, Como, Italy, 1990, (to appear in Nucl. Phys. B).
- [4] J. Ellison, S. Jerger, C. Lietzke, S.J. Wimpenny et al., "Tests of Radiation Hardness of VLSI Integrated Circuits and Silicon Strip Detectors for the SSC Under Neutron, Proton and Gamma Irradiation", IEEE Trans. Nucl. Sci. NS38 (1991) 269.

At the heart of all calculations of hard scattering cross-sections are parameterizations of the parton distributions functions $q(x, Q^2)$, $\bar{q}(x, Q^2)$ and $g(x, Q^2)$. These, in turn, are derived from measurements of the Deep Inelastic Structure Functions $F_1(x, Q^2)$, $F_2(x, Q^2)$, and $F_3(x, Q^2)$ and it is on the reliability of these measurements on which the parton distribution functions depend.

In general the experimental data are in quite good agreement with the exception of the region of small Bjorken x ($x \leq 0.2$) where significant discrepancies exist. This is particularly unfortunate as this is the most important kinematic region for calculations pertaining to cross-sections at the Tevatron and SSC.

As a part of an ongoing study of the deep inelastic data have investigating two of the principal experimental datasets - those of the EMC and BCDMS Muon Collaborations at CERN. It is the inconsistencies between these two sets of data which give rise to some of the largest uncertainties in the parton distributions.

The EMC and BCDMS have published high precision measurements on the structure function $F_2(x, Q^2)$ measured using hydrogen [1,2] and deuterium [3,4] targets. The same basic problems effect the data on both targets. For example Fig.15 shows a comparison of the published hydrogen data from which it can be seen that, in terms of their broad characteristics, the data agree. The Q^2 -dependence of $F_2(x)$ is similar for both experiments but when fitted results in significantly different results for Λ (Table 1). The x -dependence, however is significantly different and inconsistent with a simple normalization difference between the two experiments. This is inconsistent with the statistical and systematic errors quoted by the two groups.

We have studied the analysis methods used by the two groups in detail and find that there are several differences in both the theoretical input and methods used to extract F_2 . Careful studies of the treatment of the electromagnetic radiative corrections [5] and the

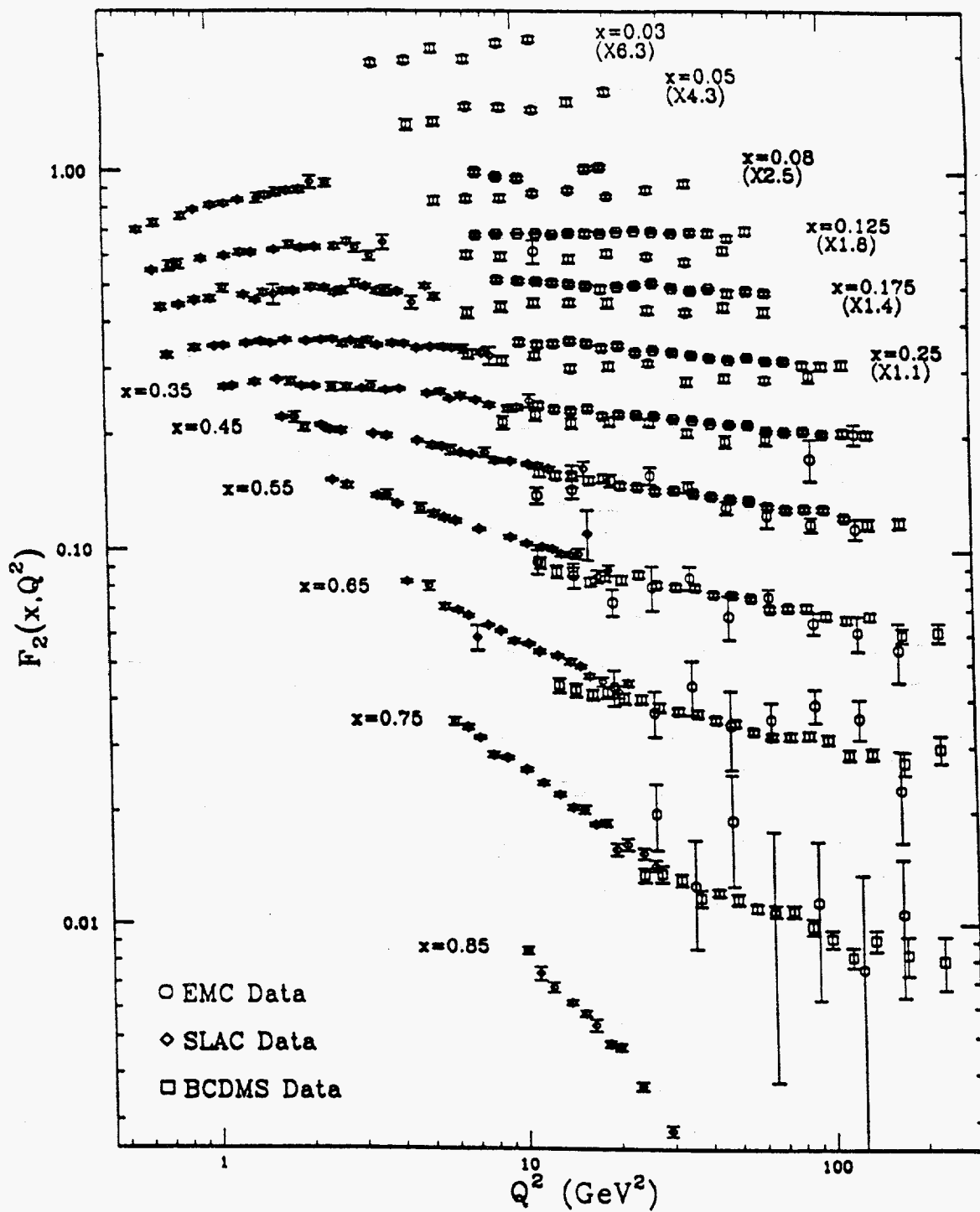


Fig.15 Comparison of the Published EMC, BCDMS and SLAC data

TABLE 1

QCD Fit Results

| QCD Fit | This Analysis | EMC[1] | BCDMS[2] |
|---|-----------------------|-------------------|------------------|
| Leading Order Singlet | 206^{+57}_{-50} MeV | 90 MeV | 215 ± 27 MeV |
| Next to Leading Order Non-Singlet | 209^{+78}_{-71} MeV | 105 ± 101 MeV | 224 ± 21 MeV |

calculations of the ratio $R = \sigma_L/\sigma_T$ [6] suggest that these may be responsible for some of the differences between the two sets of data.

To further investigate this requires the re-analysis of the two sets of data using the same assumptions. We have completed such an analysis of the hydrogen data and find that, after correction, the Q^2 -dependence of F_2 , and hence the value of Λ , are in very good agreement (see Table 1 and Figs 16). The difference in the x -dependence persists and globally we find a normalization difference of 11% between the two datasets. To study this problem further we have also compared our results to those from the re-analyzed compilation of the SLAC electron data [7,8]. While there is little kinematical overlap with the two CERN groups the data provide an independent measure of the x -dependence of F_2 .

We have two versions of these data ; one using the results direct from the SLAC analysis (open squares) and the second using results re-extracted using our treatment of R [6] (solid points) which are compared to our results for EMC in Fig.17 and for BCDMS in Fig 18. The agreement between the electron and muon datasets is good but further work is needed to see if the SLAC data is in better agreement with either set of muon data. On further study we find that the SLAC data are consistent with a constant normalization shift of 5.2 % with respect to EMC (Fig 19a) but that a single normalization shift cannot make the SLAC and BCDMS data agree (Fig 19b). The reason for the latter problem is not understood. Our final results, after correction for normalization differences are shown in Fig 20 from which we conclude that reasonable consistency can be achieved between the three datasets provided that the same modelling is used for R and that differences in relative normalization are corrected for.

We are currently working on a similar analysis of the deuterium data from SLAC EMC and BCDMS. Preliminary results show the same basic features as observed in the hydrogen analysis.

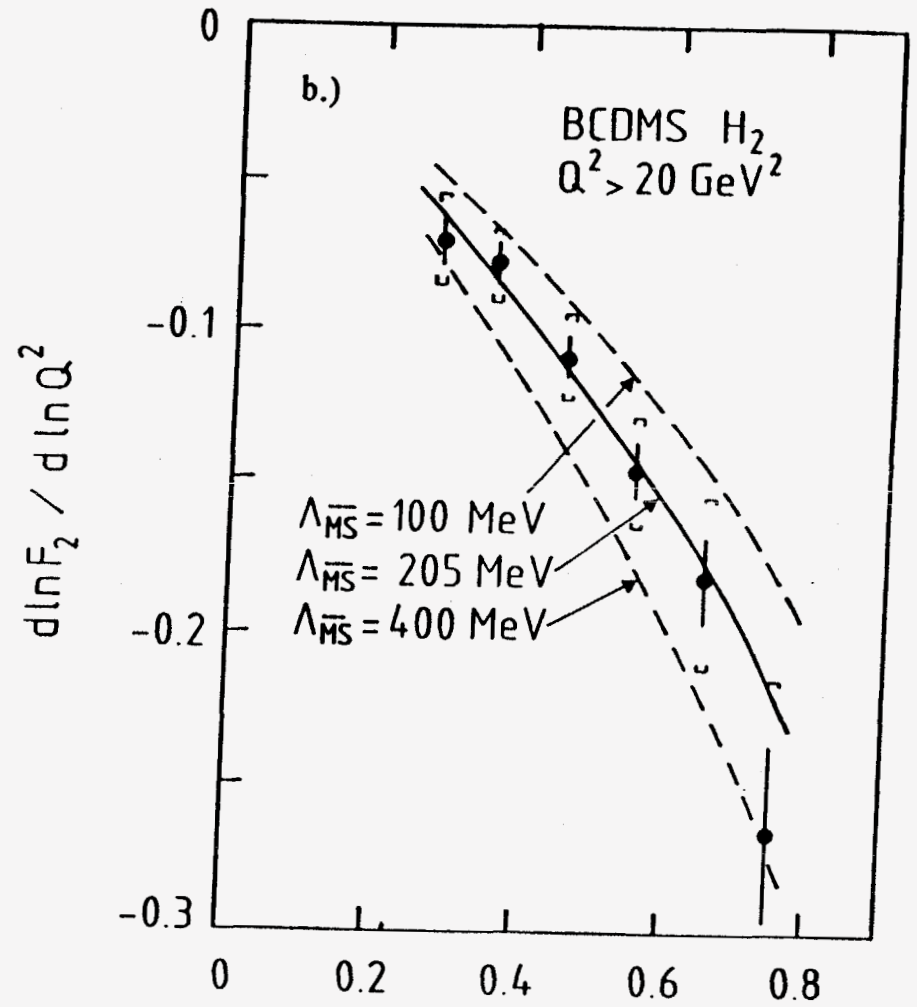
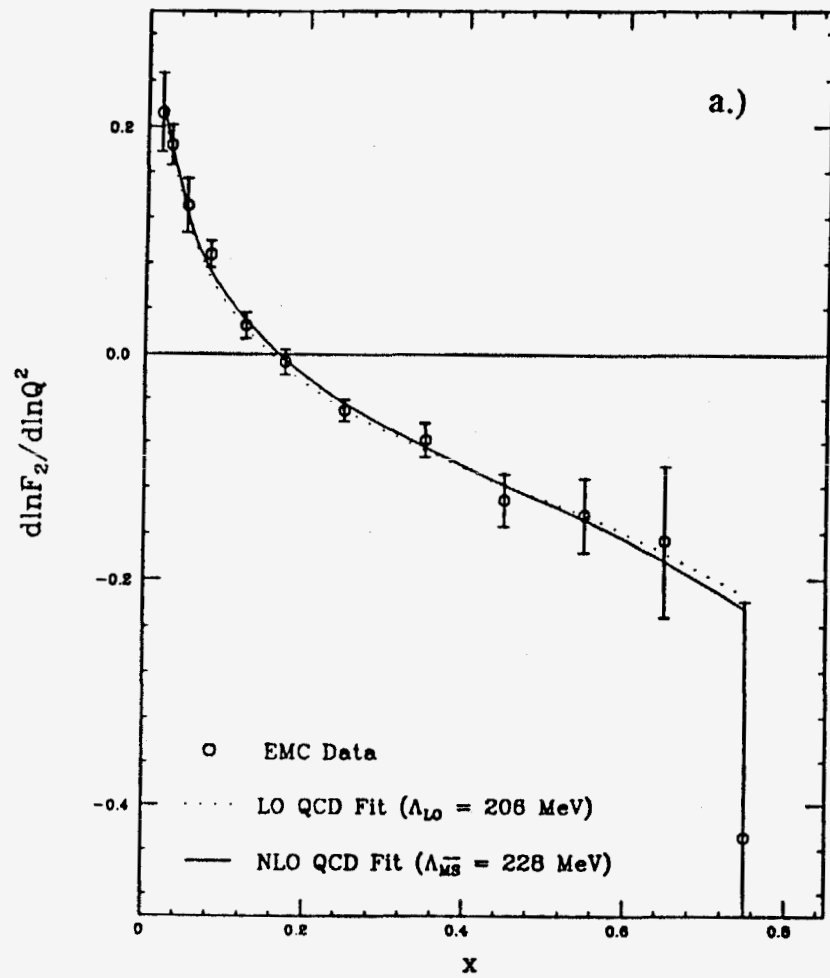


Fig.16 Comparison of the data and the predictions of QCD
 a.) EMC Data (this analysis)
 b.) BCDMS Data [2].

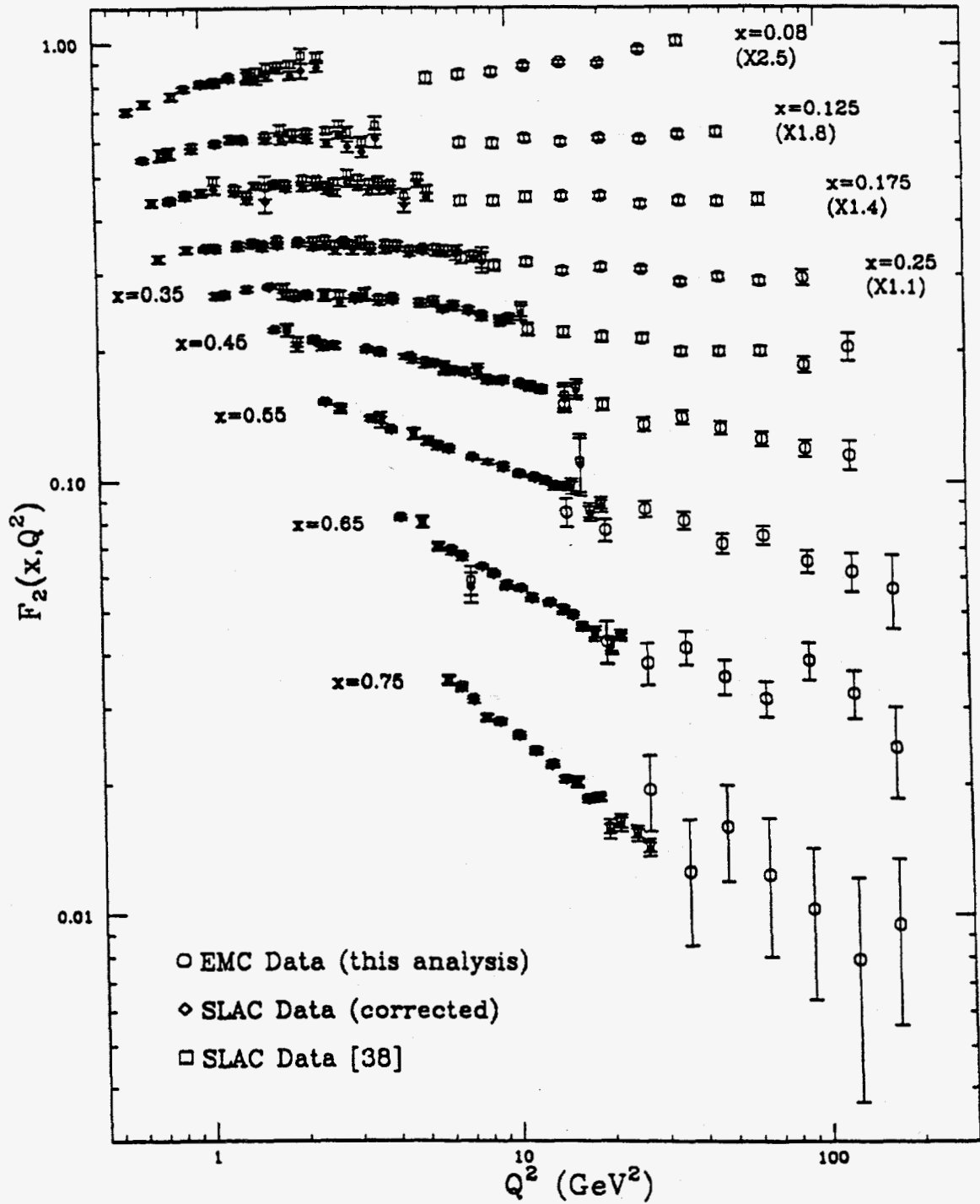


Fig.17 Comparison of the SLAC and EMC Data (this analysis)

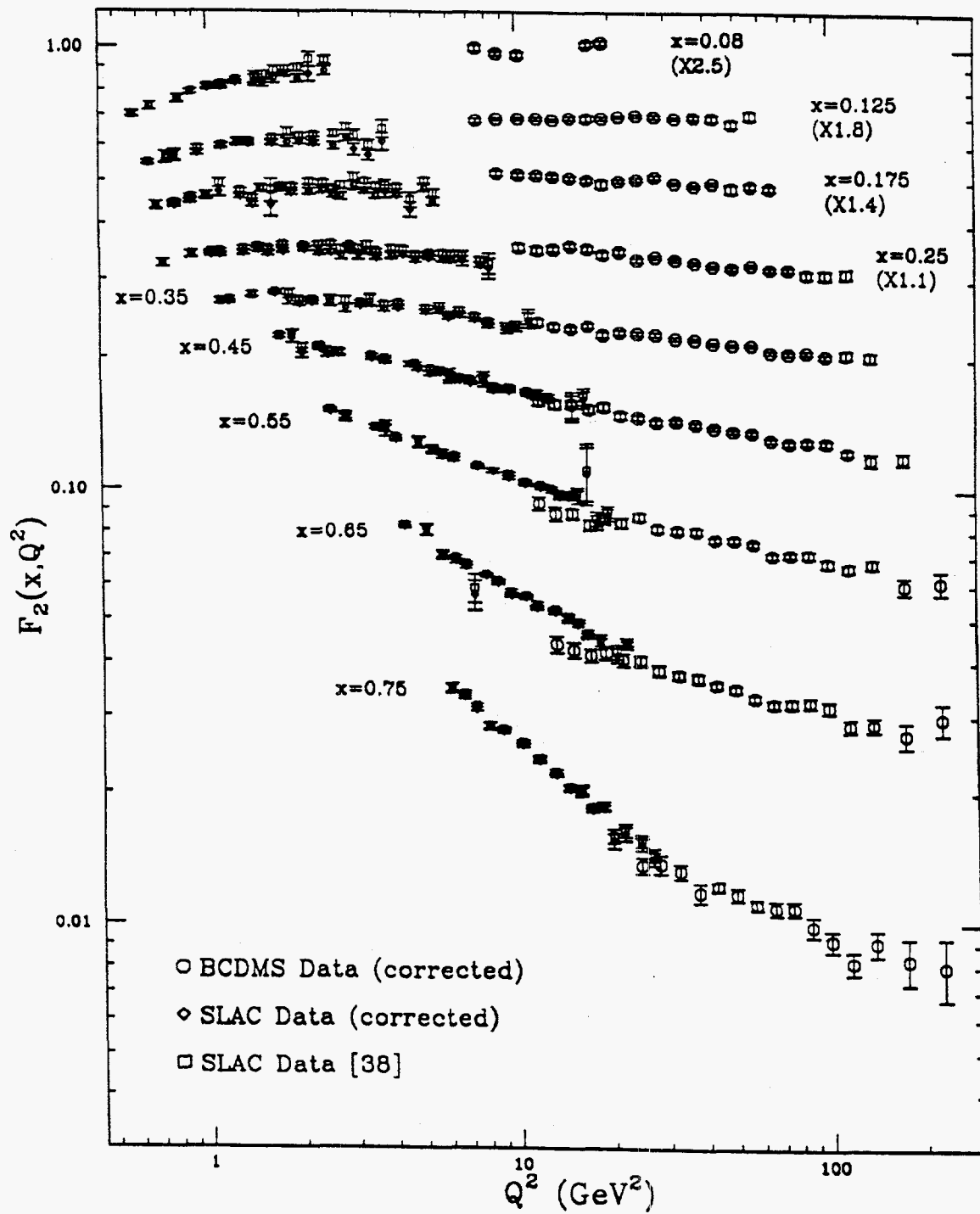


Fig.18 Comparison of the SLAC and BCDMS Data (this analysis)

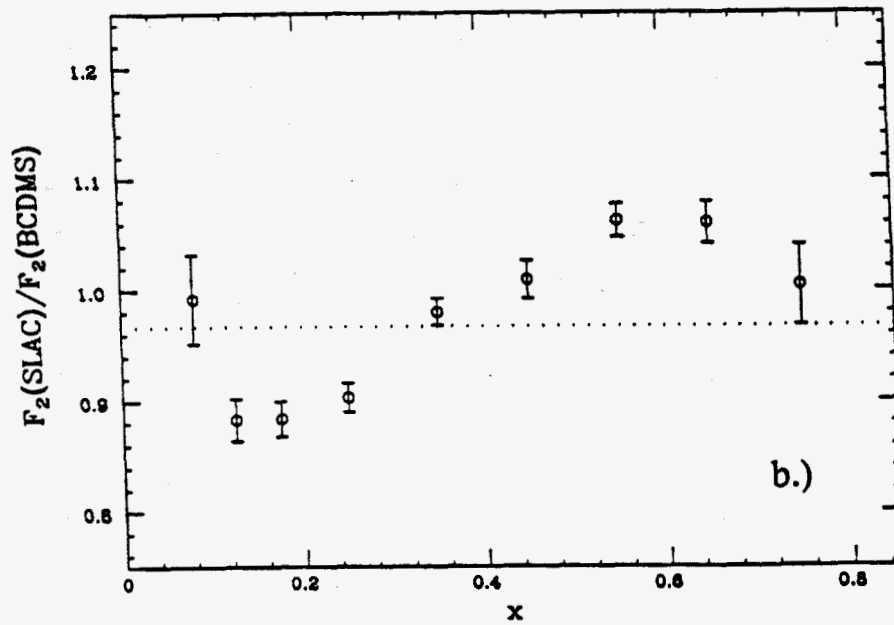
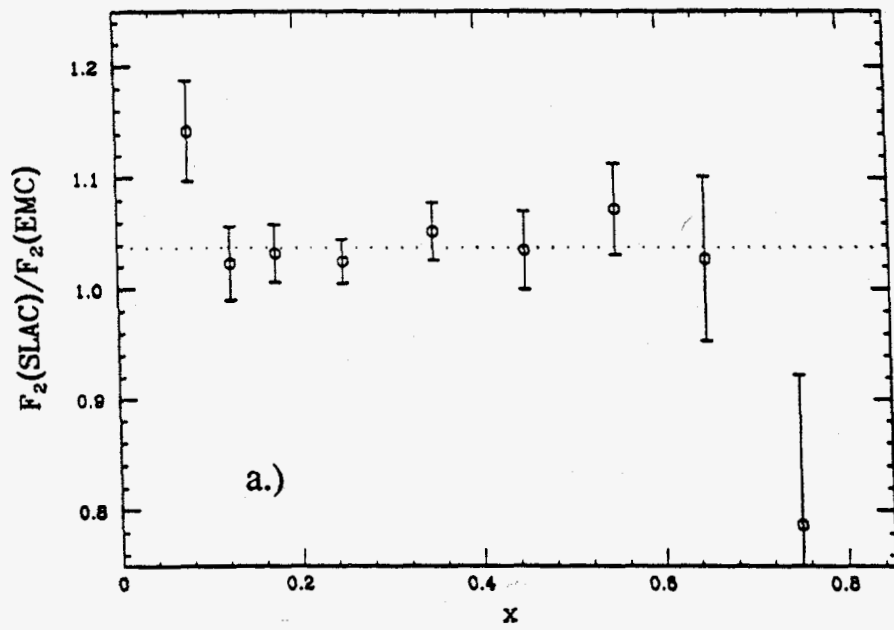


Fig.19 Comparison of the x -dependences of the Ratio of SLAC and :
 a.) EMC Data b.) BCDMS data

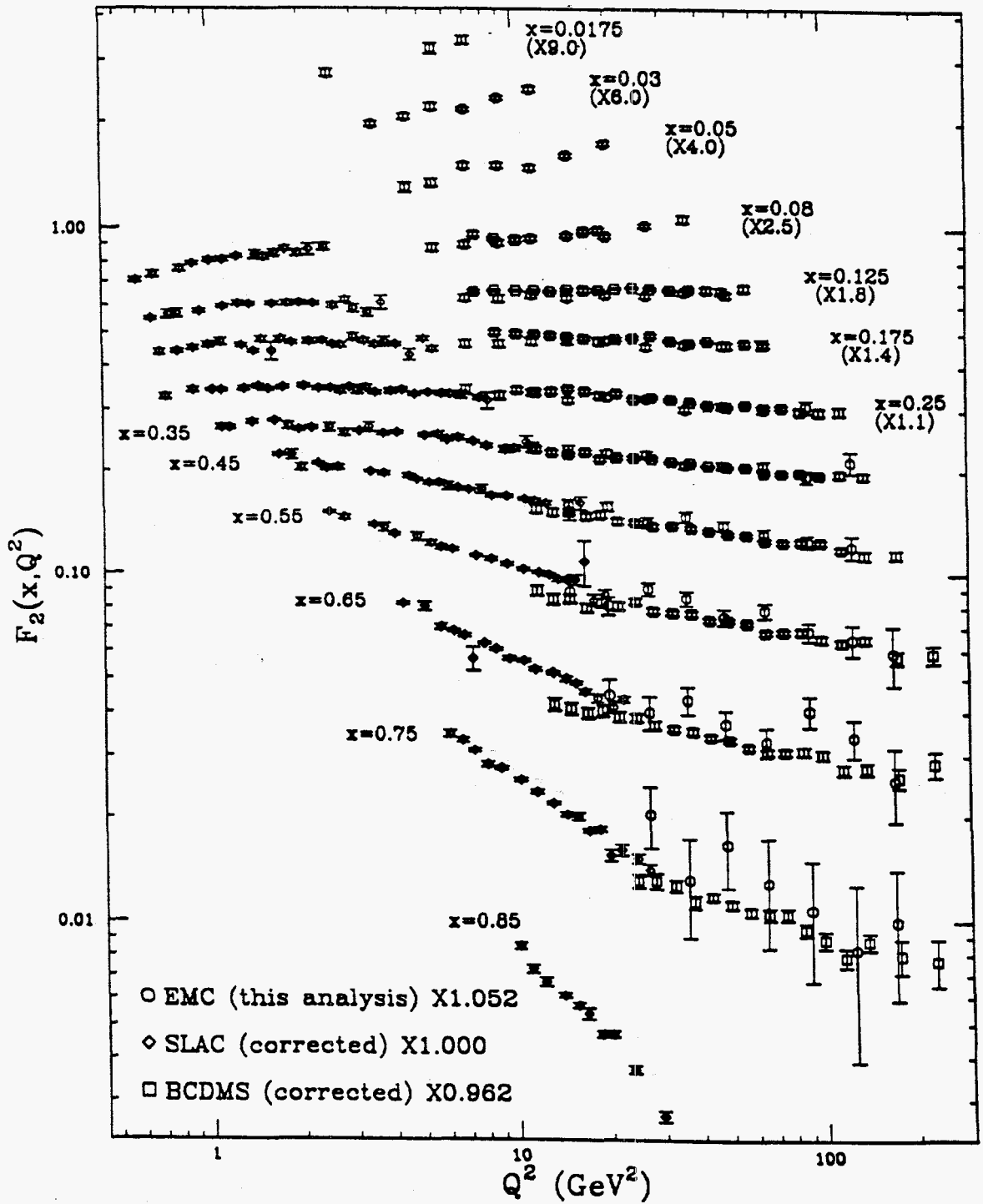


Fig.20 Comparison of the EMC, BCDMS and SLAC data from this analysis

References

- [1] J.J. Aubert et al. (EMC Collaboration), Nucl. Phys. **B259**, 189, (1985).
- [2] A.C. Benvenuti et al.(BCDMS Collaboration), Phys. Lett. **B223** (1989) 485.
- [3] J.J. Aubert et al. (EMC Collaboration), Nucl. Phys. **B293** (1987) 740.
M. Arneodo et al. (EMC Collaboration), Nucl. Phys. **B333** (1990) 1.
M. Arneodo et al. (EMC Collaboration), to be submitted to Nucl. Phys. B, 1991.
- [4] A.C. Benvenuti et al (BCDMS Collaboration), CERN-EP/89-170, (1989).
- [5] C. Lietzke, S.J. Wimpenny, "A Comparison of the RadEMC and Bardin-Shumeiko Radiative Correction Programs", U.C. Riverside Report No. UCR/DIS-89-06 , (1989).
- [6] K. Bazizi, S.J.Wimpenny, "A Study of the Properties of the Ratio $R=\sigma_L/\sigma_T$ ", U.C. Riverside Report No. UCR/DIS-90-04.
- [7] S. Dasu et al.(E139/E140 Collaboration), paper contributed to the International Europhysics Conference on High Energy Physics, Madrid, September 1989, University of Rochester Preprint No. UR-1119, 1989.
- [8] S. Rock, L.W. Whitlow, private communications.



TASK A2:

e^+e^- COLLIDER PHYSICS

AND

NEUTRINO PHYSICS



Task A2

2.1 Program

The physics program of Task A2 has been the systematic study of leptons and hadrons at e^+e^- colliders. The TPC/ 2γ experiment at PEP focussed on e^+e^- annihilation and two-photon processes in the late 70s and early 80s. The OPAL detector at LEP began taking data in 1989 and has now accumulated over 150,000 Z^0 s. Publications by the collaboration cover a broad spectrum of physics: the precision measurement of electroweak parameters, the first determination of the number of light neutrino generations by the method of single photon counting, the measurement of the running coupling constant of the strong interaction by several independent methods, the extension of the mass limit of the Higgs and other new particles, and a number of topics in heavy quark and tau physics. The continued exploitation of the rich physics potential of LEP and LEP200 will form the core of the UCR effort for the coming several years.

Conscious of the fact that the long term future of the field will involve hadron colliders, whether in the U.S. or in Europe, we have begun participating in the RD5 experiment at the CERN SPS to study muon triggering and momentum reconstruction in a strong magnetic field, the results of which will be of great utility in the design of a detector a future collider.

Several members of our group are also participating in an ongoing neutrino oscillation program LSND at Los Alamos which is expected to take data beginning in early 1993.

Personnel

Ph.D. Physicists

| | |
|---------------|--------------------------|
| M. Dittmar | Postgraduate Researcher |
| J.W. Gary | Assistant Professor |
| W. Gorn | Staff Research Associate |
| J.G. Layter | Adjunct Professor |
| K. Riles | Postgraduate Researcher |
| B.C. Shen | Professor |
| G.J. VanDalen | Professor |

Graduate Students

P.P. Altice
E.G. Heflin
J. Letts
W. Strossman

Visiting Scientist

Y.H. Yang

Invited Talks 1990-1991

1990

1. January 5, 1990
American Physical Society, Division of Particle and Fields Meeting – DPF90, Rice University, Houston
“Measurement of the Z^0 Mass and Width”, G. J. VanDalen
2. January 1990
University of California at Riverside, Seminar
“Results of OPAL Measurements of Z^0 Line Shape for Hadronic and Leptonic Decays, Along with Studies of Hadronic Event Properties”, K. Riles
3. January 1990
Stanford Linear Accelerator Center, Colloquium
“Results of OPAL Measurements of Z^0 Line Shape for Hadronic and Leptonic Decays, Along with Studies of Hadronic Event Properties”, K. Riles
4. February 1990
California State University at San Francisco
“First Results on the Z^0 ”, B. C. Shen
5. February 21, 1990
MP Division Colloquium, Los Alamos National Lab, New Mexico
“Measurement of the Z Parameters with OPAL at LEP”, G. J. VanDalen
6. March 1990 OPAL Plenary Week
“Summary of OPAL Physics Results and Future Plans”, K. Riles
7. March 1990
Institute of Physics, Academia Sinica, Taipei, Taiwan
“Recent Results and Future Developments in High Energy Physics”, B. C. Shen
8. March 1990
Physics Department, National Taiwan University, Taipei, Taiwan
“New Results in Particle Physics at Accelerators in the U.S. and Europe”, B. C. Shen
9. March 1990
Department of Physics and Astronomy, National Central University, Chung-Li, Taiwan
“Current Status and Trends in Experimental High Energy Physics”, B. C. Shen
10. March 1990
Department of Physics, National Tsing-Hwa University, Shin-Tsu, Taiwan
“Testing the Standard Model of particle Physics”, B. C. Shen

11. April 1990
Meeting of the ECFA Workshop on ep Collisions at LEP-LHC, DESY
"Supersymmetry Searches at HERA", M. Dittmar
12. May 1990
Second International Conference for Medium and High Energy Physics, Taiwan
"The Future LEP Physics Program; Some Aspects of the Next 10 Years", M. Dittmar
13. May 1990
Second International Conference for Medium and High Energy Physics, Taiwan
"Recent Results from OPAL at LEP", B. C. Shen
14. May 1990
KEK Center for High Energy Physics, Japan
"OPAL Results in 1989 and the Future LEP Program", M. Dittmar
15. May 1990
Institute for Nuclear Physics, Tokyo, Japan
"OPAL Results in 1989 and the Future LEP Program", M. Dittmar
16. May 1990
OPAL Physics Seminar
"Status of Neutrino Counting", J. G. Layter
17. May 24, 1990
Workshop on QED Structure Functions, Ann Arbor, Michigan
"Results of Study of Two-Photon backgrounds to the Neutrino Counting Experiment", K. Riles
18. May 1990
University of California at Los Angeles, Physics Seminar
"Study of the Z^0 at LEP", B. C. Shen
19. June 1, 1990
University of Oregon, Physics Seminar
"Physics at the Z^0 with OPAL at LEP", G. J. VanDalen
20. June 1990
University of Valencia, Spain
"OPAL Results in 1989 and the Future LEP Program", M. Dittmar
21. June 27, 1990
1990 Summer Study on High Energy Physics, Snowmass, Colorado
"Physics with LEP2", B. C. Shen
22. August 11, 1990
25th International Conference on High Energy Physics, Singapore
"Search for New Particles with the OPAL Detector at LEP", K. Riles

23. October, 1990
Physics Department, University of California at Riverside, Seminar
"Hunt for the Higgs with OPAL", B. C. Shen
24. November, 1990
Beyond the Standard Model II, Norman, Oklahoma
"Hunting the Higgs at LEP with OPAL", J. G. Layter
25. December 1, 1990
Southern California Modern Physics Institute, Cal Poly Pomona
"How Many Types of Matter are There? Electron Positron Collisions at the Z^0 Mass", G. J. VanDalen

1991

26. January 21, 1991
California Institute of Technology, High Energy Seminar
"Hunting the Higgs with OPAL at LEP", G. J. VanDalen
27. February 7, 1991
University of California at Riverside, Colloquium
"Low Energy Neutrino Experiments - Doing TeV Physics with MeV Neutrinos", G. J. VanDalen
28. February 25, 1991
Department of Energy, Washington DC
"Determination of Electroweak Parameters at the Z with OPAL", B. C. Shen
29. March 11, 1991
26th Rencontres de Moriond, Les Arc, France
"Tau Physics at LEP - Testing the Tau Lepton Universality", M. Dittmar
30. March 13, 1991
Neutrinos, AstroPhysics and Cosmics Rays Workshop, University of California at San Diego
"The LSND Detector at Los Alamos", G. J. VanDalen
31. April 4, 1991
University of Maryland, College Park, Seminar
"Tau Physics with OPAL at LEP", M. Dittmar
32. April 4, 1991
The 5th Spring School on Particles and Fields, Academia Sinica, Taiwan
"Precision Tests of the Electroweak Theory at the Z", B. C. Shen
33. April 8, 1991
University of California, Riverside, Seminar
"Tau Physics with OPAL at LEP", M. Dittmar

34. April 9, 1991
Dept of Physics and Astronomy, National Central Univ., Taiwan
"Study of Quantum Chromodynamics at the Z", B. C. Shen
35. April 18, 1991
University of Michigan, Ann Arbor
"Recent Results on Tau Decays from the OPAL Detector at LEP", K. Riles
36. April 20, 1991
Fermi National Accelerator Laboratory, Batavia
"Recent Results on Tau Decays from the OPAL Detector at LEP", K. Riles
37. April 24, 1991
Korean Physical Society Meeting, Seoul, Korea
"Search for Close Mass Heavy Leptons with OPAL at LEP", H. Oh

Other Talks 1990 - 1991

1990

1. March 1990
Special Plenary Week OffLine Session
"Proposal for Compressing OPAL Data Sets", K. Riles
2. March 1990
Plenary Week Lepton Physics Session
"Algorithm for Online Extraction of Anomalous Events", K. Riles
3. May 3, 1990
OPAL Heavy Lepton Working Group
"Results of First Close-Mass Lepton Study", K. Riles
4. May 12, 1990
OPAL Hadron Calorimeter Meeting, CERN
"HCAL Off-line, Status and Future", J. G. Layter
5. June 1990
OPAL Collaboration Board Meeting
"A Proposal for the Management of the OPAL VAX Cluster", J. G. Layter
6. July, 1990
OPAL Tau Physics Meeting, CERN
"An Outline of the OPAL Publication on Tau Decays", M. Dittmar
7. July 26, 1990
OPAL Weekly Meeting, CERN
"Search for Lepton Flavour Violation", M. Dittmar
8. September 3, 1990
OPAL Weekly Meeting, CERN
"Lepton Flavour Violation Search with full 89-90 Data", M. Dittmar
9. September 14, 1990
OPAL Plenary Meeting, Cesena, Italy
"Dense Data in 1991", K. Riles
10. September 18, 1990
OPAL Plenary Meeting, Cesena, Italy
"Tau Analysis: Lepton Flavour Violation and Polarization", M. Dittmar
11. October 31, 1990
OPAL ROPE Review Meeting, CERN
"Status of Hadron Calorimeter Event Reconstruction", K. Riles

12. December 13, 1990
OPAL Weekly Meeting, CERN
"Measurement of the Tau Branching Ratios of Tau \rightarrow electron", K. Riles

1991

13. February 5, 1991
OPAL Weekly Meeting, CERN
"A Detailed Investigation of Radiative Lepton Pairs", M. Dittmar
14. March 7, 1991
OPAL Plenary Meeting, CERN
"Status of Tau Polarization and Branching Ratio Analyses", K. Riles
15. March 19, 1991
OPAL Monte Carlo Group Meeting, CERN
"Status of Hadron Calorimeter Monte Carlo Simulation", K. Riles
16. April 19, 1991
Sung-Kyun-Kwan University, Seoul, Korea
"Results from OPAL", H. Oh
17. April 24, 1991
APS Meeting, Washington D.C.
"Measurement of Tau to Muon Decay Parameters with the OPAL Detector at LEP",
B. O'Neill
18. April 24, 1991
APS Meeting, Washington D.C.
"Measurement of $B(\tau \rightarrow \pi\nu)$ and the Tau Polarization with OPAL at LEP", C. Ho
19. April 24, 1991
APS Meeting, Washington D.C.
"A Direct Measurement of the Z Invisible Width by Single Photon Counting", W.
J. Larson
20. April 26, 1991
Korean Physical Society Meeting, Seoul, Korea
"Results from OPAL", H. Oh
21. April 30, 1991
Kyung-Pook National University, Daegu, Korea
"Results from OPAL", H. Oh
22. May 2, 1991
Kang-Leung National University, Kang-Leung, Korea
"Results from OPAL", H. Oh

Publications 1990 - 1991

1990

1. M. Daoudi, W. Langeveld, J. G. Layter, W. T. Lin, B. C. Shen, *et al.* (TPC/Two-Gamma Collaboration), "Investigation of the Electromagnetic Structure of η and η' Mesons by Two-Photon Interactions", *Phys. Rev. Lett.* **64** (1990) 172-175.
2. M. Daoudi, W. Langeveld, J. G. Layter, W. T. Lin, B. C. Shen, *et al.* (TPC/Two-Gamma Collaboration), "Inclusive $D^{*\pm}$ Production in Photon-Photon Collisions", *Phys. Lett.* **B252** (1990) 499-504.
3. M. Daoudi, W. Langeveld, J. G. Layter, W. T. Lin, B. C. Shen, G. J. VanDalen, *et al.* (TPC/Two-Gamma Collaboration), "A Measurement of the Total Hadronic Cross Section in Tagged $\gamma\gamma$ Reactions", *Phys. Rev.* **D41** (1990) 2667-2674.
4. M. Daoudi, J. Layter, J. K. Riles, and B. Shen, "Study of All Neutral Final State of $f_2(1270)$ Produced in Two-Photon Collision as a Background to Radiative Neutrino Counting on the Z^0 Resonance", Proceedings of the Workshop on QED Structure Functions, Ann Arbor, Michigan, May 22-25, **AIP-201** (1989).
5. M. Dittmar, W. Gorn, E. Heflin, C. Ho, W. J. Larson, J. G. Layter, J. Ma, B. P. O'Neill, H. Oh, K. Riles, B. C. Shen, G. J. VanDalen, Y. Yang *et al.* (OPAL Collaboration), "Measurement of the Decay of the Z^0 into Lepton Pairs", *Phys. Lett.* **B235** (1990) 379-388.
6. M. Dittmar, W. Gorn, E. Heflin, C. Ho, W. J. Larson, J. G. Layter, J. Ma, B. P. O'Neill, H. Oh, K. Riles, B. C. Shen, G. J. VanDalen, Y. Yang *et al.* (OPAL Collaboration), "A Study of Jet Production Rates and a Test of QCD on the Z^0 Resonance", *Phys. Lett.* **B235** (1990) 389-398.
7. M. Dittmar, W. Gorn, E. Heflin, C. Ho, W. J. Larson, J. G. Layter, J. Ma, B. P. O'Neill, H. Oh, K. Riles, B. C. Shen, G. J. VanDalen, Y. Yang *et al.* (OPAL Collaboration), "A Search for the Top and b' Quarks in Hadronic Z^0 Decays", *Phys. Lett.* **B236** (1990) 364-374.
8. M. Dittmar, W. Gorn, E. Heflin, C. Ho, W. J. Larson, J. G. Layter, J. Ma, B. P. O'Neill, H. Oh, K. Riles, B. C. Shen, G. J. VanDalen, Y. Yang *et al.* (OPAL Collaboration), "Mass Limits for a Standard Model Higgs Boson in e^+e^- Collisions at LEP", *Phys. Lett.* **B236** (1990) 224-232.
9. M. Dittmar, W. Gorn, E. Heflin, C. Ho, W. J. Larson, J. G. Layter, J. Ma, B. P. O'Neill, H. Oh, K. Riles, B. C. Shen, G. J. VanDalen, Y. Yang *et al.* (OPAL Collaboration), "A Search for Acoplanar Pairs of Leptons or Jets in Z^0 Decays; Mass Limits on Supersymmetric Particles", *Phys. Lett.* **B240** (1990) 261-270.
10. M. Dittmar, W. Gorn, E. Heflin, C. Ho, W. J. Larson, J. G. Layter, J. Ma, B. P. O'Neill, H. Oh, K. Riles, B. C. Shen, G. J. VanDalen, Y. Yang *et al.* (OPAL Collaboration), "A Direct Search for New Heavy Charged Leptons at LEP", *Phys. Lett.* **B240** (1990) 250-260.

11. M.Dittmar, W.Gorn, E.Heflin, C.Ho, W.J.Larson, J.G.Layter, J.Ma, B.P.O'Neill, H.Oh, K.Riles, B.C.Shen, G.J.VanDalen, Y.Yang *et al.* (OPAL Collaboration), "A Combined Analysis of the Hadronic and Leptonic Decays of the Z^0 ", Phys. Lett. **B240** (1990) 497-512.
12. M.Dittmar, W.Gorn, E.Heflin, C.Ho, W.J.Larson, J.G.Layter, J.Ma, B.P.O'Neill, H.Oh, K.Riles, B.C.Shen, G.J.VanDalen, Y.Yang *et al.* (OPAL Collaboration), "A Study of the Reaction $e^+e^- \rightarrow \gamma\gamma$ at LEP", Phys. Lett. **B241** (1990) 133-140.
13. M.Dittmar, W.Gorn, E.Heflin, C.Ho, W.J.Larson, J.G.Layter, J.Ma, B.P.O'Neill, H.Oh, K.Riles, B.C.Shen, G.J.VanDalen, Y.Yang *et al.* (OPAL Collaboration), "A Search for Technipions and Charged Higgs Bosons at LEP", Phys. Lett. **B242** (1990) 299-308.
14. M.Dittmar, W.Gorn, E.Heflin, C.Ho, W.J.Larson, J.G.Layter, J.Ma, B.P.O'Neill, H.Oh, K.Riles, B.C.Shen, G.J.VanDalen, Y.Yang *et al.* (OPAL Collaboration), "A Measurement of Global Event Shape Distributions in the Hadronic Decays of the Z^0 ", Zeitschrift f. Physik. **C47** (1990) 505-521.
15. M.Dittmar, W.Gorn, E.Heflin, C.Ho, W.J.Larson, J.G.Layter, J.Ma, B.P.O'Neill, H.Oh, K.Riles, B.C.Shen, G.J.VanDalen, Y.Yang *et al.* (OPAL Collaboration), "Search for Excited Leptons at LEP", Phys. Lett. **B244** (1990) 135-142.
16. M.Dittmar, W.Gorn, E.Heflin, C.Ho, W.J.Larson, J.G.Layter, J.Ma, B.P.O'Neill, H.Oh, K.Riles, B.C.Shen, G.J.VanDalen, Y.Yang *et al.* (OPAL Collaboration), "Evidence for Final State Photons in Multihadronic Decays of the Z^0 ", Phys. Lett. **B246** (1990) 285-296.
17. M.Dittmar, W.Gorn, E.Heflin, C.Ho, W.J.Larson, J.G.Layter, J.Ma, B.P.O'Neill, H.Oh, K.Riles, B.C.Shen, G.J.VanDalen, Y.Yang *et al.* (OPAL Collaboration), "Limits on Neutral Heavy Lepton Production from Z^0 Decay", Phys. Lett. **B247** (1990) 448-457.
18. M.Dittmar, W.Gorn, E.Heflin, C.Ho, W.J.Larson, J.G.Layter, J.Ma, B.P.O'Neill, H.Oh, K.Riles, B.C.Shen, G.J.VanDalen, Y.Yang *et al.* (OPAL Collaboration), "Analysis of the Z^0 Couplings to Charged Leptons", Phys. Lett. **B247** (1990) 458-472.
19. M.Dittmar, W.Gorn, E.Heflin, C.Ho, W.J.Larson, J.G.Layter, J.Ma, B.P.O'Neill, H.Oh, K.Riles, B.C.Shen, G.J.VanDalen, Y.Yang *et al.* (OPAL Collaboration), "A Study of Coherence of Soft Gluons in Hadron Jets", Phys. Lett. **B247** (1990) 617-628.
20. M.Dittmar, W.Gorn, E.Heflin, C.Ho, W.J.Larson, J.G.Layter, J.Ma, B.P.O'Neill, H.Oh, K.Riles, B.C.Shen, G.J.VanDalen, Y.Yang *et al.* (OPAL Collaboration), "A Direct Search for Neutralino Production at LEP", Phys. Lett. **B248** (1990) 211-219.

21. M.Dittmar, W.Gorn, E.Heflin, C.Ho, W.J.Larson, J.G.Layter, J.Ma, B.P.O'Neill, H.Oh, K.Riles, B.C.Shen, G.J.VanDalen, Y.Yang *et al.* (OPAL Collaboration), "Limits on a Light Higgs Boson in e^+e^- Collisions at LEP", Phys. Lett. **B251** (1990) 211-222.
22. M.Dittmar, W.Gorn, E.Heflin, C.Ho, W.J.Larson, J.G.Layter, J.Ma, B.P.O'Neill, H.Oh, K.Riles, B.C.Shen, G.J.VanDalen, Y.Yang *et al.* (OPAL Collaboration), "A Measurement of Energy Correlations and a Determination of $\alpha_s(M_{Z^0})$ in e^+e^- Anihilations at $\sqrt{s}=91$ GeV", Phys. Lett. **B252** (1990) 159-169.
23. M.Dittmar, W.Gorn, E.Heflin, C.Ho, W.J.Larson, J.G.Layter, J.Ma, B.P.O'Neill, H.Oh, K.Riles, B.C.Shen, G.J.VanDalen, Y.Yang *et al.* (OPAL Collaboration), "Search for Pair Produced Stable Singly-Charged Heavy Particles in Z^0 Decays", Phys. Lett. **B252** (1990) 290-300.
24. M. Dittmar, A. Santamaria, M.C. Gonzales-Garcia and J.W.F. Valle, "Production Mechanisms and Signatures of Isosinglet Neutral Heavy Leptons in Z^0 Decays", Nucl. Phys. **B332** (1990) 1-19.
25. G. J. VanDalen, " Z^0 Mass and Width and the Number of Neutrinos", Proceedings of the DPF90, Rice University, Houston, edited by Billy Bonner and Hannu Miettinen, World Scientific, Singapore (1990) 376-380.
26. L. Auerbach (Temple U.), S. Clearwater, T. Dombeck, T.J. Bowles, H.S. Matis (Los Alamos), W. Gorn (UC, Riverside), B. Dieterle, J. Kang, C. Leavitt (New Mexico U.), D. Koetke (Valparaiso U., Catolica), "The Response of an Aluminum Scintillator Calorimeter to Electrons near the Critical Energy from 50-MeV to 150-MeV and Comparisons with the EGS4 Program Predictions.", Nucl. Instrum. Methods **A287** (1990) 378-388.
27. K. Riles, A. Weir, *et al.*, "Upper Limits on D^\pm and B^\pm Decays to Two Leptons Plus π^\pm or K^\pm ", Phys. Rev. **D41** (1990) 1384.
28. K. Riles, *et al.*, "Search for a Nearly Degenerate Lepton Doublet (L^-, L^0)", Phys. Rev. **D42** (1990) 1-9.
29. K. Riles, S. R. Wagner, *et al.*, "Measurement of the B^0 Meson Lifetime", Phys. Rev. Lett. **64** (1990) 1095.
30. K. Riles, J. F. Kral, *et al.*, "Measurement of the $b\bar{b}$ Fraction in Hadronic Z Decays", Phys. Rev. Lett. **64** (1990) 1211.
31. K. Riles, C. K. Jung, *et al.*, "Search for Long Lived Massive Neutrinos in Z Decays", Phys. Rev. Lett. **64** (1990) 1091.
32. K. Riles, S. Komamiya, *et al.*, "Determination of α_s Using a Differential Jet Multiplicity Distribution at SLC and PEP", Phys. Rev. Lett. **64** (1990) 987.

33. K. Riles, D. Y. Wu, *et al.*, "Radiative Tau Production and Decay", Phys. Rev. **D41** (1990) 2339.
34. K. Riles, G. S. Abrams, *et al.*, "Measurements of Charged Particle Inclusive Distributions in Hadronic Decays of the Z Boson", Phys. Rev. Lett. **64** (1990) 1334.
35. K. Riles, A. Weir, *et al.*, "Reanalysis of $B^0 - \bar{B}^0$ Mixing in e^+e^- Annihilation at 29 GeV", Phys. Lett. **B240** (1990) 289.
36. K. Riles, M. L. Swartz, *et al.*, "A Search for Doubly Charged Higgs Scalars in Z Decay", Phys. Rev. Lett. **64** (1990) 2877-2880.
37. K. Riles, A. P. Burchat, *et al.*, "A Search for Decays of the Z to Unstable Neutral Leptons with Mass Between 2.5 GeV and 22 GeV", Phys. Rev. **D41** (1990) 3542.
38. K. Riles, S. Komamiya, *et al.*, "A Search for Nonminimal Higgs Bosons from Z Boson Decay", Phys. Rev. Lett. **64** (1990) 2881-2884.
39. K. Riles, T. Barklow, *et al.*, "Searches for Supersymmetric Particles Produced in Z Boson Decay", Phys. Rev. Lett. **64** (1990) 2984-2987.
40. K. Riles, M. Petradza, *et al.*, "Study of Four Lepton Final States in e^+e^- Interactions at $\sqrt{s} = 29$ GeV", Phys. Rev. **D42** (1990) 2171-2179.
41. K. Riles, E. Soderstrom, *et al.*, "A Search for Pair Production for Heavy Stable Charged Particles in Z Decays", Phys. Rev. Lett. **D64** (1990) 2980-2983.
42. K. Riles, J. Boyer, *et al.*, "Two Photon Production of Pion Pairs", Phys. Rev. **D42** (1990) 1350-1367.
43. K. Riles, F. Butler, *et al.*, "Measurement of the Two Photon Width of the $\eta'(958)$ ", Phys. Rev. **D42** (1990) 1368-1384.

1991

44. M. Daoudi, W. Langeveld, J. G. Layter, W. T. Lin, B. C. Shen, G. J. VanDalen, *et al.* (TPC/Two-Gamma Collaboration), "Test of Spin Dependence in Charm-quark Fragmentation to D^* ", Phys. Rev. **D43** (1991) 29-33.
45. M. Dittmar, W. Gorn, E. Heflin, C. Ho, W. J. Larson, J. G. Layter, J. Ma, B. P. O'Neill, H. Oh, K. Riles, B. C. Shen, G. J. VanDalen, Y. Yang *et al.* (OPAL Collaboration), "A Study of Angular Correlations in 4-jet Final States of Hadronic Z^0 Decays", Zeitschrift f. Physik. **C49** (1991) 49-57.
46. M. Dittmar, W. Gorn, E. Heflin, C. Ho, W. J. Larson, J. G. Layter, J. Ma, B. P. O'Neill, H. Oh, K. Riles, B. C. Shen, G. J. VanDalen, Y. Yang *et al.* (OPAL Collaboration), "Searches for Neutral Higgs Bosons in e^+e^- Collisions at LEP", Zeitschrift f. Physik. **C49** (1991) 1-15.

47. M.Dittmar, W.Gorn, E.Heflin, C.Ho, W.J.Larson, J.G.Layter, J.Ma, B.P.O'Neill, H.Oh, K.Riles, B.C.Shen, G.J.VanDalen, Y.Yang *et al.* (OPAL Collaboration), "A Study of the Recombination Scheme Dependence of Jet Production Rates and of $\alpha_s(M_{Z_0})$ in Hadronic Z^0 Decays", *Zeitschrift f. Physik.* **C49** (1991) 375-384.
48. M.Dittmar, W.Gorn, E.Heflin, C.Ho, W.J.Larson, J.G.Layter, J.Ma, B.P.O'Neill, H.Oh, K.Riles, B.C.Shen, G.J.VanDalen, Y.Yang *et al.* (OPAL Collaboration), "Search for the Minimal Standard Model Higgs Boson in e^+e^- Collisions at LEP", *Phys. Lett.* **B253** (1991) 511-523.
49. M.Dittmar, W.Gorn, E.Heflin, C.Ho, W.J.Larson, J.G.Layter, J.Ma, B.P.O'Neill, H.Oh, K.Riles, B.C.Shen, G.J.VanDalen, Y.Yang *et al.* (OPAL Collaboration), "A Search for Lepton Flavour Violation in Z^0 Decays", *Phys. Lett.* **B254** (1991) 293-302.
50. M.Dittmar, W.Gorn, E.Heflin, C.Ho, W.J.Larson, J.G.Layter, J.Ma, B.P.O'Neill, H.Oh, K.Riles, B.C.Shen, G.J.VanDalen, Y.Yang *et al.* (OPAL Collaboration), "Measurement of the Cross Sections of the Reactions $e^+e^- \rightarrow \gamma\gamma$ and $e^+e^- \rightarrow \gamma\gamma\gamma$ at LEP", *Phys. Lett.* **B257** (1991) 531-540.
51. M.Dittmar, W.Gorn, E.Heflin, C.Ho, W.J.Larson, J.G.Layter, J.Ma, B.P.O'Neill, H.Oh, K.Riles, B.C.Shen, G.J.VanDalen, Y.Yang *et al.* (OPAL Collaboration), "A Model Independent Observation of the String Effect using Quark Tagging at LEP", *Phys. Lett.* **B261** (1991) 334-346.
52. M.Dittmar, W.Gorn, E.Heflin, C.Ho, W.J.Larson, J.G.Layter, J.Ma, B.P.O'Neill, H.Oh, K.Riles, B.C.Shen, G.J.VanDalen, Y.Yang *et al.* (OPAL Collaboration), "A Intermittency in Hadronic Decays of the Z^0 ", *Phys. Lett.* **B262** (1991) 351-361.
53. M.Dittmar, W.Gorn, E.Heflin, C.Ho, W.J.Larson, J.G.Layter, J.Ma, B.P.O'Neill, H.Oh, K.Riles, B.C.Shen, G.J.VanDalen, Y.Yang *et al.* (OPAL Collaboration), "A Study of Heavy Flavour Production using Muons in Hadronic Z^0 Decays", *Phys. Lett.* **B263** (1991) - .
54. M.Dittmar, W.Gorn, E.Heflin, C.Ho, W.J.Larson, J.G.Layter, J.Ma, B.P.O'Neill, H.Oh, K.Riles, B.C.Shen, G.J.VanDalen, Y.Yang *et al.* (OPAL Collaboration), "A Search for Scalar Leptoquarks in Z^0 Decays", *Phys. Lett.* **B263** (1991) - .
55. M.Dittmar, W.Gorn, E.Heflin, C.Ho, W.J.Larson, J.G.Layter, J.Ma, B.P.O'Neill, H.Oh, K.Riles, B.C.Shen, G.J.VanDalen, Y.Yang *et al.* (OPAL Collaboration), "A Study of $D^{*\pm}$ Production in Z^0 Decays", *Phys. Lett.* **B262** (1991) 341-350.
56. S.-Y. Chu and B. C. Shen, "Can the Color Force be Used to Achieve Fusion?", *Mod. Phys. Lett.* **A6** (1991) 237-244.
57. M. Dittmar and 41 member working group, "Physics Possibilities", Report of the Working Group on High Luminosity at LEP, CERN 91-02 (1991) 69.

58. F. Boudjema, R. Casalbuoni, P. Chiappetta, D. Cocolicchio, M. Dittmar, F. Feruglio, B. Gavela (convener), "Higgs and New Physics", Report of the Working Group on High Luminosity at LEP, CERN 91-02 (1991) 88.
59. M. Dittmar and J.W.F. Valle, "Heavy Singlet Neutral Leptons, Flavour and CP Violation on the Z Peak", Report of the Working Group on High Luminosity at LEP, CERN 91-02 (1991) .
60. D. Cocolicchio and M. Dittmar, "The Radiative and Hadronic Flavour-Changing Decays of the Z", Report of the Working Group on High Luminosity at LEP, CERN 91-02 (1991) .
61. B. Shen, "Recent Results from OPAL at LEP", in Progress in High Energy Physics, Eds. W.-Y. P. Hwang *et al.*, North Holland (1990) 22-45.
62. M. Dittmar, "The Future LEP Physics Program; Some Aspects of the Next Ten years", in Progress in High Energy Physics, Eds. W.-Y. P. Hwang *et al.*, North Holland (1990) 89-105.
63. K. Riles, J.J. Gomez Cadenas, *et al.*, "A Search for Elastic NonDiagonal Lepton Pair Production in e^+e^- Annihilation at $\sqrt{s} = 29$ GeV", Phys. Rev. Lett. **66** (1991) 1007-1010.

Publications Submitted

1. M.Dittmar, W.Gorn, E.Heflin, C.Ho, W.J.Larson, J.G.Layter, J.Ma, B.P.O'Neill, H.Oh, K.Riles, B.C.Shen, G.J.VanDalen, Y.Yang *et al.* (OPAL Collaboration), "The OPAL Detector at LEP", CERN-EP/90-100 (14 August 1990), submitted to Nucl. Instr. and Meth.
2. M.Dittmar, W.Gorn, E.Heflin, C.Ho, W.J.Larson, J.G.Layter, J.Ma, B.P.O'Neill, H.Oh, K.Riles, B.C.Shen, G.J.VanDalen, Y.Yang *et al.* (OPAL Collaboration), "A Direct Measurement of the Z^0 Invisible Width by Single Photon Counting", CERN-PPE/90-187 (14 December 1990), submitted to Zeitschrift f. Physik.
3. M.Dittmar, W.Gorn, E.Heflin, C.Ho, W.J.Larson, J.G.Layter, J.Ma, B.P.O'Neill, H.Oh, K.Riles, B.C.Shen, G.J.VanDalen, Y.Yang *et al.* (OPAL Collaboration), "Measurement of the Z^0 Line Shape Parameters and the Electroweak Couplings of Charged Leptons", CERN-PPE/91-67 (16 April 1991), submitted to Zeitschrift f. Physik.
4. M.Dittmar, W.Gorn, E.Heflin, C.Ho, W.J.Larson, J.G.Layter, J.Ma, B.P.O'Neill, H.Oh, K.Riles, B.C.Shen, G.J.VanDalen, Y.Yang *et al.* (OPAL Collaboration), "A Measurement of the Electroweak Couplings of Up and Down Type Quarks Using Final State Photons in Hadronic Z^0 Decays", CERN-PPE/91-81 (24 May 1991), submitted to Phys. Lett. B.

5. M.Dittmar, W.Gorn, E.Heflin, C.Ho, W.J.Larson, J.G.Layter, J.Ma, B.P.O'Neill, H.Oh, K.Riles, B.C.Shen, G.J.VanDalen, Y.Yang *et al.* (OPAL Collaboration), "A Study of K_s^0 Production in Z^0 Decays", CERN-PPE/91-86 (28 May 1991), submitted to Phys. Lett. B.
6. M.Dittmar, W.Gorn, E.Heflin, C.Ho, W.J.Larson, J.G.Layter, J.Ma, B.P.O'Neill, H.Oh, K.Riles, B.C.Shen, G.J.VanDalen, Y.Yang *et al.* (OPAL Collaboration), "A Direct Observation of Quark-Gluon Jet Differences at LEP", CERN-PPE/91-91 (11 June 1991), submitted to Phys. Lett. B.
7. M.Dittmar, W.Gorn, E.Heflin, C.Ho, W.J.Larson, J.G.Layter, J.Ma, B.P.O'Neill, H.Oh, K.Riles, B.C.Shen, G.J.VanDalen, Y.Yang *et al.* (OPAL Collaboration), "Observation of J/ψ Production in Multihadronic Z^0 Decays", CERN-PPE/91-92 (12 June 1991), submitted to Phys. Lett. B.
8. M.Dittmar, W.Gorn, E.Heflin, C.Ho, W.J.Larson, J.G.Layter, J.Ma, B.P.O'Neill, H.Oh, K.Riles, B.C.Shen, G.J.VanDalen, Y.Yang *et al.* (OPAL Collaboration), "Measurement of the Three-Jet Distributions Sensitive to the Gluon Spin in e^+e^- Annihilations at $\sqrt{s} = 91$ GeV", CERN-PPE/91-97 (18 June 1991), submitted to Zeitschrift f. Physik.
9. M.Dittmar, W.Gorn, E.Heflin, C.Ho, W.J.Larson, J.G.Layter, J.Ma, B.P.O'Neill, H.Oh, K.Riles, B.C.Shen, G.J.VanDalen, Y.Yang *et al.* (OPAL Collaboration), "Measurement of Branching Ratios and τ Polarization from $\tau \rightarrow e\nu\bar{\nu}$, $\tau \rightarrow \mu\nu\bar{\nu}$, and $\tau \rightarrow \pi(K)\nu$ Decays at LEP", CERN-PPE/91-103 (25 June 1991), submitted to Phys. Lett. B.
10. M. Dittmar, M. Arignon *et al.*, "The Trigger System of the OPAL Experiment at LEP", CERN/PPE-91-32 (20 February 1991), submitted to Nucl. Instr. and Meth.
11. M. Dittmar, "Testing the Tau Lepton", to appear in the Proceedings of the 26th Rencontres de Moriond, Electroweak and Unified Theories, Les Arcs, France, 10-17 March 1991.
12. K. Riles, "Searches for New Particles with the OPAL Detector at LEP", to appear in the Proceedings of the 1990 International Conference on High Energy Physics, Singapore, August 2-8, 1991.
13. J. Layter, "Hunting the Higgs Boson at LEP with OPAL", to appear in the Proceedings of Beyond the Standard Model II, Oklahoma, November 1990.
14. B. Shen, P.C. Rowson, E. Blucher, P. Rankin, " e^+e^- Physics in the 1990s: Electroweak Measurables and Radiative Corrections", 1990 DPF Summer Study on High Energy Physics: Research Directions for the Decade, Snowmass, Colorado, June 25 - July 13, 1990.

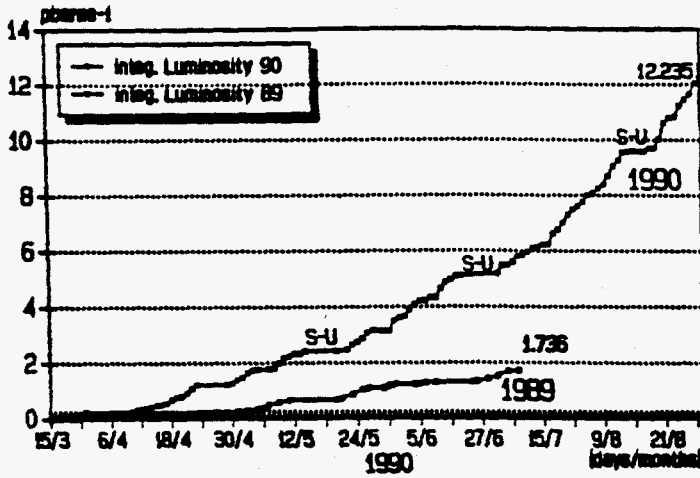
2.2 TPC/2 γ at PEP

The UCR group has participated actively in the TPC/2 γ experiment at PEP since the inception of the program. A large number of papers have been published on the study of leptons and quarks based on data taken between 1983 and 1987. A total of five students have completed their Ph.D. research on the TPC/2 γ experiment. Willis Lin and Mourad Daoudi, who received their Ph.D.'s in the Spring and Fall of 1990, are the most recent.

With the planned high luminosity running at PEP, the TPC/2 γ Collaboration expected to accumulate 1-2 fb⁻¹ of data over a period of 2-3 years and to produce unique and precise physics results. Although our group had not committed to any hardware upgrade efforts for the high luminosity operation of TPC/2 γ we agreed to contribute to the running and the physics analysis. It is extremely valuable to have large quantities of data for graduate students to carry out their research, particularly when a large fraction of the resources of the high energy physics community is devoted to detector developments for future accelerators.

Unfortunately, our hope for high luminosity running of PEP came to an end on Nov. 1, 1991 when Burton Richter announced that PEP would not be operated at SLAC for at least one year. The TPC/2 γ Collaboration decided subsequently to discontinue the operation of the detector. Nevertheless, the data accumulated so far would be still quite valuable for a number of physics topics and would be available for the groups involved in the experiment. We intend to continue our physics analysis efforts on a few specific topics, such as Bose-Einstein correlations and intermittency in annihilation hadronic processes, and resonance and hadron production in two-photon processes. These analyses will be carried out by Layter and Shen together with our recent graduates Lin and Daoudi. Only a modest amount of support is needed for computing, communication and travel for this work.

LEP OPERATIONS 1990
INTEGRATED LUMINOSITY 1990 CF 1989



LEP OPERATIONS
Z⁰ ENERGY SCAN 1989 cf 1990

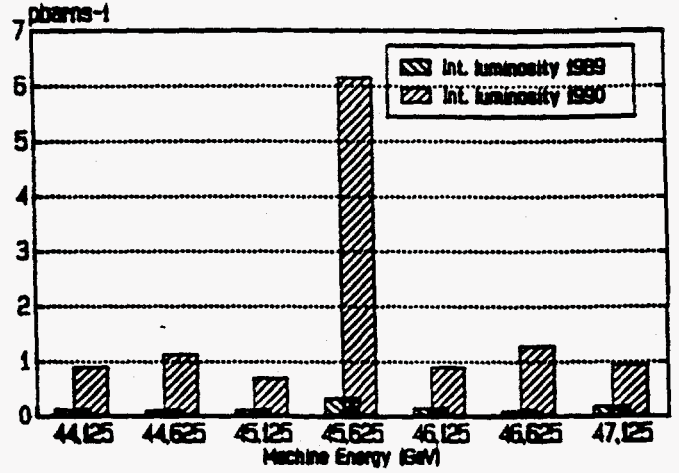


Figure 2.1: Left Theoretical integrated luminosity versus time for LEP. Right Integrated luminosity at each scan point.

2.3 OPAL at LEP

2.3.1 LEP Performance

Although in 1990 LEP did not produce the million Z^0 s that had been expected, its performance was nonetheless commendable. An integrated luminosity of 12.235 pb^{-1} was achieved, compared with 1.736 in 1989. This was the "theoretical luminosity," based on measured beam intensity. The actual luminosity delivered to OPAL was around 9.0 pb^{-1} , half on the Z^0 peak and the rest at 1 GeV increments above and below. This resulted in 144,000 multihadron events. These statistics are summarized in Figure 2.1.

Luminosity

One can rewrite the standard luminosity formula, involving the product of the electron and positron beam intensities divided by the product of the transverse cross sections of the beams, in a form that emphasizes the factors which must be manipulated to reach the goal of $10^6 Z^0$ s:

$$L = \frac{\gamma f_{rev} k_b N_b \xi_y}{2r_e \beta_{y*}} \mathcal{F},$$

where ξ_y is the "vertical beam-beam strength" parameter, N_b is the number of particles in the bunch, assumed the same for e^- and e^+ , β_{y*} is the betatron amplitude function, and \mathcal{F} is the ratio of average to peak luminosity. The prospect for increasing the number of bunches k_b will be discussed later.

The following table compares the values achieved with the design values for these and other critical parameters. [1]

| Parameter | Achieved | Design |
|--|----------|--------|
| Current per bunch (mA) | 0.780 | 0.750 |
| Total current per beam (mA) | 2.98 | 3.00 |
| Total current in both beams (mA) | 4.7 | 6.0 |
| Vertical beam-beam strength | 0.016 | 0.040 |
| Horizontal beam-beam strength | 0.035 | 0.040 |
| Emittance ratio | < 0.040 | 0.040 |
| Betatron amplitude function at IP (cm) | 3.7 | 7.0 |
| Luminosity ($\times 10^{30}$) | 7 | 16 |

The vertical beam-beam strength parameter is considerably off from its design value as a result of operation of the machine at transverse tune values Q_h and Q_v which are not optimized for production of beam-beam effects. This choice of tune values is necessitate by the presence of skew quadrupole fields arising from the "nickel layer," the magnetic flashing deposited on the beam pipe during the fabrication stage. Efforts to neutralize the skew fields have not eliminated the problem, and the search for a better set of tune values continues.

The bunch intensity should be limited by the Transverse Mode Coupling Instability to the value of 0.85 mA given in the table. The fact that this value has not been reached is thought to be due to vertical beam blowup caused by an uncompensated coupling between synchrotron motion and vertical betatron oscillation, which should in principle be zero. This coupling seems to be caused by the presence of dispersion at the RF cavities which converts the large energy gain of acceleration into increased betatron oscillation. Although the RF regions were designed to be dispersion-free, there is apparently a residual dispersion of from three to eight times what was expected, and the cause is not yet fully understood. The first step in correcting this situation is to obtain better measurements of the dispersion itself.

The betatron amplitude function β^* is the one factor that already exceeds design specifications. The value of 3.7 cm has been achieved in Machine Development sessions, and an attempt is being made to find an optics which permits dependable running at 4.0 for physics runs. Greater efficiency in the β^* "squeezing" step is also being sought. One problem of a "jump" in the value of β^* at the end of ramping was traced to the frequency response of the power supplies for the superconducting low- β quadrupoles and has now been cured.

The average to peak luminosity ratio is given by

$$\mathcal{F} = \eta \frac{1 - \exp^{-t_{phys}/\tau}}{t_{phys}/\tau}.$$

For large values of τ , which is the actual case, \mathcal{F} reduces to η , the "availability" for physics, which is just $\eta = t_{phys}/(t_{phys} + t_{reload})$. Since the uptime for physics t_{phys} is on the order of 12 hours, η will be large if the time for reloading of the beam is small. Unfortunately t_{reload} in 1990 was also on the order of 12 hours, so η was about 0.5. Currently operations personnel are fighting to get the reloading time down to something like 4 hours. It must be borne in mind that the reloading operation involves five accelerating components: LIL,

EPA, PS, SPS, and LEP itself, so a reduction in reloading time demands high efficiency from all the accelerators.

Energy Calibration

During the past year, a "Working Group on LEP Energy" was set up to involve experimenters in the task of determining the LEP energy calibration, inasmuch as the energy formed an integral part of many of the physics results that were presented. This group has refined the techniques that were described in detail in last year's proposal, namely proton calibration and magnetic measurements, to determine a correction to be applied to the "field display energy" which is available online during running.

To recapitulate briefly, the proton calibration method measures the momentum of a proton beam on the same orbit as the electron beam by measuring the revolution frequency f^{rev} for electrons and for protons. Since this can only be done at the injection energy of 20 GeV, it must be combined with the magnetic measurements technique which tries to find all relevant corrections to the field of the reference magnet, among them the magnet aging factors, off-axis corrections, effect of the earth's field, effect of nickel flashing on the vacuum chamber, etc, to permit the best possible extrapolation to the field used for physics running.

The consensus of the working group[2] is that the correction factor to be applied to the 1990 data is $-6.4 \pm 2.4 \times 10^{-4}$, corresponding to an energy uncertainty of ± 0.02 GeV. This error contains only one significant digit in recognition of the fact that the component errors are imperfectly known.

The observation made in the last hours of the 1990 running, using backscattered photons from polarized laser light recorded in a Compton polarimeter, that transverse polarization existed at a level of 10% renewed hope that the resonance depolarization technique could be implemented to make very precise energy measurements, potentially of order $\Delta E/E \approx 10^{-5}$. At the present time the initial observation of polarization has been confirmed, but no energy value from this method has been circulated. The LEP scan strategy has been altered however, so that the increments are 880 MeV rather than 1 GeV. This puts more scan points in the vicinity of the depolarizing resonances. The ultimate precision of the method depends on the number of points at which a measurement can be made. An ultimate error of 5 MeV is hoped for.

The LEP running strategy for the remainder of the year will change slightly from last year's in that more time will be spent on the Z^0 peak and less at the higher and lower energy points. A 2/3, 1/3 sharing seems to be favored by all groups but L3. Of the 184 days scheduled this year, 25% will be devoted to machine development.

In a longer perspective, LEP will introduce 8-on-8 bunch running in 1992, making use of electrostatic beam separators from SPPS. Some trigger tests have already been carried out in this mode. The move to 18-on-18 will require at least 2 years' work by the experiments and an expenditure of 10 MSF. No commitment has been made to take this step yet. LEP will have superconducting cavities in sufficient quantities to reach W^+W^- threshold in 1994, which will mark the beginning of the LEP200 era. Present planning still calls for LHC installation to begin in 1997 and commissioning to start in 1998. After that time LHC and LEP would share time in a manner not yet decided.

2.3.2 The OPAL Detector

The definitive article describing the OPAL detector[3] has been accepted for publication in Nuclear Instruments and Methods. Consequently we will limit the discussion here to a few salient points.

Detector Performance

The Central Jet Chamber is the principal tracking chamber of OPAL. It not only provides the primary momentum measurement of the tracks and the means of event visualization, but also it is a key element in particle identification through its measurement of specific ionization. Position resolution in the r - ϕ plane is 120 microns. With the 50 micron resolution of the vertex detector, this leads to a momentum resolution of $\sigma_p/p^2 = 1.51 \times 10^{-3}$, or σ_p/p of 6.8% at 45 GeV, and an impact parameter resolution for μ pairs of 40 microns. The same quantity in the r - z plane is 1.7 mm, a considerable improvement over the situation a year ago.

The dE/dx capabilities have also undergone marked improvement during the past year. The resolution for μ pairs is now 2.9% and for single electrons is 3.0%. The corresponding number for minimum ionizing pions is 3.8%. The figures are valid for tracks with more than 40 wire hits, corresponding to 89% of all tracks. With this improved resolution in dE/dx , the 2σ separation of electrons and pions has been extended to 11 GeV/c, and the separation of pions and kaons to 15 GeV/c. Kaon-proton separation at the 1.5σ level can now be achieved between 7 and 13 GeV/c. The effect of this improvement can be seen in the enhancement of the ϕ signal shown in Figure 2.2.

The electromagnetic barrel lead glass resolution is 2.6% at 45 GeV. This detector system is extremely quiet. A study of random beam crossings shows that fewer than 1% of these events have more than 300 MeV summed over all 12000 blocks. This makes it possible to run a single-element trigger with a very low threshold, as discussed in below in the section on the single photon signal.

The installation of the silicon vertex detector is the most significant upgrade carried out during the long winter shutdown. The first phase of this detector incorporates two layers of single-sided strips read out with the MX3 multiplexor chip developed at RAL. Beam tests of these strips gave a position resolution of 5 microns and a signal to noise ratio of 10, as expected. Calibration of this detector system is now under way. The second phase of the detector will use two-sided strips and the new MX5 multiplexor chip. To be installed during the coming winter shutdown, this new version will offer dramatic improvement in z resolution.

Luminosity Measurement

The OPAL Forward Detector was initially felt to be somewhat inferior to those of the other LEP detectors. However, persistent attention to all the sources of uncertainties has reduced the overall experimental uncertainty in the luminosity determination to below 1%. The current level of the systematic errors from all sources is presented in the section on the line shape.

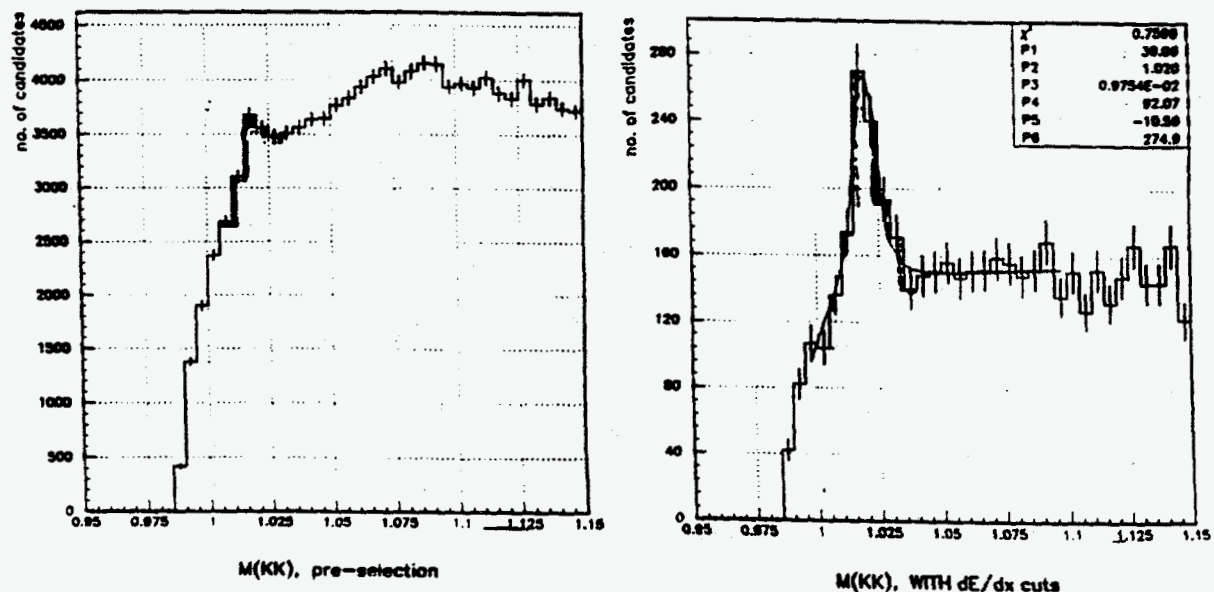


Figure 2.2: The ϕ signal a) without and b) with dE/dx selection.

Trigger and Readout

A comprehensive article describing the OPAL trigger system has been accepted for publication in *Nuclear Instruments and Methods*. [4] The trigger system, involving single-element triggers and coincidences in $\theta - \phi$ bins between different detector elements, provides triggers for all the main physics processes at close to 100% efficiency, and the large number of redundant triggers makes it possible to evaluate systematics precisely. During the 1990 running, OPAL triggered at an average rate of 2 Hz, of which 0.12 Hz came from multihadron events, 0.2 Hz from forward detector bhabhas, 0.02 Hz from dilepton events, 0.6 Hz from cosmics and noise, and the remainder from a variety of junk sources such as beam-gas, beam-wall, halo muons, synchrotron radiation, and off-momentum particles.

Current efforts are directed to extending the coverage and lowering the thresholds of a number of special purpose triggers. Triggers from the hadron calorimeter are being incorporated into the $\theta - \phi$ matrix. Preparations are also far advanced for lowering the trigger decision time in anticipation of 8-on-8 bunch running next year.

The distributed computing power of the front-end readout systems have been upgraded during the past year to lower the average readout deadtime to 10 ms and reduce long tails from a number of the "problem" detectors. At the same time OPAL has brought into operation a high performance online processing capability built around Apollo processors to carry out the function originally planned for the 370/E emulators judged to be obsolete before LEP began physics running two years ago.

The raw data load from multihadron events is 200 kilobytes and from other physics processes 60 kB. The Filter Processor, an Apollo DN10000 replacing a battery of 68020 pro-

processors, produces "compressed raw data" or CRD, which average 40 kB for multihadrons and 8 kB for other types of events. The CRD is buffered via large capacity optical disks before a first pass processing through the event reconstruction program running on several DN10000s. The DST output from these machines is available for online monitoring and is sent to the offline analysis "farms" within hours of the original data collection. Up to date calibration files are elaborated in this same processing step. Proposed upgrades to the online cluster which supervises these operations are discussed in a later section.

Offline Analysis Farms

During the past year an advanced offline analysis capability has come into being through the cooperative effort of CERN's CN division and members of the OPAL collaboration. This facility, known as SHIFT, is designed to eventually supplant CERN's central main-frame computers and is built around the high speed Ultranet network running at gigabit speed. Ultranet links a variety of fast processors such as the DN10000s and the newer Silicon Graphics 4D/340S machines, together with the Cray X-MP/48 to provide access to cartridge tapes. Some 25 Gbytes of disks space is interfaced via Digital 5000 workstations and is designed to accommodate all the data to be acquired during this year's running. Analysis jobs can be submitted to this facility from a variety of sources, such as the CERN central IBM and the OPAL offline cluster, and the results, incorporating the latest available calibration files, are returned within a few hours.

The SHIFT facility was originally expected to come into service in 1992 but is already being used by many members of the collaboration for data analysis, even though a number of problems remain to be solved. The slower but more thoroughly debugged MAW system, running on a subset of the OPAL offline VAX cluster machines, continues to be used for data analysis by the majority of the collaboration. The MAW strategy is more sophisticated than that of SHIFT. The MAW software transparently splits up a user-submitted job into subjobs, each of which runs on a workstation which contains the desired data files on its local disk. In this way movement of large disk files over the network is avoided. The SHIFT approach is more elemental: it simply transfers the files over its high speed net. Since the overall disk capacity on MAW and SHIFT is limited by financial constraints, the likely evolution of the MAW system will be toward a "nanoDST" farm, to be used in the advanced stages of analysis projects when the event samples are well defined and limited in size.

Hadron Calorimeter Strip Readout

During the past year of operation, the HCAL strip readout, the responsibility of the UCR group, has continued to perform at an acceptably trouble-free level. Indeed, the HCAL strips are among the most reliable of the OPAL detector components. Software monitoring tools which have been improved during this period include command procedures to check the integrity of the online data acquisition software permanent storage media and to back up these stored files automatically once a day. Our ability to perform online monitoring, using the available network tools such as TCP/IP, and offline monitoring, using the DST files which arrive quickly to the DST farm, has improved to the point that we are frequently

aware of minor problems before the shift crew manning the experiment in the tunnel. During the long LEP shutdown all of the front-end electronics faults were repaired. The installation of monitor streamer tubes in the experimental hall has been carried out so that gas gain monitoring is not affected by temperature variation effects in the gas mixing room.

The principal task to be accomplished in the coming 12 months is the upgrading of the Hadron Calorimeter strip readout electronics and software to accommodate the expected ever-higher luminosity at LEP. We will study the possibility of double-buffering events, which promises to cut our readout time to one fourth of its current value. This will prepare us to handle the event rate at even the highest level of multi-bunch running and appears to be possible with minimal changes to the existing system.

2.3.3 Electroweak Studies at the Z^0

Introduction

Within the framework of the Standard Model, M_Z , the mass of the Z^0 boson, the massive neutral carrier of the electroweak field, is a fundamental parameter. Its precise determination, in conjunction with the knowledge of the fine structure constant α and the Fermi coupling constant G_F leads to well defined predictions for the couplings of the Z^0 to all fermions. Since these couplings, as well as the mass of the Z^0 , are measured to high precision at LEP, comparison with predictions provides a stringent test of the Standard Model and places bounds on the allowed ranges of M_t and M_H .

The OPAL Collaboration has recently submitted for publication an exhaustive analysis of measurements of the Z^0 mass M_Z , its total width Γ_{Z^0} , and partial decay widths into hadrons, charged leptons, and invisible final states. The axial vector and vector couplings of the Z^0 to charged leptons are extracted from measurements of the leptonic partial widths and forward-backward asymmetries. The analysis combines data from 1989 and 1990 and is based on a total of some 165,700 hadronic and 18,300 leptonic Z^0 decays. The cross sections and forward-backward asymmetries are measured at seven center of mass energies, spanning an interval of ± 3 GeV about the Z^0 peak.

At each machine energy, the multihadron cross section is calculated as

$$\sigma(e^+e^- \rightarrow \text{hadrons}) = \frac{1}{\epsilon \int \mathcal{L} dt} (N_{had} - N_{bkgd})$$

where ϵ encompasses all selection and acceptance factors, and $\int \mathcal{L} dt$ is the integrated luminosity at the point in question. We describe briefly the luminosity determination and the event selection criteria, then summarize the fitting techniques and present some of the results obtained. Full details can be found in the published paper. [6]

The Luminosity Determination

Three methods were employed in making the luminosity measurement: (I) an absolute determination using proportional tube chambers, (II) a second absolute measurement using scintillators, and (III) a relative measurement, stable and with high statistics, using the forward calorimeters alone.

In method I, the track angle was determined by proportional tube chambers forming part of the forward detector complex. An energy cut was made using the calorimeters to eliminate off-momentum background. The principal limitation of this method last year was the lack of knowledge of the exact position of the tube chambers. This limitation has been overcome using very accurately surveyed drift chambers placed in the immediate vicinity of the tube chambers. By studying single electron tracks, one can transfer the survey precision of the drift chambers to the tube chambers. However, since the drift chambers do not overlap fully with the tube chambers, a residual uncertainty remains in the definition of the inner edge of the acceptance of the tube chambers as a consequence of the uncertainty in the exact pitch of the tube chambers. The uncertainties are summarized in the table.

| Source of Error | Uncertainty [%] |
|--------------------------------|-----------------|
| Inhomogeneity in tube chambers | 0.5 |
| Pitch of tubes | 0.4 |
| Survey (with drift chambers) | 0.3 |
| Data statistics | 0.3 |
| Monte Carlo statistics | 0.2 |
| Calorimeter coordinates | 0.1 |
| Distance to interaction point | 0.1 |
| Trigger efficiency | < 0.1 |
| Tube chamber inefficiency | < 0.1 |
| overall | 0.8 |

Table 2.1: Summary of uncertainties in the tube chamber, calorimeter, and drift chamber (Method I) absolute luminosity analysis.

Method II makes use of precisely machined and surveyed scintillator counters placed in four symmetric arrays around the beam pipe at each end of the detector. As in method I, calorimeter cuts are made to remove backgrounds. Averaging the luminosity over the four quadrants removes sensitivity to the position of the interaction point relative to the counter positions. The accepted cross section for this scintillator array was found to be 8.2 nb at $\sqrt{s} = 91.1$ GeV using the BABAMC Monte Carlo program. The overall experimental error for this counter system is 1.5%.

The integrated luminosities determined by methods I and II for the 1990 data were 6.58 ± 0.05 pb⁻¹ and 6.68 ± 0.10 pb⁻¹ respectively. The final luminosity value was taken as the weighted average of the two values, with an overall experimental uncertainty of 0.7%. A theoretical error of 0.4% comes from the approximative character of the Monte Carlo programs used to calculate the acceptance. A dramatic improvement has been achieved in this component of the error on the luminosity, taken last year to be 1%. A cooperative effort between theoreticians and members of the experimental groups, particularly those from the OPAL forward detector group, has succeeded in reducing this component of the error to 0.4%. [5] Including this, the total absolute luminosity uncertainty is 0.8%.

Method III is used for actually calculating the cross sections in the paper. This method uses the forward calorimeter alone with considerable larger acceptance to increase statistics. An energy cut and a coplanarity cut are imposed on tracks, and background levels are negligible. The fill-to-fill uncertainty in this measurement is 0.8%, and the uncertainty at each energy point is then $0.8\% / \sqrt{N_{fills}}$. The results of method III track those of the other two methods very well fill by fill and are then normalized to the absolute results.

Hadronic Event Selection

Charged track multiplicity has been added to the selection criteria for multihadronic events, in addition to cluster counting in the electromagnetic calorimeter, which was the sole criterion in our earlier paper. [7] "Tracks" are required to have at least 20 measured

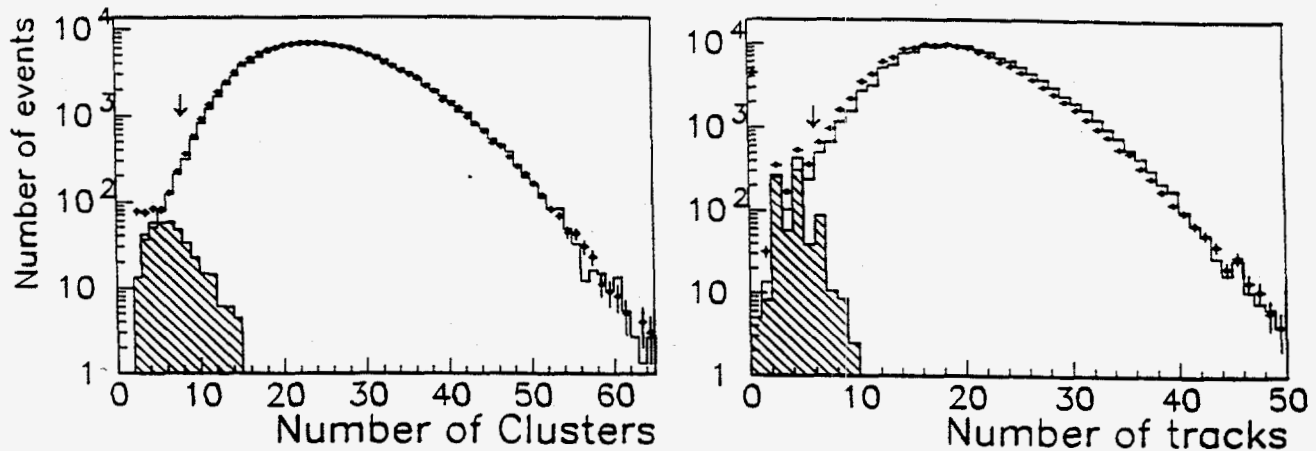


Figure 2.3: left Distribution of clusters (data points), compared with Monte Carlo (histogram), and right Distribution of numbers of tracks. The hatched areas are Monte Carlo estimates of the contribution from tau pairs.

space points, and the distance of closest approach to the nominal interaction point is 2 cm in $r\text{-}\phi$ and 40 cm in z . At least 50 MeV/c transverse momentum is also required. Calorimeter hits are grouped into “clusters” which can involve only one lead glass block in the barrel, over a threshold of 100 MeV, or two adjacent blocks in the endcaps whose energy sums to at least 200 MeV. The requirements for multihadron candidates are then:

- at least 7 clusters and at least 5 tracks, to eliminate decays to e^+e^- and $\tau^+\tau^-$,
- total energy deposited in the lead glass of at least 10 % of the center of mass energy, to discard two-photon and beam-gas events,
- a limited energy imbalance along the beam direction, to reject beam-gas, beam-wall, and beam-halo events and endcap cosmic rays. Further cosmic ray rejection is provided by the TOF counters.

Backgrounds from various sources still present in the multihadron sample after all the selection requirements have been applied are estimated in several ways: from event scans, from Monte Carlo calculations, and from the data themselves by varying the cuts. Estimated contaminations are: $\tau^+\tau^-$ $0.11 \pm 0.03\%$, two-photon $0.2 \pm 0.2\%$ (at extremes of the scan), $e^+e^- < 0.1\%$, cosmic $< 0.1\%$, beam-wall, beam-gas, and beam-halo all $< 0.1\%$. The acceptance of the selection procedure was evaluated from Monte Carlo to be 98.4% with negligible error. Agreement of the Monte Carlo with the distribution of clusters and tracks is shown in Figure 2.3.

The Lepton Channels

To select e^+e^- candidates, one requires two lead glass clusters in the angular range $|\cos\theta| < 0.85$, each of which has at least 50% of the beam energy. The total energy

reconstructed from the calorimeter information has to be at least 80% of the center of mass energy, and no more than 8 clusters or 8 tracks could be present in the detector. Since improved Monte Carlo programs are available this year for calculating t -channel effects, the cross section is evaluated over the symmetric region $|\cos\theta_{e^-}| < 0.7$. Contamination from the $\tau^+\tau^-$ channel is determined to be $0.2 \pm 0.1\%$ using the KORALZ program, and background contributions from multihadrons and from two-photon processes are less than 0.1%. Because the cross section rises steeply with increasing $\cos\theta$, a small imprecision in the definition of the acceptance cut could lead to a significant error in the cross section and asymmetry. Careful investigation of this question established that the cross section uncertainty is 0.5% and the asymmetry uncertainty is 0.002 from this source.

Dimuon candidates are identified by requiring two tracks in the angular region $|\cos\theta| < 0.95$, separated by at least 320 mrad in ϕ . Requiring a track momentum of 6 GeV/c suppresses $\tau^+\tau^-$ contamination. Each of the two tracks must further be identified as a muon by one of the following criteria: i) 2 hits in either the barrel or endcap muon chambers that fall within $\Delta\phi = (100 + 100/p)$ mrad of the projected extrapolated track; ii) at least 4 of a possible 9 hits in a similar road in the hadron calorimeter; iii) a momentum measured in the central detector of more than 15 GeV/c accompanied by a deposition in the calorimeter of less than 3 GeV.

Tau pairs and mu pairs coming from the two-photon process are rejected by a cut on visible energy, while cosmic rays are removed by vertex cuts and time of flight measurements. Monte Carlo estimated contamination from the first source is $1.3 \pm 0.1\%$ and essentially zero from the second. The overall selection efficiency is $91.6 \pm 0.2\%$, the rather large inefficiency being due to gaps in the outer detector acceptance. For the measurement of the forward-backward charge asymmetry, several more cuts were imposed to guarantee unambiguous charge determination.

Tau pair candidates have two back-to-back, collimated, low multiplicity jets. One selects them by asking that the number of charged tracks be between 2 and 6. To suppress multihadron candidates, there must be fewer than 15 charged tracks and electromagnetic clusters, summed together. Dimuon pairs are removed by previous application of the muon requirements. Cuts on the visible energy are imposed to reject radiative bhabhas and two-photon processes, and cosmic rays are removed by vertex and TOF cuts.

Once these criteria are satisfied, one picks the taus out of the tracks by an iterative procedure which begins by defining a cone of 35° half angle around the highest energy cluster, summing the momenta of all tracks in the cone, then defining a new direction. This process is repeated until there are no further particles in the vicinity, and the resulting agglomeration is considered a tau if it contains at least one charged particle with at least 1% of the beam energy. If two taus are found by the procedure, the event is a $\tau^+\tau^-$ candidate if the acolinearity of the particles is less than 15° , and if they are within an angular acceptance of $|\cos\theta| < 0.9$.

The overall efficiency of the selection procedure is determined by Monte Carlo to be $76.9 \pm 0.2\%$, and within the polar angular acceptance it is 88.8%. Background from multihadrons is studied with the JETSET 7.2 and HERWIG 4.3 Monte Carlo programs and found to be $0.4 \pm 0.4\%$. Similarly contamination from $\mu^+\mu^-$ pairs is determined to be $0.6 \pm 0.2\%$. The QED process e^+e^- contributes $0.3 \pm 0.3\%$. A requirement of opposite

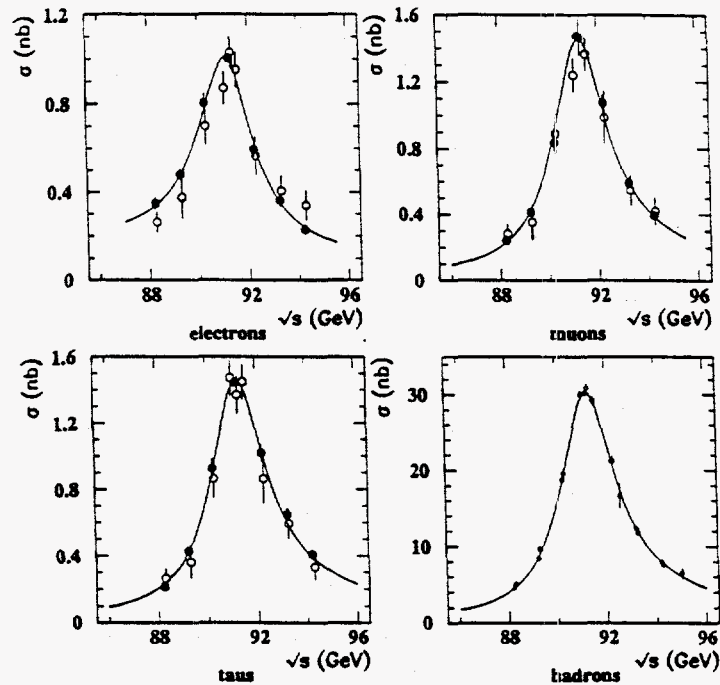


Figure 2.4: Cross sections as functions of center of mass energy for:
a) $e^+e^- \rightarrow e^+e^-$, integrated over $|\cos\theta_{e^-}| < 0.7$ and corrected for efficiency with the geometrical acceptance;
b) $e^+e^- \rightarrow \mu^+\mu^-$, corrected for acceptance;
c) $e^+e^- \rightarrow \tau^+\tau^-$, corrected for acceptance;
d) $e^+e^- \rightarrow \text{hadrons}$, corrected for acceptance.
The solid lines are the results of the fit to the combined e^+e^- , $\mu^+\mu^-$, $\tau^+\tau^-$ and hadronic data described in the text. The solid points show the 1990 data and the open points the 1989 data.

sign eliminates 1.7% of the events.

Figure 2.4 shows the corrected cross sections for the leptonic and hadronic channels

Analysis of the Data

The uncertainty of the LEP energy scale, 0.02 GeV, dominates the uncertainty in M_Z . The point-to-point energy uncertainty, 10 MeV, contributes approximately 5 MeV to the determination of the width, while the beam energy spread of 51 ± 2.5 MeV contributes a 4 MeV uncertainty in the opposite direction. Radiative corrections are treated with the ZFITTER program, the successor to ZBISON, which contains a complete $\mathcal{O}(\alpha)$ calculation, leading $\mathcal{O}(\alpha^2)$ corrections, and exponentiation of soft photons. For the e^+e^- channel, the program ALIBABA has been employed to calculate the contribution to the cross section and forward-backward asymmetry due to t -channel exchange and s - t interference terms.

The fits are based on a χ^2 minimization procedure which takes into account the full correlation matrix of the experimental uncertainties. For the hadronic line shape, a model

independent fit to the data is performed based on a Breit-Wigner line shape with s -dependent width.

$$\tilde{\sigma}(s) = \sigma_{had}^{pole} \frac{s\Gamma_Z^2}{(s - m_Z^2)^2 + s^2\Gamma_Z^2/m_Z^2}$$

plus additional QED terms that contribute less than 1%. The pole cross section

$$\sigma_{had}^{pole} = \frac{12\pi}{m_Z^2} \frac{\Gamma_e \Gamma_f}{\Gamma_Z^2}$$

represents the resonance hadronic cross section at $s = m_Z^2$ without photonic corrections. The fit, including the convolution of this cross section with photonic corrections, is performed with the program ZFITTER, treating m_Z , Γ_Z , and σ_{had}^{pole} as free parameters.

In the so-called "combined" fit, including the hadronic and leptonic data, the leptonic cross sections are described by a generalization of the improved Born approximation (IBA) given by

$$\begin{aligned} \frac{2s}{\pi\alpha^2} \frac{d\sigma}{d\cos\theta}(e^+e^- \rightarrow l^+l^-) = & \\ & \left(\frac{1}{1 - \Delta\alpha} \right)^2 (1 + \cos^2\theta) \\ & + \frac{2}{1 - \Delta\alpha} \text{Re}\{\chi(s)\} \left[\kappa_{\gamma Z}^2 \hat{v}_l^2 (1 + \cos^2\theta) + 2\kappa_{\gamma Z}^2 \hat{a}_l^2 \cos\theta \right] \\ & + |\chi(s)|^2 \left[\kappa_{ZZ}^2 (\hat{a}_l^2 + \hat{v}_l^2)^2 (1 + \cos^2\theta) + 8\kappa_{ZZ}^2 \hat{a}_l^2 \hat{v}_l^2 \cos\theta \right] \end{aligned}$$

with

$$\chi(s) = \frac{G_F m_Z^2}{8\pi\alpha\sqrt{2}} \frac{s}{s - m_Z^2 + is\Gamma_Z/m_Z}$$

In this fearsome expression the first term accounts for pure photon exchange, the second term for γZ^0 interference, and the third term for pure Z^0 exchange. $\Delta\alpha$ is the QED vacuum polarization correction evaluated at $M_t = 100$ GeV. In the IBA, \hat{a}_l and \hat{v}_l are taken to be real, and the four κ coefficients are equal to 1.

Results of the Fits

Results are given in the table, where, it should be noted, the values given come from different fitting operations and not from one global fit. The original paper must be consulted for details. In most fits the top mass M_t is taken to be 150 GeV, and that of the Higgs 100 GeV. Results are from the combined fit unless otherwise noted.

| Quantity | Fit | Value |
|----------------------------------|-----------------|-----------------------------|
| M_Z | hadronic data | $91.156 \pm 0.009 \pm 0.02$ |
| Γ_Z | " | 2.496 ± 0.017 |
| σ_{had}^{pole} | " | 41.01 ± 0.041 |
| N_ν | 2 parameter | 3.046 ± 0.068 |
| M_Z | combined fit | $91.161 \pm 0.009 \pm 0.02$ |
| Γ_Z | " | 2.492 ± 0.016 |
| Γ_{had} | | 1.740 ± 0.021 |
| $R_Z (\Gamma_{had}/\Gamma_{ll})$ | | 20.95 ± 0.22 |
| Γ_{ee} | combined fit | 82.9 ± 1.0 (MeV) |
| $\Gamma_{\mu\mu}$ | " | 83.2 ± 1.5 |
| $\Gamma_{\tau\tau}$ | " | 82.7 ± 1.9 |
| Γ_{ll} | universality | 83.00 ± 0.69 |
| \hat{a}_f^2 | | 0.998 ± 0.009 |
| \hat{v}_f^2 | | 0.0023 ± 0.0028 |
| ρ_Z | | 0.998 ± 0.009 |
| $\sin^2 \theta_W$ | | $0.238^{+0.030}_{-0.006}$ |
| $\sin^2 \theta_W$ (IBA) | | 0.2337 ± 0.0021 |
| M_W | | 79.93 ± 0.36 (GeV) |
| α_S | | 0.122 ± 0.007 |
| M_t | (OPAL + M_W) | $129^{+42+24}_{-39-16} M_H$ |
| $\Lambda_{\overline{MS}}$ | | 280^{+120}_{-95} |

Finally we present the results graphically in the following figures. Figure 2.5 gives the forward-backward asymmetries as a function of \sqrt{s} for the leptonic channels. Figure 2.6 plots R_Z , i.e., Γ_{had} versus Γ_{ll} and shows the central values and confidence contours for the measurement of Γ_Z and σ_{had}^{pole} .

Dittmar and VanDalen participated in this work.

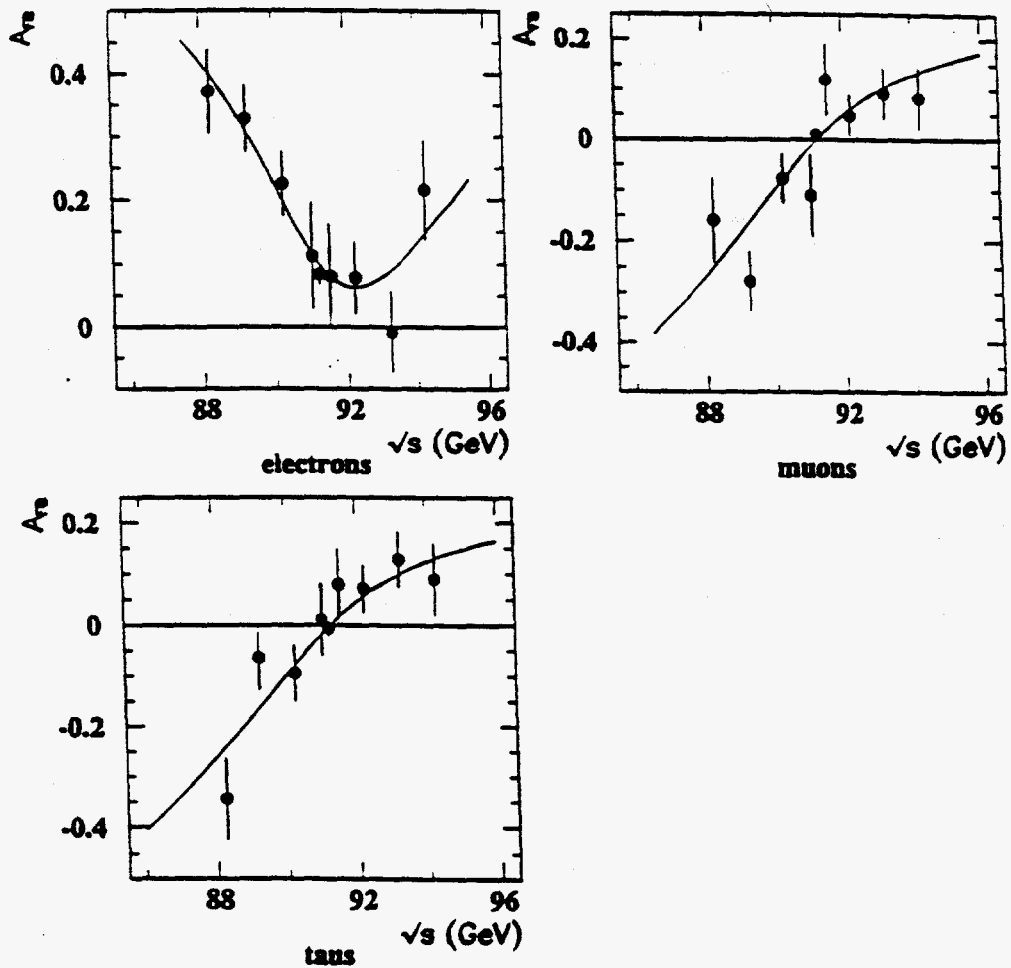


Figure 2.5: Forward-backward charge asymmetries for:

- a) $e^+e^- \rightarrow e^+e^-$, within $|\cos\theta_{e^-}| < 0.7$;
- b) $e^+e^- \rightarrow \mu^+\mu^-$, within $|\cos\theta| < 0.95$;
- c) $e^+e^- \rightarrow \tau^+\tau^-$, within $|\cos\theta| < 0.90$.

The solid lines are the results of the fit to the combined e^+e^- , $\mu^+\mu^-$, $\tau^+\tau^-$ and hadronic data described in the text.

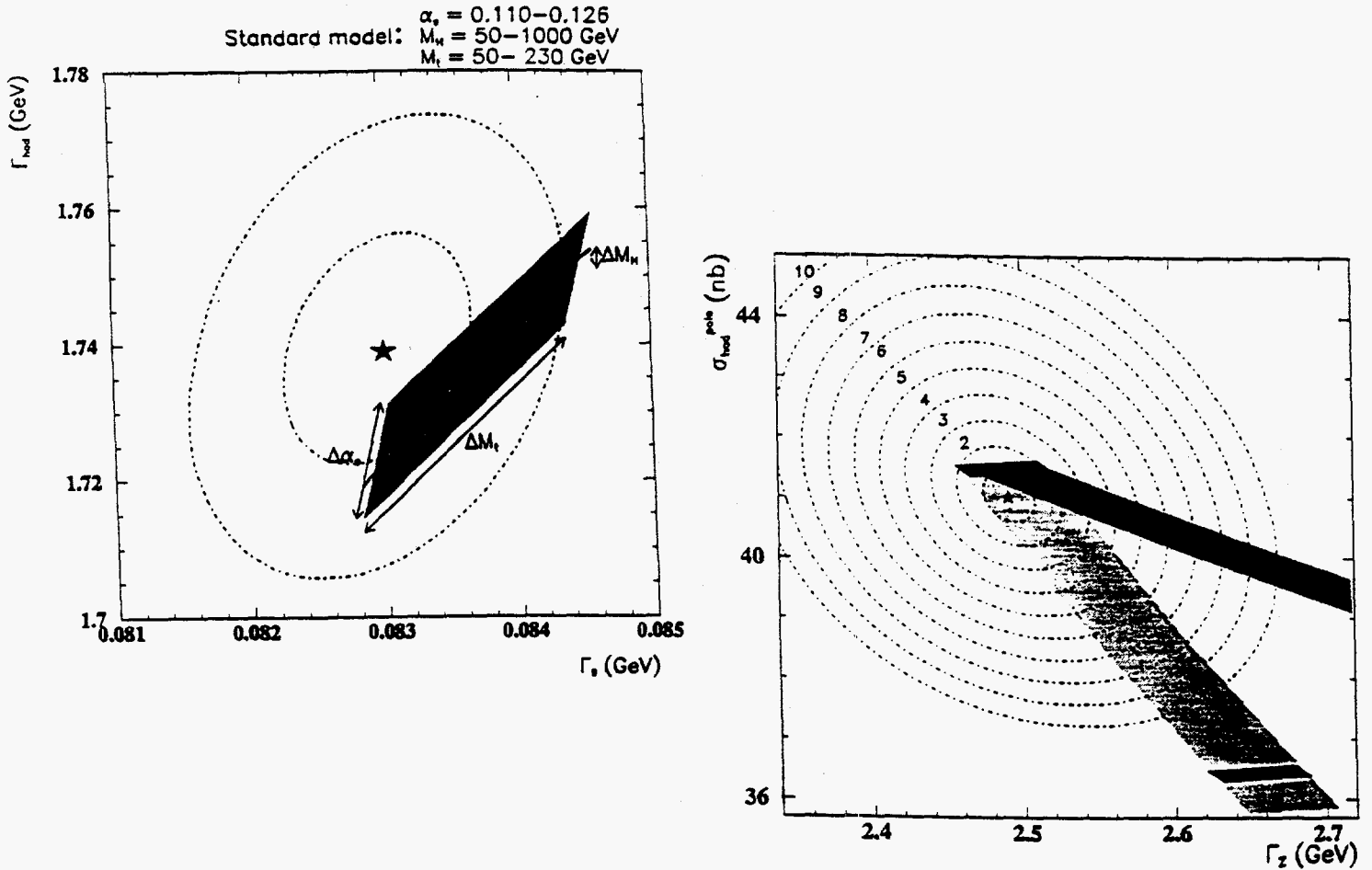


Figure 2.6: left One and two standard deviation confidence level contours in the Γ_{had} vs. Γ_{l+l-} planes. The star indicate our best fitted values; The shaded areas shows the variation in the Standard Model prediction for $50 < m_t < 230$ GeV/c², $50 < m_{H^0} < 1000$ GeV/c² and $\alpha_s = 0.118 \pm 0.008$.

right Confidence level contours for the measurement of Γ_Z and σ_{had}^{pole} . The black parallelograms of bars indicate the Standard Model prediction for 3 and 4 light neutrino species. The range spanned by each parallelogram shows the variation in the Standard Model prediction for $50 < m_t < 230$ GeV/c², $50 < m_{H^0} < 1000$ GeV/c² The shaded bar linking the two parallelograms marks the expected modification introduced by an additional contribution to the invisible Z^0 decay width exclusively. The second, darker, shaded bar indicates the modification introduced by an additional contribution to the hadronic Z^0 decay width exclusively.

2.3.4 QCD Studies

Determination of α_S

The multihadronic decays of the Z^0 provide an excellent laboratory for the determination of α_S . OPAL has measured α_S in a number of ways by analyzing parameters which are sensitive to this quantity. In each case, we have evaluated the uncertainties from all sources of error: (i) experimental statistics, (ii) hadronization in various models, (iii) Q_0 , the cutoff mass of the parton shower, (iv) $f = u^2/E_{cm}^2$, the renormalization scale factor.

Jet Rates

The relative jet production rates can be calculated to $\mathcal{O}(\alpha^2)$ in perturbative QCD, and thus are functions of α_S . In our latest analysis we compared the experimental differential two-jet rates with the predictions of a second order matrix element calculation for various jet recombination schemes. [8] The results of the detailed fits are summarized in Table 2.2.

| Scheme | $\alpha_S(M_{Z^0})$ | $\Delta\alpha_S(\text{exp.})$ | $\Delta\alpha_S(\text{had.})$ | $\Delta\alpha_S(Q_0)$ | $\Delta\alpha_S(\text{scale})$ | $\Delta\alpha_S(\text{tot.})$ |
|--------|---------------------|-------------------------------|-------------------------------|-----------------------|--------------------------------|-------------------------------|
| $E0$ | 0.118 | ± 0.003 | ± 0.003 | ± 0.003 | ± 0.007 | ± 0.007 |
| E | 0.126 | ± 0.003 | ± 0.003 | ± 0.003 | ± 0.013 | ± 0.014 |
| $p0$ | 0.118 | ± 0.003 | ± 0.003 | ± 0.005 | ± 0.004 | ± 0.008 |
| p | 0.118 | ± 0.003 | ± 0.003 | ± 0.006 | ± 0.003 | ± 0.008 |

Table 2.2: $\alpha_S(M_{Z^0})$ for different recombination schemes

EEC, AEEC, PTEC

The energy-energy correlations (EEC) are defined as the histogram of the angle between all combinations of pairs of tracks in hadronic events, weighted by their energies, suitably normalized, and averaged over all events:

$$EEC(\chi) = \frac{1}{\Delta\chi \cdot N} \int_{\chi - \frac{\Delta\chi}{2}}^{\chi + \frac{\Delta\chi}{2}} \sum_{\text{events}} \sum_{i \neq j} \frac{E_i E_j}{E_{vis}^2} \delta(\chi' - \chi_{ij}) d\chi'$$

where χ_{ij} is the angle between particles i and j and $\Delta\chi$ is the width of the histogram bin. The distribution is sensitive to α_S since the 2-jet contribution is peaked around 0° and 180° whereas 3-jet events will fill the central angular region. Calculations to $\mathcal{O}(\alpha)$ have been performed by several groups [9],[10] with good, although in some cases only fair agreement.

The asymmetry of the EEC correlations, or $AEEC(\chi) = EEC(\pi - \chi) - EEC(\chi)$ is also sensitive to α_S since the 2-jet contribution cancels whereas in 3-jet events, because of energy-weighting, jets with large opening angles contribute more than those with small opening angles. In addition, it is found to be less sensitive to fragmentation corrections and to systematic effects which are likely to have a symmetric dependence on χ .

In analogy with EEC, the planar triple-energy correlation (PTEC) can also serve as a measure of α_S . Here, one looks for triplets of tracks instead of pairs and imposes a

planarity condition: $\chi_1 + \chi_2 + \chi_3 > 2\pi - \delta$, where $\chi_{1,2,3}$ are the angles between the tracks and δ is a parameter. In order to exclude further a region of phase space sensitive to 2-jet events, one also requires that each of the angles be greater than an angle β .

The short tables below summarize the results from the three distributions. In each case, the integral over the appropriate angular region is used for the calculation of α_S . The error estimates are indications of the sensitivity of these distributions to the various effects. Included here are theoretical uncertainties arising from the different predictions of the $\mathcal{O}(\alpha)$ calculations.

| | $\alpha_S(M_Z)$ | $\Delta\alpha_S(\text{exp})$ | $\Delta\alpha_S(\text{had})$ | $\Delta\alpha_S(Q_0)$ | $\Delta\alpha_S(\text{th})$ | $\Delta\alpha_S(\text{scale})$ | $\Delta\alpha_S(\text{tot})$ |
|------|-----------------|------------------------------|------------------------------|-----------------------|-----------------------------|--------------------------------|------------------------------|
| EEC | 0.124 | ± 0.004 | ± 0.002 | ± 0.004 | ± 0.007 | ± 0.007 | ± 0.012 |
| AEEC | 0.117 | ± 0.007 | ± 0.001 | ± 0.003 | $^{+0.006}_{-0.002}$ | - | ± 0.009 |

Table 2.3: $\alpha_S(M_{Z^0})$ for EEC and AEEC

| $\alpha_S(M_{Z^0})$ | $\Delta\alpha_S(\text{stat.})$ | $\Delta\alpha_S(\text{syst.})$ | $\Delta\alpha_S(\text{th.})$ | $\Delta\alpha_S(\text{scale})$ | $\Delta\alpha_S(\text{tot.})$ |
|---------------------|--------------------------------|--------------------------------|------------------------------|--------------------------------|-------------------------------|
| 0.108 | ± 0.002 | $^{+0.008}_{\pm 0.004}$ | $^{+0.004}_{\pm 0.005}$ | ± 0.001 | $^{+0.009}_{\pm 0.007}$ |

Table 2.4: *Preliminary* results on $\alpha_S(M_{Z^0})$ from PTEC

Event Shape Variables

Among the event shape variables some are relatively stable when a particle is added to the final state (infrared safe) or when a particle in the final state is split into two (collinear safe). Three such variables have been analyzed by OPAL in a determination of α_S .

- *C-Planarity*: It is defined in terms of the eigenvalues λ_n of the momentum tensor θ_{ij} :

$$\theta_{ij} = \frac{\sum_a \frac{P_a^i P_a^j}{|P_a|}}{\sum_a |P_a|}$$

$$C = 3 (\lambda_1 \lambda_2 + \lambda_2 \lambda_3 + \lambda_3 \lambda_1)$$

where P_a^i is the i^{th} component of the momentum of particle a . The value of C vanishes for two-parton states.

- *Thrust*:

$$T = \max \left(\frac{\sum_i |\vec{p}_i \cdot \hat{n}_t|}{\sum_i |\vec{p}_i|} \right)$$

where the direction of the unit vector \hat{n}_t is chosen to maximize the quantity in parentheses. The thrust has a value of unity for 2-parton final states, smeared by hadronization, but varies between $\frac{2}{3} < T < 1$ for 3-parton states.

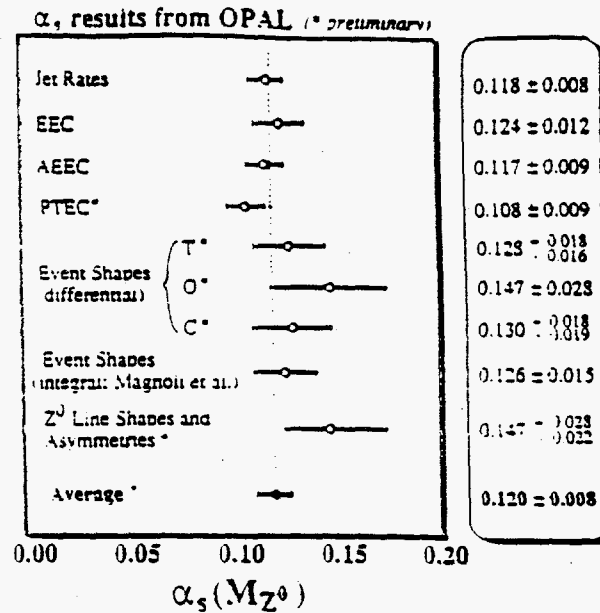


Figure 2.7: Summary of OPAL α_s measurements.

- *Oblateness*: Defining t_{major} in the same way as thrust above, but with the constraint $\hat{n}_{major} \cdot \hat{n}_t = 0$, and t_{minor} with $\hat{n}_{minor} = \hat{n}_t \times \hat{n}_{major}$, then

$$O = t_{major} - t_{minor}$$

The following table is a summary of the α_s measurements from these observables.

| Observable | $\alpha_s(M_Z)$ | $\Delta\alpha_s(\text{exp})$ | $\Delta\alpha_s(\text{had})$ | $\Delta\alpha_s(Q_0)$ | $\Delta\alpha_s(\text{scale})$ | $\Delta\alpha_s(\text{tot})$ |
|-------------|-----------------|-------------------------------------|------------------------------|-----------------------|--------------------------------|-------------------------------------|
| C planarity | 0.128 | ±0.002 | + 0.008 | ±0.001 | ± 0.016 | ± ^{0.018} _{0.016} |
| Oblateness | 0.123 | ± ^{0.002} _{0.004} | + 0.001 | + 0.052 | ±0.00 | ± ^{0.052} _{0.004} |
| Thrust | 0.130 | ± 0.002 | +0.001 | -0.006 | ±0.018 | ± ^{0.018} _{0.019} |

Table 2.5: Final results of $\alpha_s(M_{Z^0})$ for different observables.

The measurements of α_s from the various methods are graphically summarized in Figure 2.7. Also listed are the values of α_s obtained from a Standard Model fit of the experimental Z^0 line shape and asymmetries. We obtain from these a weighted average of $\alpha_s = 0.320 \pm 0.008$, where the overall uncertainty is chosen to be equal to the smallest of the individual errors.

Intermittency

Intermittency refers to the existence anomalous fluctuations in phase space distributions of hadronic events, in particular the existence of "self-similar" fluctuations, which may hint

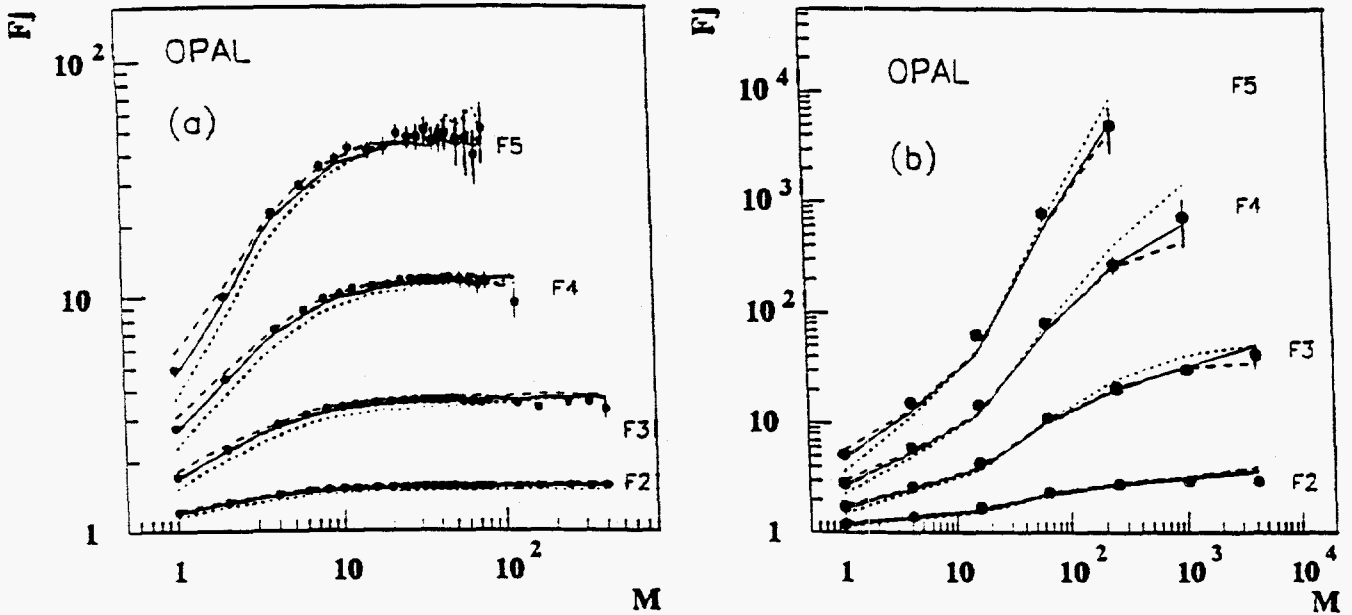


Figure 2.8: The corrected 2nd to 5th factorial moments, F_j (solid circles) versus number of bins, M for the rapidity (a) and rapidity vs azimuth (b) distributions compared with the predictions of the JETSET 7.2 parton shower (solid line), HERWIG 4.3, (dashed line) and JETSET/ERT matrix element (dotted line) Monte Carlo programs.

at a fractal structure in hadronic final states. [13] Assessing the statistical significance of rare or anomalous fluctuations is a difficult problem. However, a quantitative measure is provided by the method of *factorial moments* as proposed by Bialas and Peschanski. [14] This technique is normally applied to the experimental rapidity distribution as follows. The central rapidity plateau Y is divided into M bins of size $\delta y = Y/M$. If the number of particles in the m^{th} bin is n_m then the factorial moment of order j is given by:

$$F_j(M) = \frac{1}{\langle \bar{n}_m \rangle^j} \left\langle \frac{1}{M} \sum_{m=1}^M n_m (n_m - 1) \dots (n_m - j + 1) \right\rangle$$

where

$$\bar{n}_m = \frac{1}{M} \sum_{m=1}^M n_m$$

and where the angle bracket indicates an average over all events. With this definition it is trivial to extend the calculation to other distributions such as the two dimensional rapidity vs azimuth (azimuthal angle around the reference axis) distribution.

Factorial moments of order 2 to 5 have been determined from the OPAL multihadronic Z^0 decay sample in the rapidity range $-2 < y < 2$. The excellent momentum resolution and two particle separation provided by the OPAL detector allow us to measure the factorial moments with rapidity bin size down to 0.01 units. The measured moments for both the rapidity and rapidity versus azimuthal angle are shown in Figure 2.8 compared with the predictions of the HERWIG [15] and JETSET [16] (using both parton shower

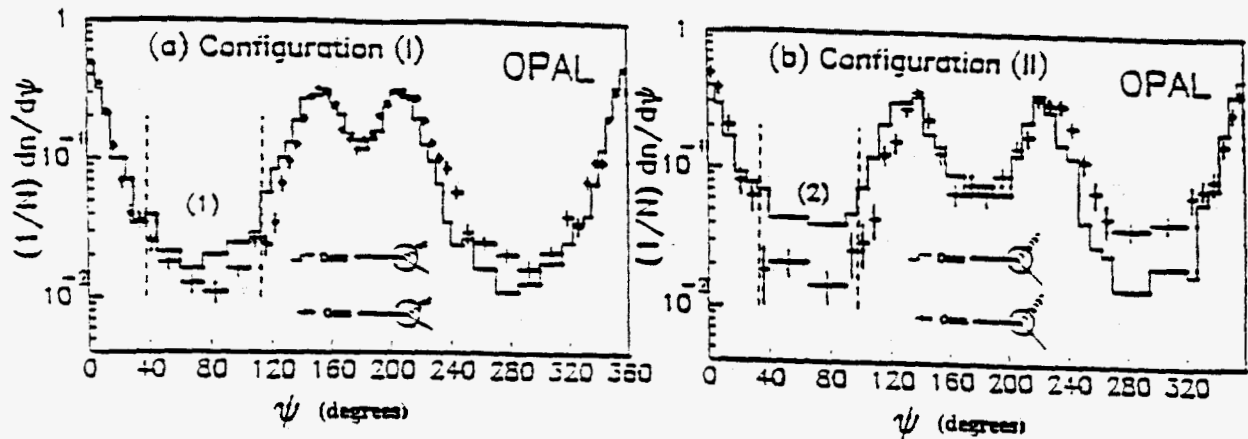


Figure 2.9: String effect from OPAL

and ERT [10] matrix element formalism) Monte Carlo programs. There is good agreement between all three models and the data [12]. Detailed investigations of the source of the observed signals in the Monte Carlo programs reveals that the major source is the jet structure of the events and the presence of 3 and 4 jet events.

The String Effect

A study of the population asymmetry between jets in 3-jet events, known as the "string effect," has been performed by OPAL [11]. The highest energy jet in the 3-jet events for this study is assumed to be a quark jet q because the gluon jet g , as the radiated entity, rarely has the highest energy in $ee \rightarrow q\bar{q}g$ events. Of the two lower energy jets, one is required to have an electron or muon track candidate; this e or μ is assumed to come from a semi-leptonic charm or bottom quark decay and so identifies the jet as being a quark jet q or an antiquark jet \bar{q} . The remaining jet is the gluon jet. Use of the lepton tag to identify the two lower energy jets allows events with a symmetric topology to be studied, for which the angle $\psi_{q\bar{q}}$ between the two quark jets is the same as the angle ψ_{qg} between the high energy quark and the gluon jet. Because of this geometric symmetry, the particle populations between the jets can be compared in a simple and model independent way.

As an example of the OPAL results, Figure 2.9 (a) shows the inclusive multiplicity distribution $(1/N) dn/d\psi$ with respect to the azimuthal angle ψ in the 3-jet event plane, for an event sample in which the angles between jets are $\psi_{q\bar{q}} = 150^\circ$ and $\psi_{qg} = 150^\circ$. In the interval enclosed by dashed lines and labeled (1), the region between the higher energy quark jet and the gluon jet is shown by the histogram while the region between the quark and antiquark jets is shown by the points with errors. The histogram lies above the points with errors in this interval: thus the particle population between the q and g is larger than that between the q and \bar{q} .

A second example is given in Figure 2.9 (b) for a different event sample in which the angles between jets are $\psi_{q\bar{q}} = 130^\circ$ and $\psi_{qg} = 130^\circ$: again the histogram (qg region) lies above the points with errors ($q\bar{q}$ region) in the region between jets, labeled (2) in figure 2.9 (b). These measurements are not strongly affected by the requirement of the lepton tag,

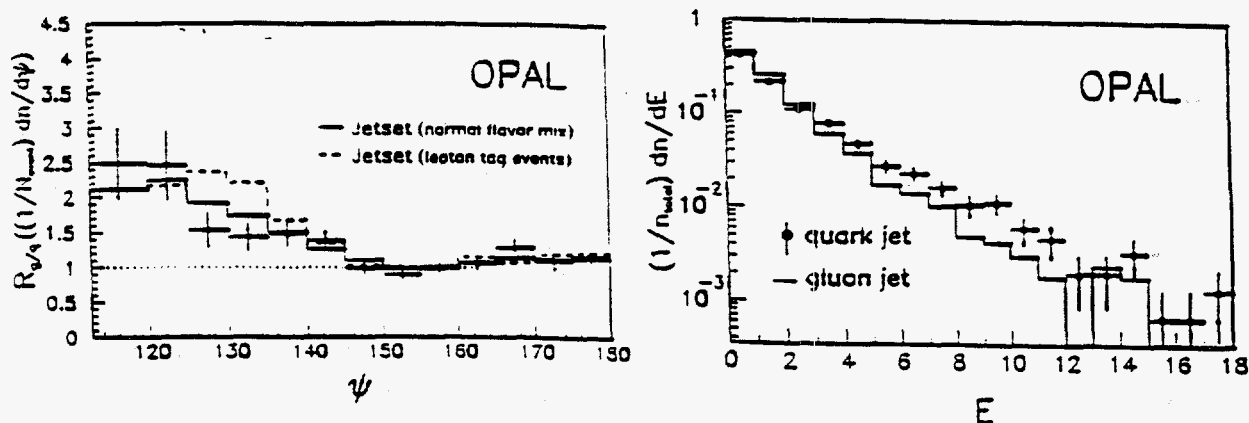


Figure 2.10: (a). The ratio of $(1/N_{evt})dn/d\psi$ in for gluon jets to that for quark jets in the region around the jet peak. (b). The inclusive energy spectrum $(1/n_{total})dn/dE$ of particles in the jet core regions ($135^\circ < \psi < 165^\circ$).

and thus these asymmetries in particle population cannot be of kinematic origin, due to the geometric symmetry in the events. This analysis establishes that dynamical differences exist between quarks and gluons or between $q\bar{q}$ and qg systems, with respect to their particle production properties.

Quark and Gluon Fragmentation

Using the symmetric quark-gluon jet events selected above, it is possible to compare directly the properties of gluon jets and quark jets of similar energies embedded in similar environments. For this comparison, we exclude that region of the event plane used for the string effect studies. Figure 2.10 shows the ratio of the particle flow for gluon jets to that for the quark jets in the region around the jet axis. Although the multiplicity of the quark and gluon jets is similar in the central region around the jet axis, the gluon jets clearly have more particles in the wings than the quark jets. Also shown in Figure 2.10 is the differential energy spectrum for particles in the cores of quark and gluon jets, defined as the region $135^\circ < \psi < 165^\circ$. The quark jet spectrum is clearly harder, implying that particles in the cores of quark jets tend to be more energetic than those in gluon jets.

Gary, a new faculty member of our group, has been a major contributor to the QCD program of OPAL.

2.3.5 Studies of Events with Photons

Neutrino counting

The number of light-mass neutrino generations can be determined directly by a method, first suggested by Ma and Okada in 1978 [19], involving the "direct" observation of the reaction $e^+e^- \rightarrow Z \rightarrow \nu\bar{\nu}$ by observing single photons from initial state radiation. Because it is a direct measurement and because it is sensitive to the radiative production of any otherwise undetectable particle pair, the single photon method provides an excellent complementary confirmation of the results of the width method.

Using the 1990 data sample of 5.3 pb^{-1} integrated luminosity with the "single photon" trigger, OPAL has measured the cross section of $e^+e^- \rightarrow \nu\bar{\nu}$ as a function of the c.m. energy. This is tabulated below and is shown in Figure 2.11, in which the data are compared with analytically calculated cross sections for 2, 3 and 4 neutrino generations. The fitted value of the invisible width is $0.50 \pm 0.07 \pm 0.03 \text{ GeV}$, corresponding to $3.0 \pm 0.4 \pm 0.2$ light neutrino generations.

| E_{cm} (GeV) | \mathcal{L} (pb^{-1}) | $E < 1.5 \text{ GeV}$ | $E > 1.5 \text{ GeV}$ | σ (pb) |
|----------------|------------------------------------|-----------------------|-----------------------|---------------|
| 88.22 | 0.400 | 5 | 2 | 6 ± 6 |
| 89.22 | 0.546 | 3 | 2 | 4 ± 4 |
| 90.22 | 0.264 | 2 | 2 | 10 ± 9 |
| 91.22 | 2.752 | 26 | 20 | 12 ± 4 |
| 92.22 | 0.379 | 5 | 5 | 21 ± 11 |
| 93.22 | 0.498 | 11 | 17 | 56 ± 14 |
| 94.22 | 0.473 | 11 | 25 | 87 ± 18 |

The luminosity and the number of single photon candidates which deposit between 1.0 and 1.5 GeV and more than 1.5 GeV in the calorimeter at each centre-of-mass energy point. The corrected cross sections, σ , are listed for single photon production for photons above 1.5 GeV in the angular region $|\cos\theta| < 0.7$ and with no restrictions against additional photons. The errors indicate the uncorrelated uncertainties only. In addition there are correlated uncertainties of 5.6 % and 0.8 pb.

Our participants in the Neutrino Counting Working Group include Layter, Shen and graduate students Larson and Heflin. Larson is working on his Ph.D. dissertation based on the analysis of the data of 1990. Heflin is working on the improvement and optimization of a single photon trigger for the 1991 run. He will concentrate on the new data to be taken in the latter part of the 1991 run at an energy several GeV above the Z^0 mass for a more precise determination of the number of light-mass neutrino generations.

Final State Photons in Hadronic Decays

One of the major goals in the study of Z^0 decays is the determination of the couplings of the fundamental fermions to the Z^0 . Since photons couple to the square of the electric charge of the quark, the fraction of charge 2/3 quarks is enriched in a sample containing final state photons. Measuring the rate of final state radiation in Z^0 decay into hadrons thus provides a simple way to disentangle the weak coupling of up- and down-type quarks.

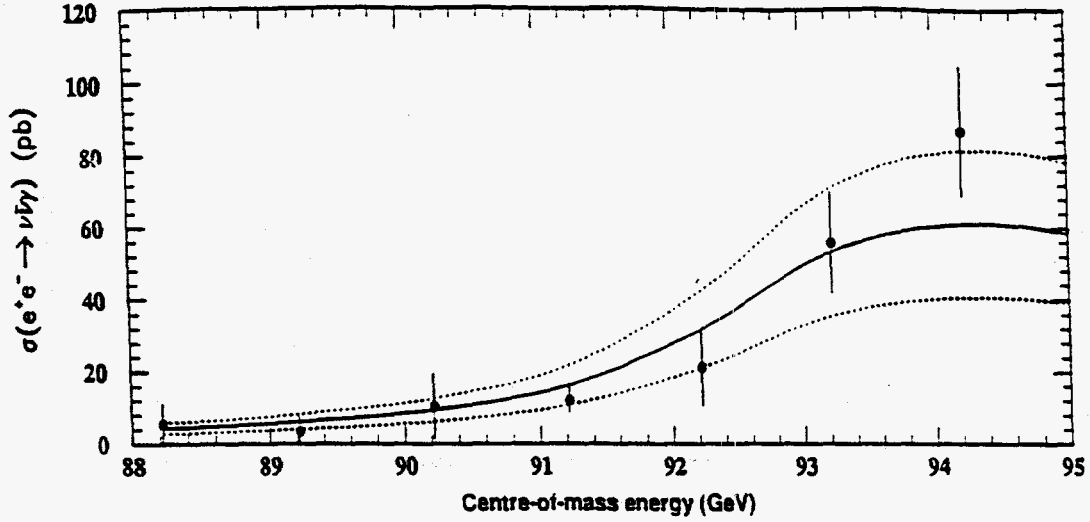


Figure 2.11: The corrected cross sections (pb) at each center-of-mass energy point for single photons above 1.5 GeV in the angular range $|\cos(\theta)| < 0.7$ from the process $e^+e^- \rightarrow \nu\bar{\nu}\gamma$. The solid curve shows the result corresponding to 3.0 light neutrino species. The expectations from two and four light neutrino species are shown by the lower and upper dashed curves respectively.

Assuming that all d-type and u-type quarks are produced equally, the hadronic width is given in the Standard Model in first order QCD as

$$\Gamma_{had} = N_c \frac{G_\mu M_Z^3}{24\pi\sqrt{2}} \cdot \left(1 + \frac{\alpha_s}{\pi}\right) \cdot (3c_d + 2c_u)$$

where N_c is the number of colors, G_μ the muon decay constant, and the $c_i = v_i^2 + a_i^2$ are the magnitudes of the weak couplings of up- and down-type quarks. The radiative width in first order QED is

$$\Gamma_{q\bar{q}\gamma} = N_c \frac{G_\mu M_Z^3}{24\pi\sqrt{2}} \cdot \frac{3}{4\pi} \cdot \frac{\alpha}{9} (3c_d + 8c_u)$$

If Γ_{had} and $\Gamma_{q\bar{q}\gamma}$ are measured, one can solve for c_u and c_d .

OPAL has updated the measurement of the radiative $q\bar{q}$ width analyzing a multi-hadron sample of about 150,000 events, corresponding to a integrated luminosity of 6.6 pb^{-1} . Candidate events are selected requiring that there be an isolated photon of at least 7.5 GeV with no neutral or charged particles within a half-angle cone of 15 degrees. The production rate of final state radiation is studied as a function of $y_{cut} = M_{ij}^2/E_{cm}^2$, the jet resolution parameter and minimum mass of the photon-jet system. 276 events were selected with $y_{cut} = 0.005$. The data are compared with theoretical matrix element calculations of Kramer and Lampe [17] to $\mathcal{O}(\alpha \cdot \alpha_s)$ in Figure 2.12, and with the predictions of two QCD shower models JETSET [16] and ARIADNE [18] in Figure 2.12. The matrix element calculation is in very good agreement with the data for $0.02 < y_{cut} < 0.12$. While ARIADNE reproduces the data well at low y_{cut} , JETSET underestimates the photon yield by about 30%.

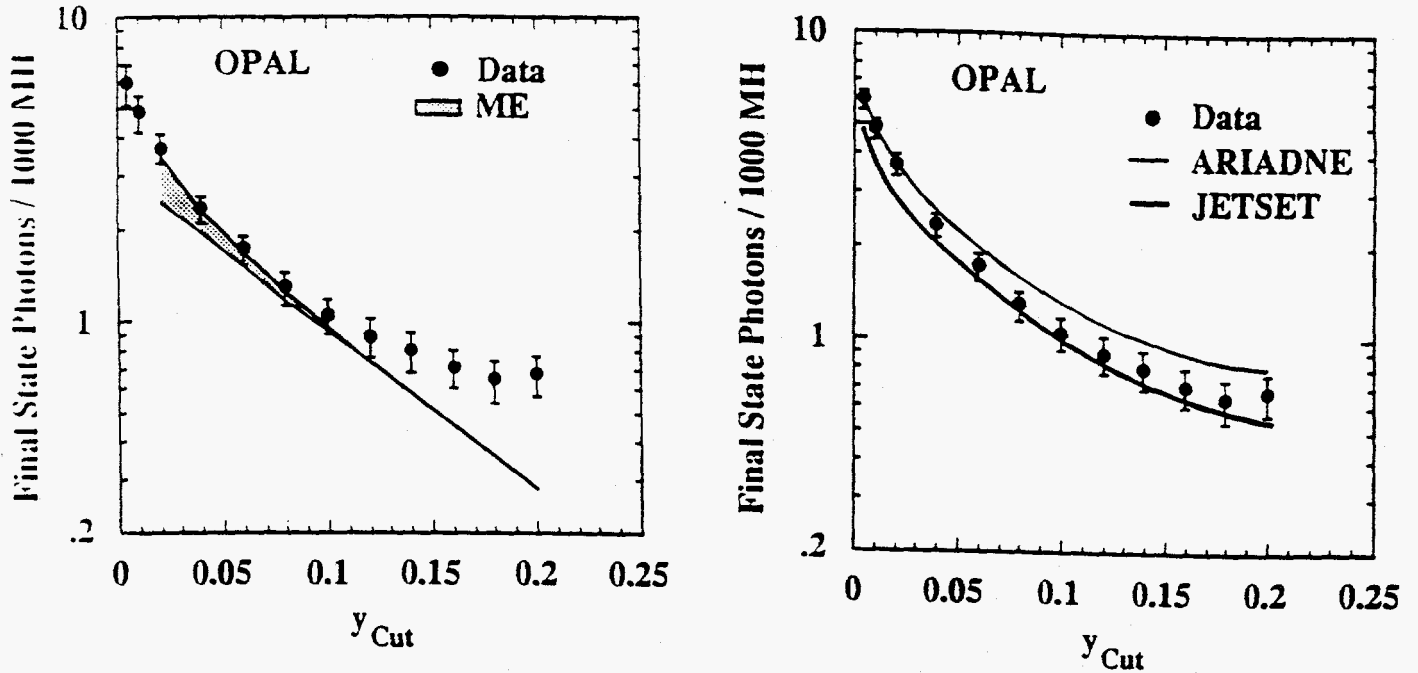


Figure 2.12: Observed fraction of multihadronic events with final state radiation of all multihadronic events as a function of y_{cut} and comparison with theoretical predictions: (a) matrix element calculations of Kramer and Lampe (The shaded area indicates the theoretical uncertainty due to α_s), and (b) QCD shower models JETSET (thick curve) and ARIADNE (thin curve).

Comparing the measurement and the prediction for $y_{cut} = 0.06$, where the experimental errors and systematics and theoretical uncertainties are small, and combining this measurement with our measured hadronic width of the Z^0 , we derive partial widths of up and down type quarks to be

$$\Gamma_u = 333 \pm 55 \pm 72 \text{ MeV} \quad \text{and} \quad \Gamma_d = 388 \pm 37 \pm 48 \text{ MeV},$$

in agreement with Standard Model expectations as shown in Figure 2.13.

The reactions $e^+e^- \rightarrow \gamma\gamma$ and $e^+e^- \rightarrow \gamma\gamma\gamma$

The reaction $e^+e^- \rightarrow \gamma\gamma$ provides a clean test of QED at energies near the Z^0 in contrast to lepton pair production where the weak interaction is dominant. The study of this reaction can also be used to set limits on non-standard properties of the Z^0 . The high order reaction $e^+e^- \rightarrow \gamma\gamma\gamma$ can be analyzed to study the validity of QED and to search for exotic decay of the Z^0 into three photons.

Events corresponding to these reactions are selected from the 1989 and 1990 data sample of an integrated luminosity of 7.21 pb^{-1} over an energy range between 88 and 95 GeV. The measured cross section of $e^+e^- \rightarrow \gamma\gamma$ as functions of energy and polar angle, as shown in Figure 2.14 a and b, are in excellent agreement with QED calculations. We determine the upper limits on the branching ratios of $Z^0 \rightarrow \gamma\gamma$, $Z^0 \rightarrow \pi^0$, $Z^0 \rightarrow \eta\gamma$, and $Z^0 \rightarrow \gamma\gamma\gamma$. Our results represent a substantial improvement over previous limits as summarized in the following table.

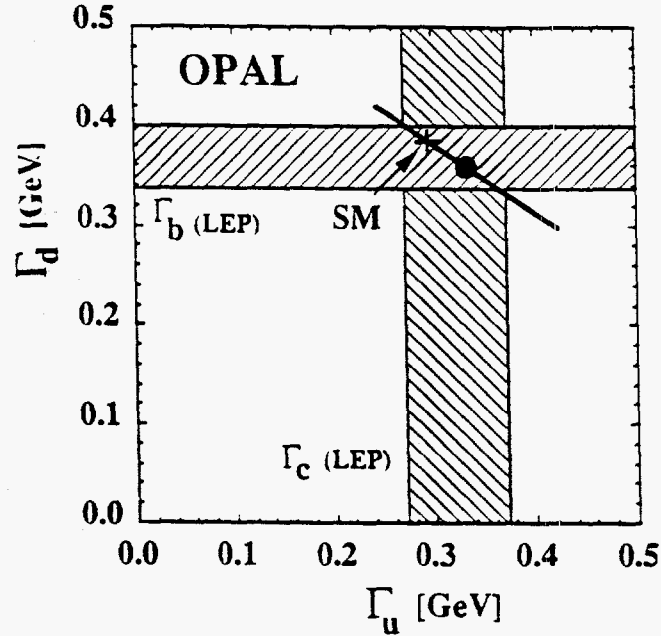


Figure 2.13: Correlation plot Γ_u vs Γ_d as obtained from this measurement. The one standard deviation contour is displayed by the bar. Also shown are the partial widths of the Z^0 into charm and bottom quarks, combined from all LEP experiments. The Standard Model value is indicated by the cross.

| Experiment | $BR(Z^0 \rightarrow \gamma\gamma)$ | $BR(Z^0 \rightarrow \pi^0\gamma)$ | $BR(Z^0 \rightarrow \eta\gamma)$ | $BR(Z^0 \rightarrow \gamma\gamma\gamma)$ |
|------------|------------------------------------|-----------------------------------|----------------------------------|--|
| OPAL (new) | 1.4×10^{-4} | 1.4×10^{-4} | 2.0×10^{-4} | 6.6×10^{-5} |
| ALEPH | | 4.9×10^{-4} | 4.6×10^{-4} | |
| DELPHI | | 3.0×10^{-4} | 4.8×10^{-4} | |
| L3 | 2.9×10^{-4} | 2.9×10^{-4} | 4.1×10^{-4} | 1.2×10^{-4} |
| OPAL [20] | 3.7×10^{-4} | 3.9×10^{-4} | 5.8×10^{-4} | 2.8×10^{-4} |

A deviation from QED can be parametrized by introducing a cutoff parameter into the electron propagator as follows

$$\frac{d\sigma}{d\Omega} = \frac{\alpha^2}{s} \frac{1 + \cos^2 \theta}{1 - \cos^2 \theta} \left[1 \pm \frac{s^2}{2\Lambda_{\pm}^4} (1 - \cos^2 \theta) \right]$$

Comparing this with our measured cross section, we obtain lower limits on the cutoff parameters of $\Lambda_+ > 117$ GeV and $\Lambda_- > 110$ GeV, at 95% confidence level.

Radiative Lepton pairs

Photon radiation from initial and final states and radiative decays are well described by quantum electrodynamics. Nevertheless, there is considerable interest in the study of radiative lepton pairs in e^+e^- collisions at the Z^0 . A higher yield in radiative tau pair events alone could indicate anomalous magnetic properties of the tau. No direct searches

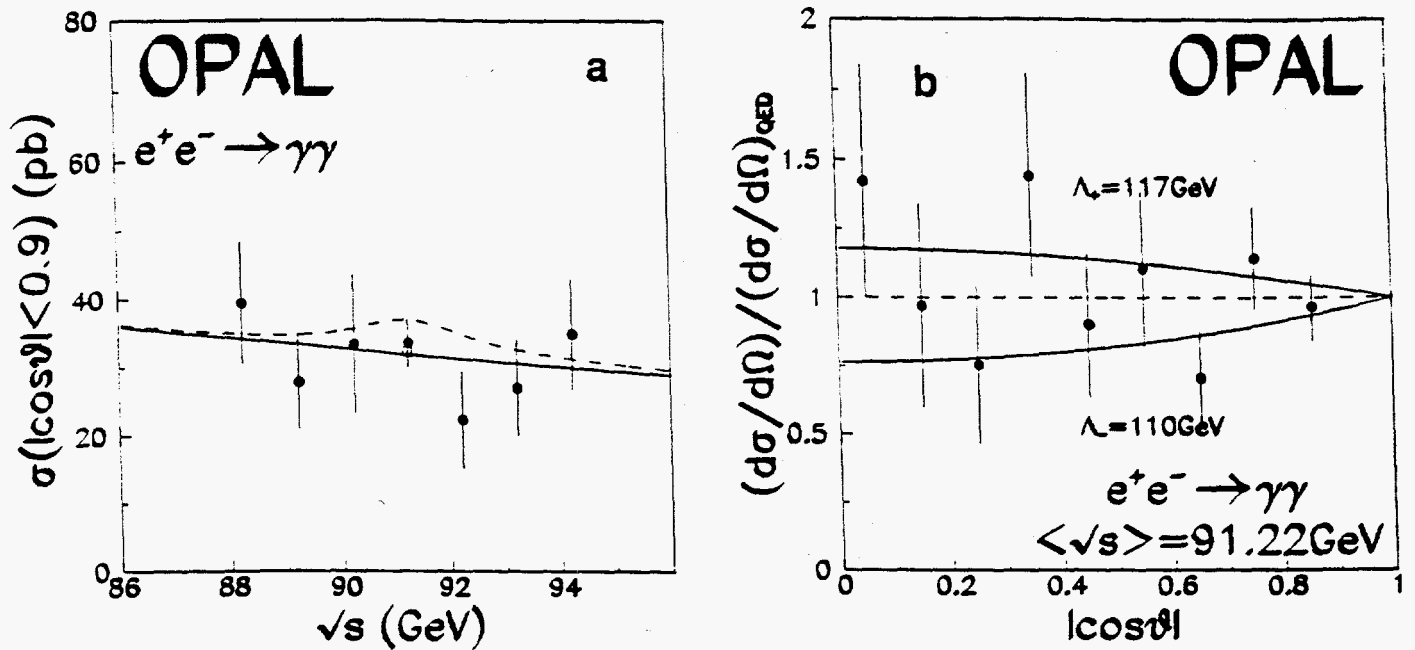


Figure 2.14: a) The measured integrated lowest order cross section for $e^+e^- \rightarrow \gamma\gamma$ (points with error bars), compared with the QED prediction (solid curve), with the polar angular range $|\cos(\theta)| < 0.9$. The average cross section is shown by a square with an error bar. The dashed curve shows the expectation with a Z^0 decay width $\Gamma_{\gamma\gamma} = 0.36$ MeV (95% confidence level limit). b) The ratio of the measured differential cross section for $e^+e^- \rightarrow \gamma\gamma$ to the QED prediction (points with error bars). The solid curves show the expectations with the cutoff parameters $\Lambda_+ = 117$ GeV and $\Lambda_- = 110$ GeV (95% confidence level limits).

for three body Z^0 decays into a photon and a pair of leptons have been performed so far. The events with hard initial state radiation allow a measurement of the cross section at energies between 60 GeV (TRISTAN) and the Z^0 .

Analyzing the data of 1989 and 1990 corresponding to an integrated luminosity of 7.1 pb^{-1} we select radiative lepton pair events and separate into $e^+e^-(\gamma)$, $\mu^+\mu^-(\gamma)$, and $\tau^+\tau^-(\gamma)$ channels. We plan to carry out the following studies:

- (i) comparing the experimentally measured yields for the three radiative lepton pair processes with those calculated with QED as functions of photon energy and angle,
- (ii) measuring the cross section of $e^+e^- \rightarrow \mu^+\mu^-$ at an average energy of 75 GeV by analyzing the $\mu^+\mu^-$ events with hard initial radiation,
- (iii) establishing limits for the branching ratios for $Z^0 \rightarrow X + \gamma$, where $X \rightarrow l+l^-$.

These analyses are being carried out by Dittmar with assistance from Shen. A draft for a letter will be available in the summer of 1991.

2.3.6 Quarks of Heavy Flavor

D* Production

D* mesons provide a powerful tool to study the production mechanism of heavy quarks since they occur almost exclusively in jets from primary b and c quarks. The D*s from c quarks directly coupled to the Z⁰ have relatively high energy fraction $\langle x_{D^*} \rangle \approx 0.5$, whereas the D*s from the decay of b quarks tend to have lower $\langle x_{D^*} \rangle \approx 0.3$. OPAL has analyzed D* production by investigating the two-body decay sequence $D^{*+} \rightarrow D^0 \pi^+ \rightarrow (K^- \pi^+) \pi^+$ and its charge conjugate. The low Q-value of the D* decay is exploited to minimize the combinatorial background. Further reduction is achieved by requiring $|\cos \theta^*| < 0.9$ for $\langle x_{D^*} \rangle > 0.5$ and $|\cos \theta^*| < 0.8$ for $\langle x_{D^*} \rangle < 0.5$, since the decay angular distribution of D⁰ is expected to be isotropic. The D* signal can be easily identified in the distribution of the mass difference $\Delta M = M(K\pi\pi) - M(K\pi)$ as shown in Figure 2.15 (a). Backgrounds and systematic uncertainties are determined by three different methods as a function of x_{D^*} . The signal and background yields are listed in Table 2.6 and shown in Figure 2.15 (b).

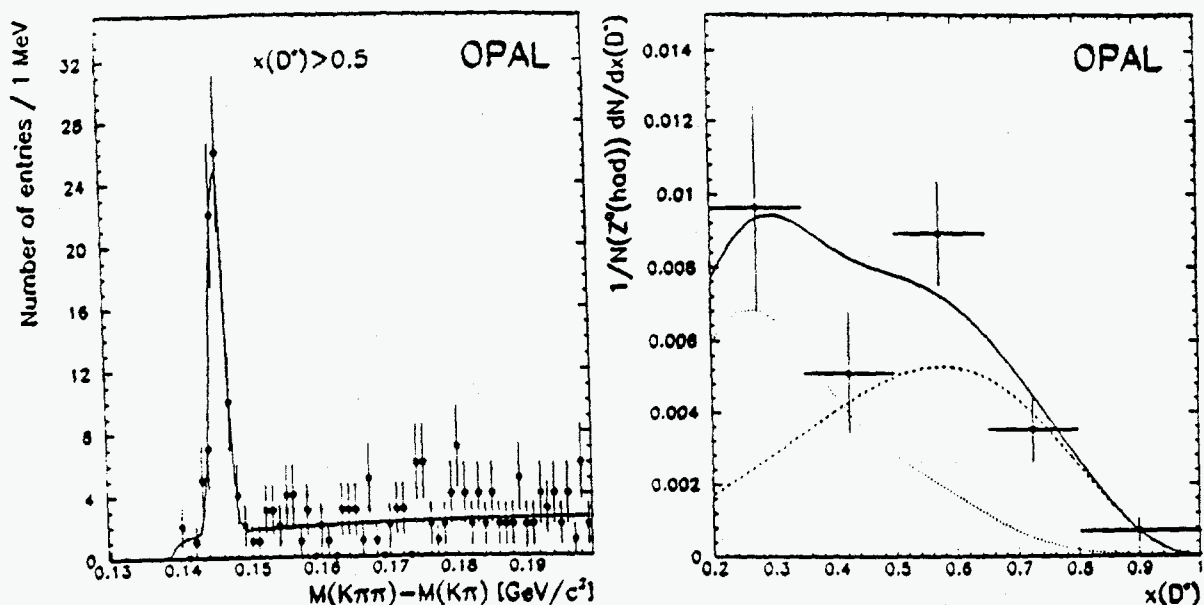


Figure 2.15: (a) Observed distribution of $\Delta M = M(K\pi\pi) - M(K\pi)$ for $x_{D^*} > 0.5$. The line shows the result from a fit of a Gaussian distribution for the signal over a smooth background.

(b) Total D* yield $\frac{1}{N_{had}} \frac{dN(D^* \rightarrow \pi K \pi)}{dx_{D^*}}$. The error bars displayed are statistical errors only. Also shown is the D* contribution from Z⁰ decays into bottom quarks (dotted line) and the fitted contribution from Z⁰ → c c̄ (dashed line). The solid line shows the combined contribution from b and c quarks.

The observed x_{D^*} distribution has contributions from both charm and bottom quarks

| x_{D^*} | $N_{D^*}^{\text{obs}}$ | N_{backgr} | $N_{D^*}^{\text{corr}}$ | syst. err. | $f_{c\bar{c}}$ |
|-----------|------------------------|---------------------|-------------------------|------------|-----------------|
| 0.20-0.35 | 32.5 ± 9.6 | 51.5 | 214 ± 63 | ± 32 | 0.27 ± 0.11 |
| 0.35-0.50 | 17.2 ± 5.7 | 14.8 | 113 ± 38 | ± 17 | 0.49 ± 0.13 |
| 0.50-0.65 | 43.4 ± 7.0 | 5.6 | 198 ± 33 | ± 19 | 0.72 ± 0.09 |
| 0.65-0.80 | 17.1 ± 4.5 | 2.9 | 78 ± 21 | ± 7.4 | 0.87 ± 0.05 |
| 0.80-1.00 | 4.5 ± 2.2 | 0.4 | 21 ± 10 | ± 2.0 | 0.95 ± 0.04 |

Table 2.6: The observed and corrected D^* yields are listed for various intervals of x_{D^*} . The error quoted for $N_{D^*}^{\text{obs}}$ includes the statistical errors for the number of events and the background fit. The systematic error takes into account contributions from the uncertainty in the efficiency calculation and variations between different methods of background determination. In the last column $f_{c\bar{c}}$ denotes the fraction of D^* mesons from primary charmed quarks as derived from the fit.

coupling directly to the Z^0 . The yield depends on: a) the fractions

$$F_c = \frac{\Gamma_{Z^0 \rightarrow c\bar{c}}}{\Gamma_{Z^0 \rightarrow \text{Hadrons}}}$$

and

$$F_b = \frac{\Gamma_{Z^0 \rightarrow b\bar{b}}}{\Gamma_{Z^0 \rightarrow \text{Hadrons}}};$$

b) the product branching ratio $P_{q \rightarrow D^*}$ of a quark species q to turn into a D^* and the D^* to decay into $\pi(K\pi)$, and c) the fragmentation functions of the charm and bottom quarks, parametrized in the Peterson form

$$d(x) = \frac{N}{x \left[1 - \frac{1}{x} - \frac{\epsilon}{1-x}\right]^2},$$

A maximum likelihood fit to the D^* events is performed. Fixing the yield and the fragmentation function of the b quarks to the values obtained and LEP and the decay branching fractions of the c quarks measured at PEP/PETRA, we obtain a partial width of Z^0 decay into $c\bar{c}$ of

$$\Gamma_{Z^0 \rightarrow c\bar{c}} = 323 \pm 61 \pm 35 \text{ MeV},$$

and an energy fraction of the D^* from primary quarks of

$$\langle x_{c \rightarrow D^*} \rangle = 0.52 \pm 0.03 \pm 0.01.$$

Study of b-quarks With Lepton Tagging

The study of b quarks from Z^0 decays is of great interest. A precision measurement of the partial width for $Z^0 \rightarrow b\bar{b}$ provides an important test of radiative corrections in the electroweak model, and the forward-backward asymmetry is sensitive to the value of the

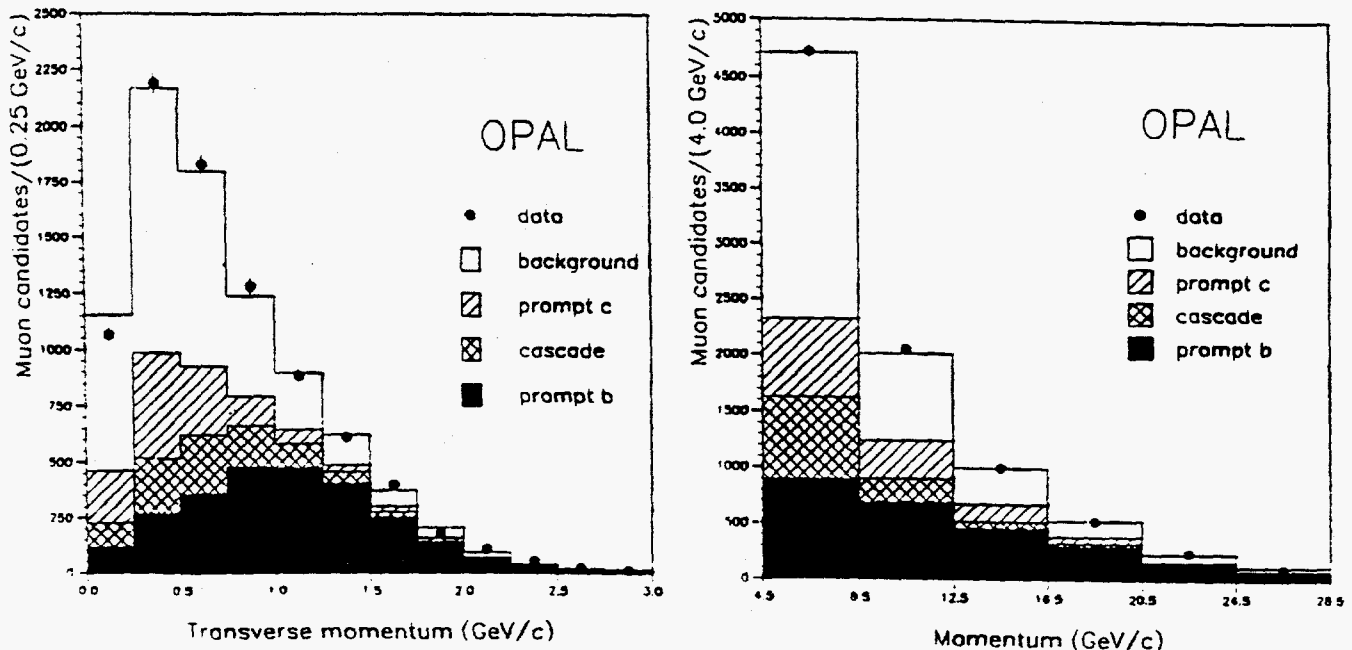


Figure 2.16: Results of fitting for the composition of the observed p vs p_T distribution for $p > 4.5$ GeV/c and for all p_T , shown superimposed on: a) the p_T distribution for $p > 4.5$ GeV/c; b) the p distribution for $p > 4.5$ GeV/c and for all p_T . (The process $b \rightarrow \tau \rightarrow \mu$ is included in the cascade contribution.)

weak mixing angle. OPAL has made a measurement of the partial width and the forward-backward asymmetry for $Z^0 \rightarrow b\bar{b}$, the partial width for $Z^0 \rightarrow c\bar{c}$, and the fragmentation parameters of the b and c quarks from an analysis of muon tagged hadronic decays based on a data sample of 6.4 pb^{-1} integrated luminosity.

Prompt muons can come from: direct decays of primary b quarks, cascade decays of $b \rightarrow c \rightarrow \mu$, cascade decays of $b \rightarrow \tau \rightarrow \mu$, and decays of primary c quarks. Penetrating tracks which mimic signal muons come from sail-through, punch-through, and decays of kaons and pions. The hard fragmentation of the b quark and its large mass results in muons of high p and p_T relative to the direction of the parent hadron. In contrast, muons from charm and cascade decays have much softer distributions in these variables, allowing the separation of b and c quarks on a statistical basis by applying kinematical cuts.

Muon candidates are identified by associating central detector tracks with track segments inside the hadron calorimeter and the muon chambers. The overall efficiency is found to be 85% in the range $|\cos\theta| < 0.8$, and 77% in the range $0.8 < |\cos\theta| < 0.9$. The efficiency is approximately independent of p and p_T for $p > 4.5$ GeV/c. The scaled mass jet finding algorithm of JADE is used to group charged tracks into jets. The jet resolution parameter y_{cut} is chosen to be 0.02. Only jets with polar angle with $|\cos\theta| < 0.8$ are accepted. The observed p vs p_T spectrum is fitted by a combination of the p vs p_T distributions for each of the separate sources of prompt and nonprompt muons. The fitted contributions are shown superimposed on the data in Figures 2.16 a and b. This fit gives the result:

$$\begin{aligned}
(\Gamma(Z^0 \rightarrow b\bar{b})/\Gamma(Z^0 \rightarrow \text{hadrons})) \times \text{Br}(b \rightarrow \mu) &= 0.0226 \pm 0.0007(\text{stat}) \pm 0.0013(\text{syst}). \\
(\Gamma(Z^0 \rightarrow c\bar{c})/\Gamma(Z^0 \rightarrow \text{hadrons})) \times \text{Br}(c \rightarrow \mu) &= 0.0176 \pm 0.0025(\text{stat}) \pm 0.0042(\text{syst}),
\end{aligned}$$

$$\langle x_E \rangle_b = 0.726 \pm 0.007(\text{stat}) \pm 0.022(\text{syst}),$$

$$\langle x_E \rangle_c = 0.56 \pm 0.02(\text{stat}) \pm 0.03(\text{syst}),$$

A complementary analysis of the $b\bar{b}$ fraction, based on counting the number of muons with $p_T > 1.0 \text{ GeV}/c$ and $p > 4.5 \text{ GeV}/c$, and subtracting the contributions from background and c quark decays, gave:

$$(\Gamma(Z^0 \rightarrow b\bar{b})/\Gamma(Z^0 \rightarrow \text{hadrons})) \times \text{Br}(b \rightarrow \mu) = 0.0218 \pm 0.0007(\text{stat}) \pm 0.0026(\text{syst}).$$

which supports the fitting result and is subject to different systematic uncertainties.

Using events with high p_T muons, the forward-backward asymmetry of the reaction $e^+e^- \rightarrow Z^0 \rightarrow b\bar{b}$ at the Z^0 peak, before correction for $B^0\bar{B}^0$ mixing, was measured to be:

$$A_b^{FB} = 0.072 \pm 0.042(\text{stat}) \pm 0.010(\text{syst}).$$

2.3.7 Studies of $\tau^+\tau^-$ Pair Production and Decay

The heaviest known lepton, the τ , can be used as a laboratory to study electroweak phenomena and answer some fundamental questions. The main points of interest are:

- Lepton universality
- τ lepton number conservation
- τ neutrino mass
- The determination of the τ couplings to the W and the Z^0
- Indirect searches for new interactions and massive particles (right handed W 's and extra Z^0 's)
- Searches for exotic particles decaying into τ 's.

Experiments at LEP can give detailed answers to the above questions. The expected number of $\tau^+\tau^-$ (and $b\bar{b}$) events at LEP is competitive with previous e^+e^- experiments at lower energies.

During the last year, the OPAL collaboration has performed several measurements which answer some of these questions. The number of neutrinos has been measured to be 3.046 ± 0.068 from the hadronic line shape [6], giving strong evidence for the τ neutrino and excluding the existence of more lepton families with small neutrino masses. As discussed earlier, our data give strong confirmation to the concept of lepton universality. We have also searched for Z^0 decays into exotic particles, like supersymmetric τ 's, charged Higgses, and heavy neutral leptons which could decay subsequently into τ 's. A method – developed for our search for supersymmetry in events with low charged and neutral particle multiplicity – has also been used to search for charged Higgses and to analyze the production of τ pair events [21]. Recently we have used this method to perform a combined lepton pair analysis [6]. These measurements will continue during the next years and much higher precisions can be expected.

The Tau Working Group, which includes the chairman K. Riles, M. Dittmar, B. Shen, G. J. VanDalen, and two graduate students C. Ho and B. O'Neill, had for its main physics goals for the 1990 data:

- Evidence for non-zero forward backward charge asymmetry of τ 's at the Z^0 pole.
- The observation of τ polarization, a proof of parity violation in Z^0 decays. The observation of τ polarization, in addition to a precision measurement of $\sin^2 \theta_W$, makes possible the determination of the absolute sign of the axial and vector couplings of the leptons.
- The search for violation of the τ lepton number in Z^0 decays.
- A precise measurement of τ branching ratios, which would demonstrate the feasibility of precision τ studies at the Z^0 pole.

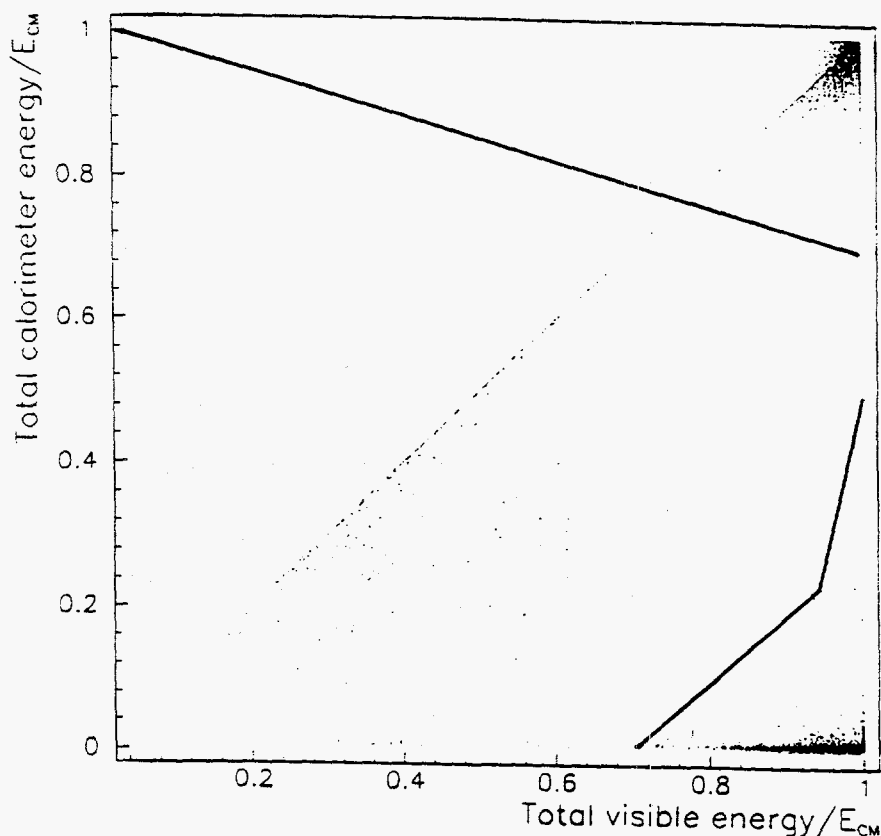


Figure 2.17: Visible energy versus calorimeter energy for low multiplicity events

Selection of Lepton Pair Events

We have performed an analysis which uses the information from the central detector and the lead glass calorimeter to select the different types of lepton pairs with high efficiency and very small background. As can be seen from Figure 2.17, the different types of lepton pairs (e^+e^- , $\mu^+\mu^-$, and $\tau^+\tau^-$) are well separated from each other. This combined analysis of the different types of lepton pairs simplifies some measurements considerably, since efficiencies and accuracies can be determined directly from the data. Starting from this lepton pair selection, different detailed studies are now in progress.

Study of the different τ decay modes

Considerable effort has been spent in recent years at previous e^+e^- experiments to measure different τ decay modes. We have analyzed a sample of about 6,600 τ decays and obtained results on τ decays into 1 and 3 charged particles and also for the τ decay into μ 's, and electrons.

Using a subset of the data, preliminary topological branching ratios were determined by finding an identified τ using the criteria just mentioned. This constitutes the "tagging side" of the event, and it can be a one-prong or a three-prong track. One then observes the charged multiplicity on the opposite side of the event. All events with a tagged τ on both sides were counted twice. Table 2.7 contains the observed branching ratios of

| tagged side | opposite side | BR (%) | PDG 1988 (%) |
|-------------|---------------|------------------------|------------------|
| 1 track | 1 | $84.4 \pm 1.5 \pm 1.2$ | 86.7 ± 0.4 |
| 1 track | 3 | $15.1 \pm 1.5 \pm 1.2$ | 13.19 ± 0.26 |
| 3 track | 1 | $83.5 \pm 3.1 \pm 2.2$ | 86.7 ± 0.4 |

Table 2.7: Topological branching ratios from OPAL data compared with world averages

the τ into 1 and 3 charged tracks using the different tagging conditions. Our results, even uncorrected for uncertainties due to unobserved photon conversions (enhancing the 3 charged particle mode), are in agreement with the current world averages on topological branching ratios. [22].

We have also unambiguously identified μ 's and electrons from τ decays. To determine the lepton efficiency, we use Z^0 decays into $\mu^+\mu^-$ and e^+e^- pairs which allow us to measure efficiencies with very small systematic errors. Our results for the branching ratio using all the data are [23]:

$$\text{BR}(\tau \rightarrow \mu\nu\bar{\nu}) = 16.8 \pm 0.5 \pm 0.4\%$$

and

$$\text{BR}(\tau \rightarrow e\nu\bar{\nu}X) = 17.4 \pm 0.5 \pm 0.4\%$$

This is in excellent agreement with the current world averages of $17.8 \pm 0.4\%$ and $17.7 \pm 0.4\%$. It should also be compared with the best measurements from single experiments with errors of about 0.8%.

The measured lepton branching ratios, when combined with the world-average measured value for the τ lifetime, yield a ratio of the τ Fermi coupling constant to that of the lighter leptons given by $G_\tau/G_{e,\mu} = 0.92 \pm 0.04$, where it is assumed $G_e = G_\mu \equiv G_{e,\mu}$. These results are consistent with previous measurements and increase slightly the statistical significance of both the discrepancy between the τ lifetime and leptonic branching ratios and the discrepancy between the inclusive and the sum of the exclusive 1-prong branching ratios of the τ .

The τ polarization measurement

The τ polarization can be measured using the 2-body τ decays into spin 0 + spin 1/2 particles ($\pi\nu$ and $K\nu$). Within the context of the standard model the polarization of the τ^- for unpolarised beams at the Z^0 peak is:

$$P(\theta) = -\frac{2a_\tau v_\tau}{a_\tau^2 + v_\tau^2} - \frac{2a_e v_e}{a_e^2 + v_e^2} \cdot \frac{\cos \theta}{1 + \cos^2 \theta}$$

Thus, within the Standard Model one expects to see three different regions for the τ polarization: the forward region with about 30% polarization, the backward region with a polarization close to 0, and the average polarization of about 15% for any range symmetric in $\cos \theta_\tau$ around 0. The π momentum spectrum can be used to measure the τ polarization according to:

$$\frac{dn}{dx_\pi} = 1 + P(\tau)(2x - 1)$$

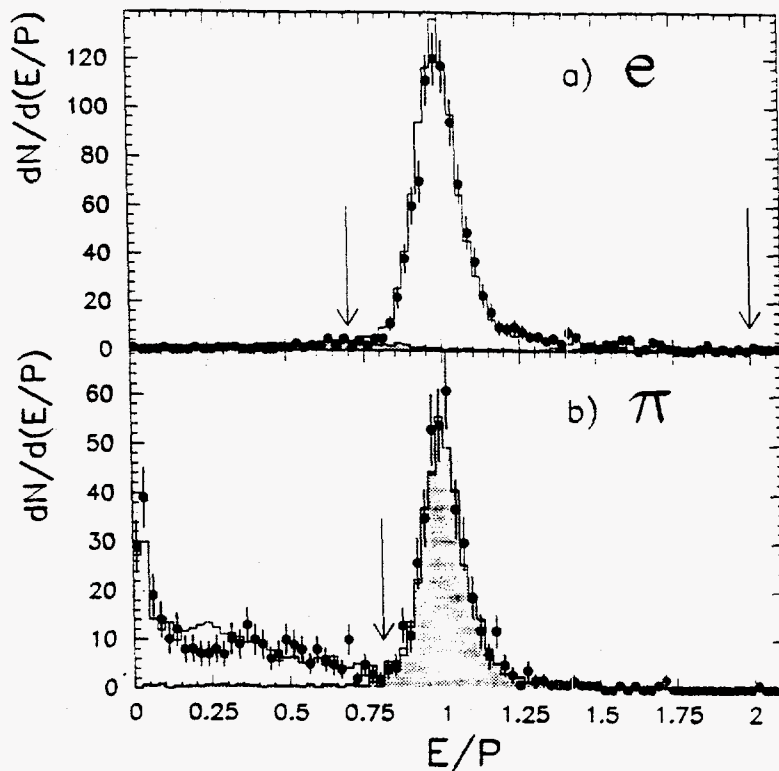


Figure 2.18: Distributions in E/p for a) $\tau \rightarrow e\nu\bar{\nu}$ candidates and b) $\tau \rightarrow \pi(K)\nu$ candidates after *all other* selection requirements except the E/p requirements have been imposed. In each figure the data are indicated by the points with error bars, the expected signal from Monte Carlo by the open histogram, and the expected background from Monte Carlo by the shaded histogram. Monte Carlo predictions are normalized to the world-average values for $B(\tau \rightarrow e\nu\bar{\nu})$ and $B(\tau \rightarrow \pi(K)\nu)$. The arrows indicate the cut values.

Only about 13% of the 1 prong τ decays are $\pi(K)\nu$ decays. (In the following we consider the $\pi\nu$ and $K\nu$ together since we did not try to distinguish the two experimentally.) In addition, the momentum spectrum of the background from ρ , e and μ decays is peaked at low x . These decay modes, if not perfectly rejected, might lead to a non-negligible asymmetry. A further complication is the final state radiation. It reduces the τ energy and therefore shifts the pion (kaon) energy spectrum to lower x values, leading to an additional asymmetry.

Figure 2.18 illustrates the separation of the one prong decays into $\tau \rightarrow \pi(K)\nu$, $\tau \rightarrow \mu\nu\bar{\nu}$, and $\tau \rightarrow e\nu\bar{\nu}$ samples. Figure 2.19 shows the final unfolded (for efficiency and backgrounds) momentum distributions for the three τ decays, along with polarization fits.

From an analysis of the momentum spectra of the decay products, assuming V-A charged current couplings of the τ , we obtain a combined average τ polarization at the peak of the Z resonance of -0.01 ± 0.09 , implying $v_\tau/a_\tau = 0.01 \pm 0.04$. From the spectra of identified decays in the forward and backward hemispheres, we obtain a value for the

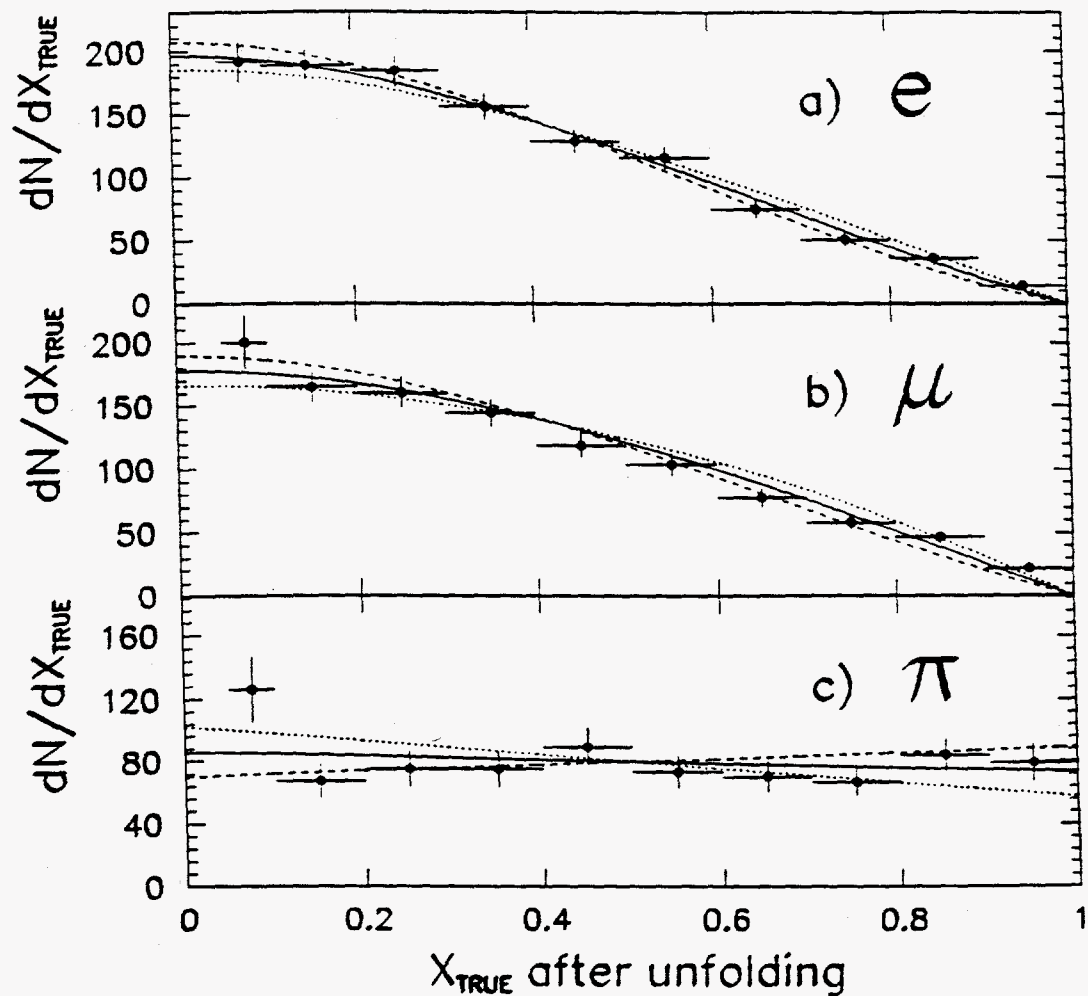


Figure 2.19: Final, unfolded, corrected momentum distributions for a) $\tau \rightarrow e\nu\bar{\nu}$, b) $\tau \rightarrow \mu\nu\bar{\nu}$, and c) $\tau \rightarrow \pi(K)\nu$ candidates. Data are indicated by points with error bars. The solid curves show the distributions corresponding to the fitted polarizations for each channel. The dashed/dotted curves show the distributions corresponding to values of polarization at ± 2 standard deviations from the fitted values. The error bars shown are the square roots of the diagonal terms of the error matrices for the unfolded distributions, but in fitting for polarization, full account is taken of the correlations among the unfolded bins, described by the off-diagonal terms of the error matrices.

efficiency-corrected, forward-backward polarization asymmetry of -0.22 ± 0.10 , implying $v_e/a_e = 0.15 \pm 0.07$. Imposing lepton universality and combining the forward and backward hemisphere measurements leads to $v/a = 0.05 \pm 0.04$ or $\sin^2 \bar{\theta}_W = 0.237 \pm 0.009$, where there is no ambiguity introduced by the relative signs of v and a .

Search for Lepton Flavor Violation in Z^0 Decays

We have performed a direct search for Z^0 decays into $e^\pm \tau^\mp$ and $\mu^\pm \tau^\mp$ using a sample of about 2×10^5 Z^0 decays which have been recorded with the OPAL experiment during 1989 and 1990. Such events can be identified by back to back low multiplicity jets with one electron or muon with an energy close to the beam energy. At least one of the τ decay products is a neutrino, which carries energy and momentum. The τ side can therefore be identified by its low visible energy.

One candidate is found for $Z \rightarrow e\tau$, 31 candidates for $Z \rightarrow \mu\tau$, and no candidates for $Z \rightarrow e\mu$. All observations are consistent with expected backgrounds, allowing the following 95% c.l. limits to be placed on such decays: $BR(Z \rightarrow e\tau) \leq 7.2 \times 10^{-5}$, $BR(Z \rightarrow \mu\tau) \leq 35. \times 10^{-5}$, and $BR(Z \rightarrow e\mu) \leq 4.6 \times 10^{-5}$.

τ Lifetime Measurement

The τ lifetime has been measured at OPAL using two independent techniques on the same τ -pair sample. Application of the impact parameter method to 1-prong tau decays, and decay length analysis of the 3-prong tau decays.

From the OPAL 1990 run at LEP 5130 $e^+e^- \rightarrow \tau\tau$ events have been isolated corresponding to an integrated luminosity of 6.3 pb^{-1} . The selection procedure used information from the central tracking detectors and electromagnetic calorimetry to identify events with two back-to-back collimated, low multiplicity jets. Time-of-flight measurements were used to reject cosmic ray events and muon identification to reject $e^+e^- \rightarrow \mu\mu$ events. Hadronic events were rejected by applying multiplicity cuts on the charged tracks and electromagnetic clusters. Total energy cuts allow a rejection of $e^+e^- \rightarrow e^+e^-$ events and two-photon processes. The angular region of acceptance covers the range $|\cos \theta_{thrust}| < 0.9$.

Figure 2.20 shows the decay length distribution for the three prong τ decays. Similar distributions are obtained for the impact parameter for one prong decays.

The final results of the two statistically independent measurements are respectively:

$$\tau_\tau = 0.294 \pm 0.013(\text{stat.}) \pm 0.021(\text{syst.}) \text{ ps}$$

$$\tau_\tau = 0.330 \pm 0.018(\text{stat.}) \pm 0.014(\text{syst.}) \text{ ps}$$

Future τ Analysis Projects

Our goals on τ physics are precision measurements of lepton universality, the forward backward charge asymmetry and the τ polarization. Accuracies in $\sin^2 \theta_W$ of 0.004 can be expected. We will also continue to perform detailed studies of the different τ decay modes. The searches for lepton flavor violation and neutrino singlet production will continue in the future.

OPAL 3-prong tau decay length distribution

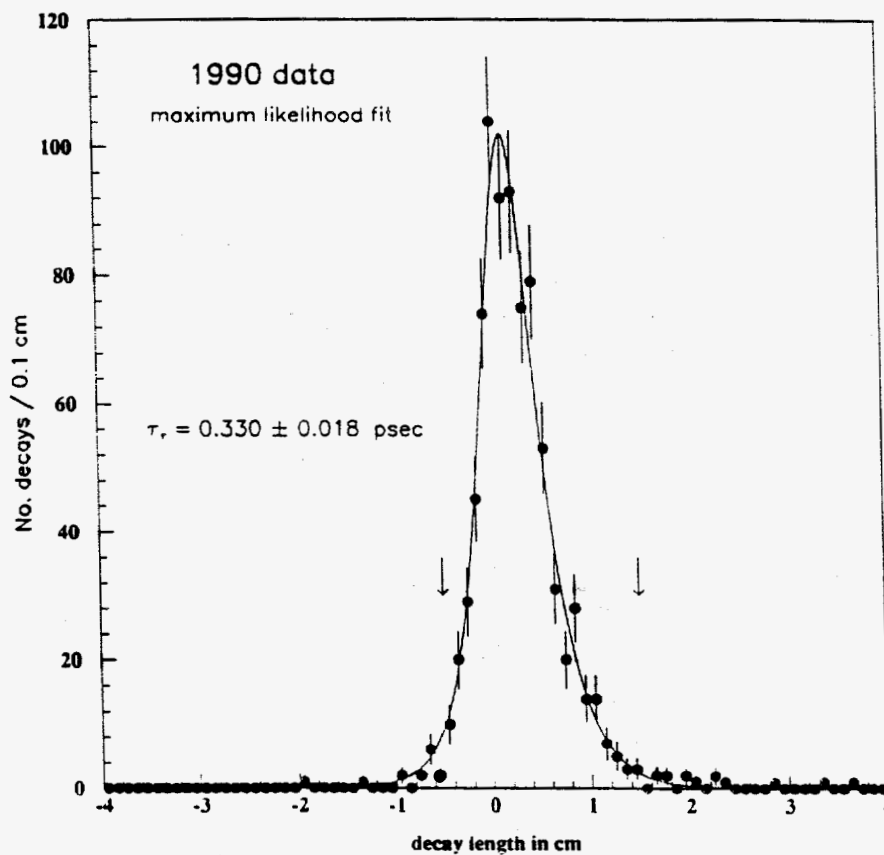


Figure 2.20: The maximum likelihood fit to the decay lengths from 1990 OPAL data. The fit was for the 799 events which had decay lengths within the range $[-0.5, +1.5]$ cm, and length error less than 0.5 cm.

2.3.8 Searches

There have been many different searches performed at LEP for signatures characteristic of new particles. In particular, searches have been made for the Higgs boson in minimal Standard Model form and for supersymmetric extensions, for fourth generation leptons, excited leptons, and leptoquarks. However the very impressive agreement between the predictions of the Standard Model and the measured lineshape of the Z^0 leaves very little room for new physics at LEP, and in fact no evidence for new physics has been reported. We update briefly the status of the principal searches that have been performed.

Very Light Standard Model Higgs

The OPAL detector has been used to set an upper limit on the decay of the Higgs boson to e^+e^- in the reaction $e^+e^- \rightarrow Z^0 \rightarrow Z^{0*} H^0$ as a function of the mass of the Higgs. In the context of the Standard Model, this study rules out a Higgs mass between 40 MeV and the threshold for decay into two muons. The limit does not extend below 40 MeV because as the Higgs mass decreases, an increasing proportion of the bosons are predicted to decay outside the detector volume. However, combining this analysis with that for unobserved Higgs decay, such as when the Higgs decays outside the detector, the Standard Model Higgs is ruled out for all masses up to the muon threshold.

The "Higgs Gap"

Higgs searches published by the OPAL Collaboration through the end of 1990 were characterized by a "gap" region between $2m_\mu$ and $3 \text{ GeV}/c^2$ where the Higgs could not be excluded. This was due to the fact that models used for Higgs boson decay were not considered accurate due to the presence of large QCD corrections to the couplings of the Higgs boson to its decay products. OPAL has recently presented the results of a new search in this gap region in which no assumptions are made about these couplings.

The standard mechanism for Higgs boson production at LEP is the "Bjorken Process," $Z^0 \rightarrow Z^{0*} H^0$. This search involves the "lepton channel" $Z^{0*} \rightarrow e^+e^-$ or $\mu^+\mu^-$, and the "neutrino channel" $Z^{0*} \rightarrow \nu\bar{\nu}$. The search is model independent in the sense that it is based on the kinematics of $Z^{0*} H^0$ production, where the Higgs boson recoils against the Z^{0*} with an average momentum of $7 \text{ GeV}/c^2$ in the mass region in question. Independence from Higgs boson decay models can be achieved in the following manner.

In the lepton channel analysis, the acoplanarity angle between the two leptons is required to be large, and the missing momentum (i.e., the momentum of the Higgs boson), constructed using the lepton momenta, is required to point into the acceptance of the detector. In this way the analysis is sensitive to all Higgs bosons of arbitrary decay mode, since requirements are placed only on the leptons. Only events whose topologies are consistent with known physics backgrounds, such as $l^+l^-\gamma$, $l^+l^-\gamma$, $\gamma \rightarrow$ conversion electron, and $l^+l^-\gamma\gamma$ with $m_{\gamma\gamma}$ large, are removed.

Although this veto makes the analysis insensitive to Higgs boson decays to photons, such decays are well covered by the search in the neutrino channel, where one looks for isolated electromagnetic activity in the detector. Hence the combined results from both channels, shown in Figure 2.21, are sensitive to any decay mode of the Higgs boson.

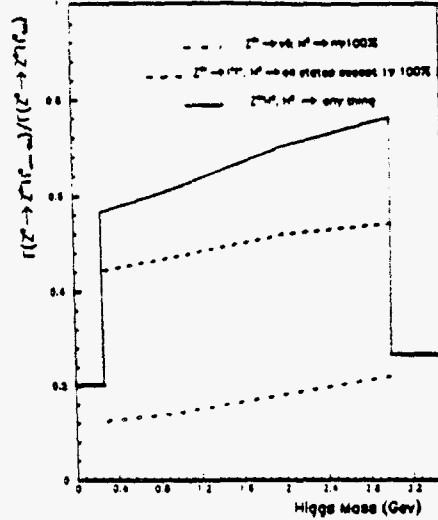


Figure 2.21: The OPAL 95% confidence level limits on the process $Z^0 \rightarrow Z^0 * h^0$, $Z^{0*} \rightarrow \nu\bar{\nu}$, $H^0 \rightarrow$ neutral states giving a single photon cluster, and $Z^0 \rightarrow Z^0 * h^0$, $Z^{0*} \rightarrow e^+e^-$, $\mu^+\mu^-$, $h^0 \rightarrow$ states other than a single photon cluster. Also shown is the 95% confidence level limit on the process $Z^0 \rightarrow Z^0 * h^0$, $h^0 \rightarrow$ anything.

Minimal Standard Model Higgs

The main focus of attention of Higgs searches has been in the high mass region. Here one again makes use of the Bjorken process, followed by the decay of the Higgs boson to heavy particles, either $b\bar{b}/c\bar{c}$ or $\tau^+\tau^-$, and the decay of the Z^{0*} to all possible fermion-antifermion pairs. Distinctive signatures with significant branching ratios are $H^0 \rightarrow b\bar{b}/c\bar{c}$ and $Z^{0*} \rightarrow \nu\bar{\nu}$, the missing energy channel; $H^0 \rightarrow b\bar{b}/c\bar{c}$ and $Z^{0*} \rightarrow e^+e^-$ or $\mu^+\mu^-$, the isolated lepton channel; and the $\tau\tau$ -jet-jet channel, in which either the Higgs or the Z^{0*} contributes the $\tau^+\tau^-$ pair. The search strategy in each of these channels is optimized for a mass reach from 25 to 50 GeV/c^2 . Concretely, as the supposed Higgs mass increases, its decay would change appearance from a monojet to a pair of jets. Analysis of the full event sample of 8.0 pb^{-1} leads to mass limit of $44 \text{ GeV}/c^2$ at the 95% confidence level.

Minimal Supersymmetric Model Higgs

In a more general case, two Higgs doublets are considered and the Higgs sector contains five physical Higgs bosons. A popular theory with such a Higgs sector is supersymmetry (SUSY). In the minimal SUSY Model (MSSM) one of the Higgs doublets couples to up-type fermions only, while the other couples only to down-type fermions, thus preventing flavor-changing neutral currents. Of the two neutral scalar Higgs bosons in this model, one (h^0) must be lighter than the Z^0 , while the other must be heavier than the Z^0 . There is also a charged Higgs pair which has to be heavier than the W , and a neutral CP-odd or pseudoscalar Higgs (A^0) which has to be heavier than the h^0 but can be lighter than the Z^0 and might therefore also be accessible to experiments running near the Z^0 resonance. In this model, two independent parameters are needed to specify the Higgs sector. There

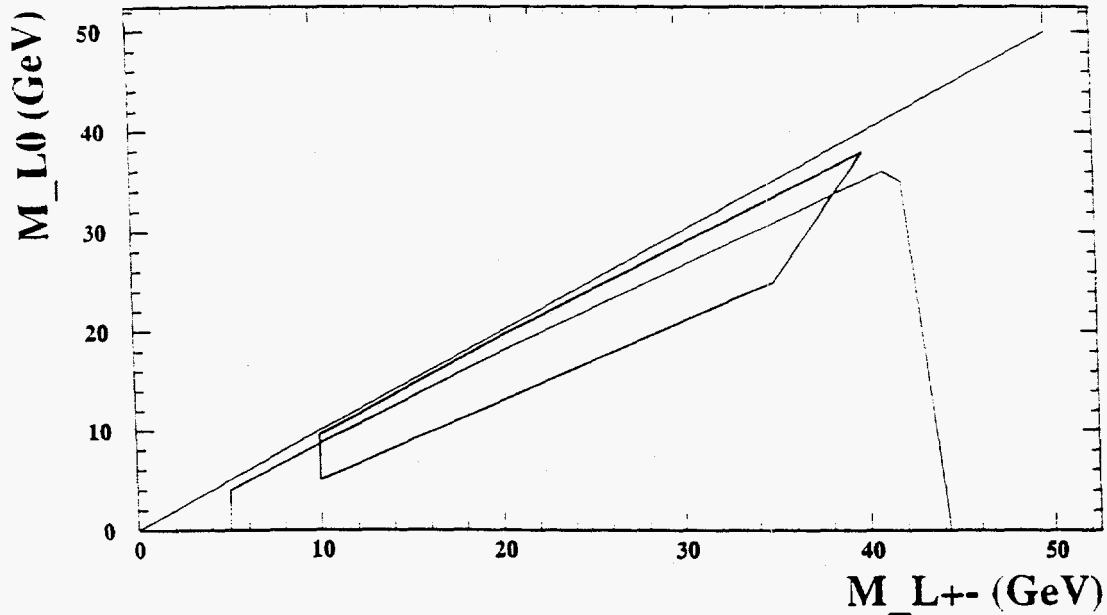


Figure 2.22: Exclusion contours at 95% confidence level in the $(M_{L\pm}, M_{L0})$ mass plane. The thin line is the mass limit from the missing p_T and E_{vis} analysis. The area surrounded by the thick line is excluded by the $L^+L^- \rightarrow e\bar{e}$ search.

are two common choices for these parameters: i) $\tan\beta = v_2/v_1$, the ratio of the vacuum expectation values of the doublets, and m_{h^0} , the mass of the lightest Higgs; and ii) m_{A^0} , and m_{A^0} , the mass of the pseudoscalar Higgs.

The search for the MSM Higgs described previously can be applied directly to the mode $Z^0 \rightarrow Z^0 h^0$ to exclude a significant region of the m_{h^0}, m_{A^0} parameter space. Consequently, the higher limit described above translates into an extension of the excluded region in the space. Other regions of the parameter space have been excluded using the decay $Z^0 \rightarrow h^0 A^0$, where the Higgs bosons could be identified by their decays into $c\bar{c}$, $b\bar{b}$, and $\tau^+\tau^-$. These processes must be examined separately for the assumptions $\tan\beta > 1$ (where $A^0 \rightarrow b\bar{b}, \tau^+\tau^-$ mostly) and $\tan\beta < 1$ (where $A^0 \rightarrow c\bar{c}$ predominantly). The m_{h^0}, m_{A^0} parameter space has been updated.

Heavy Leptons

Members of the UCR group Layter, Oh and Riles are preparing a publication which will describe a search for a new heavy lepton doublet with nonzero neutrino mass, using the entire data set. Although this analysis has much in common with a previous search with 1989 data, its primary value lies in greater sensitivity to the case of near degeneracy in mass for a large range in charged lepton mass. Two different search techniques have been used. The first, sensitive to lepton doublets over a wide range in mass splitting, is based on missing energy and missing momentum transverse to the beam. The second technique, sensitive to small mass splitting, is based on the presence of exactly two good charged tracks, one of which is identified as an electron and the other as a non-electron. For the case of a massless neutrino, a charged lepton is excluded at the 95% confidence level in

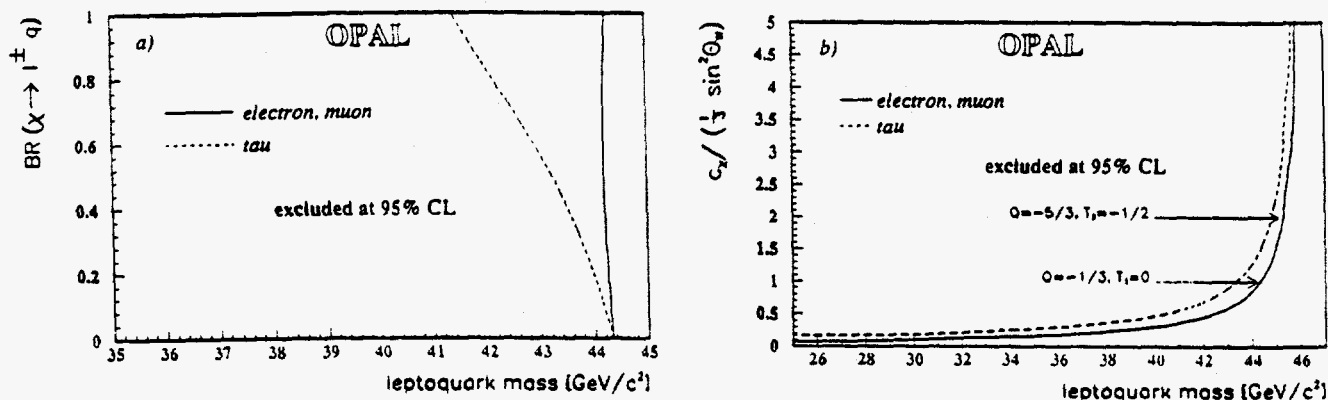


Figure 2.23: OPAL lower mass limit for leptoquarks as a function of the branching ratio for $q_\chi = -1/3, T_3 = 0$.

the mass range $5-44.3 GeV/c^2$. For a mass splitting $\approx 0.5 GeV/c^2$, the excluded range is $10-20 GeV/c^2$, as shown in Figure 2.22

Excited Leptons

A search for excited leptons has been carried out using the full data sample. The channels considered were $e^+e^- \rightarrow l^+l^-\gamma$ and $e^+e^- \rightarrow l^+l^-\gamma\gamma$. The search assumed that the excited lepton $l^* \equiv e^*, \mu^*, \text{ or } \tau^*$ is a spin $\frac{1}{2}$ particle and decays exclusively through $l^* \rightarrow l\gamma$. This newly updated search is essentially the same as that done last year and described previously, although some improvements have been made in the tau analysis.

Leptoquarks

Several models, including compositeness models, predict the existence of particles carrying lepton as well as baryon number. These leptoquarks, χ , could be pair produced at LEP if light enough. They would decay via $\chi\chi \rightarrow l^+l^-q\bar{q}$, where l can be a charged lepton or a neutrino. The OPAL Collaboration has searched for them using the signatures of two jets plus either two isolated leptons, an isolated lepton plus missing energy, or just missing energy alone. Limits are placed assuming minimal coupling, $c_\chi = 1/3 \sin^2 \theta_w$, which occurs for charge $1/3$ leptoquarks. The limit on m_χ is shown in Figure 2.23 as a function of the branching ratio to charged leptons. The limit is only dependent on the branching ratio to tau: for 100% branching to the tau the limit is $41.4 GeV/c^2$, which for 0% branching the limit is $46.4 GeV/c^2$.

2.3.9 Personnel

The OPAL experiment at LEP is the major project of our group, and our responsibilities include operation of the Hadron Calorimeter strip system, the online VAX computer in the OPAL data acquisition system, maintenance and development of online data acquisition and offline reconstruction software, and physics analysis.

The physicists participating in OPAL are M. Dittmar, J.W. Gary, W. Gorn, J.G. Layter, K. Riles, B.C. Shen, and G.J. VanDalen. Four graduate students C. Ho, W. Larson, H. Oh, and B. O'Neill, will complete their Ph.D. research this summer. E. Heflin will finish during this coming academic year, and J. Letts in about two years. P. Altice has worked on OPAL for two summers and will move to CERN next spring. We will accept two new students to replace the ones graduating. The University will also provide J.W. Gary sufficient funds for graduate students as part of his startup support. In addition we have one visiting scientist, Y. Yang, from the People's Republic of China who will be at CERN for the remainder of this year.

2.4 Neutrino Physics at LAMPF

Neutrino interactions have been used throughout the development of particle physics to study a wide range of fundamental questions including the nature of the electroweak interaction, lepton number conservation, and as a probe of cosmology. Low energy neutrinos, such as those available at LAMPF, offer significant advantages in testing the fundamental properties of the neutrinos themselves. In the decade of the 80's a series of experiments at LAMPF have measured neutrino interactions at low energies. Since 1982 several members of our group, notably William Gorn and Gordon VanDalen, have participated in an experiment at LAMPF which established significant limits in the search for neutrino oscillations [27].

We are now collaborating in a new program which is a natural successor to the previous experiment, and serves as a logical next step in the entire LAMPF neutrino program. The primary goal of the experiment is to search for neutrino oscillations to the levels of 10^{-2} eV² in mass difference and 2×10^{-4} in mixing. This greatly extends the range explored by accelerator based searches.

The new experiment, called the Large Scintillation Neutrino Detector, or LSND, will consist of 200 tons of dilute mineral oil-liquid scintillator located near the LAMPF beam stop neutrino source. The primary focus of LSND is neutrino oscillations, although a range of related neutrino interactions will also be investigated. The collaboration of 33 physicists from LAMPF and 5 universities has prepared a proposal which has been approved with the highest ranking by the Los Alamos PAC. The first stages of construction are taking place in 1990-91, and data acquisition with the complete detector will begin in summer of 1992.

2.4.1 The Detector

The detector is similar to a large water Cherenkov device but with better angular, position, and energy resolution due to more light collected from scintillation, and the improvements in Cherenkov imaging from higher index of refraction, longer radiation length, and lower density of mineral oil compared to water. The expected energy, position and angular resolutions for a 45 MeV electron are $< 5\%$, < 25 cm, and $< 15^\circ$ respectively. Protons are identified by the absence of a Cherenkov cone, and neutrons will be tagged by the 2.2 MeV photon from neutron absorption on a free proton. The superb event timing and vertex reconstruction allows us to separate neutrino induced events from pion decay in flight, decay at rest, and cosmic ray backgrounds using the 200 MHz fine structure in the LAMPF beam. The LSND detector is based on an extension of a technique that has been used in large water Cherenkov devices such as Kamioka and IMB. These detectors are capable of reconstructing the energy and direction of low-energy electrons through the Cherenkov light emitted in the liquid. Kamioka, in particular, has observed recoil electrons from solar neutrinos below 10 MeV. The technique of imaging-Cherenkov detectors for observing low-energy, simple-topology events is well established. Instead of using water as the target medium, it is proposed to use mineral oil with a refractive index of 1.47. This medium is composed approximately of CH_2 which is superior for detection of low-energy electrons by virtue of its lower density, higher refractive index, and lower radiation length. The

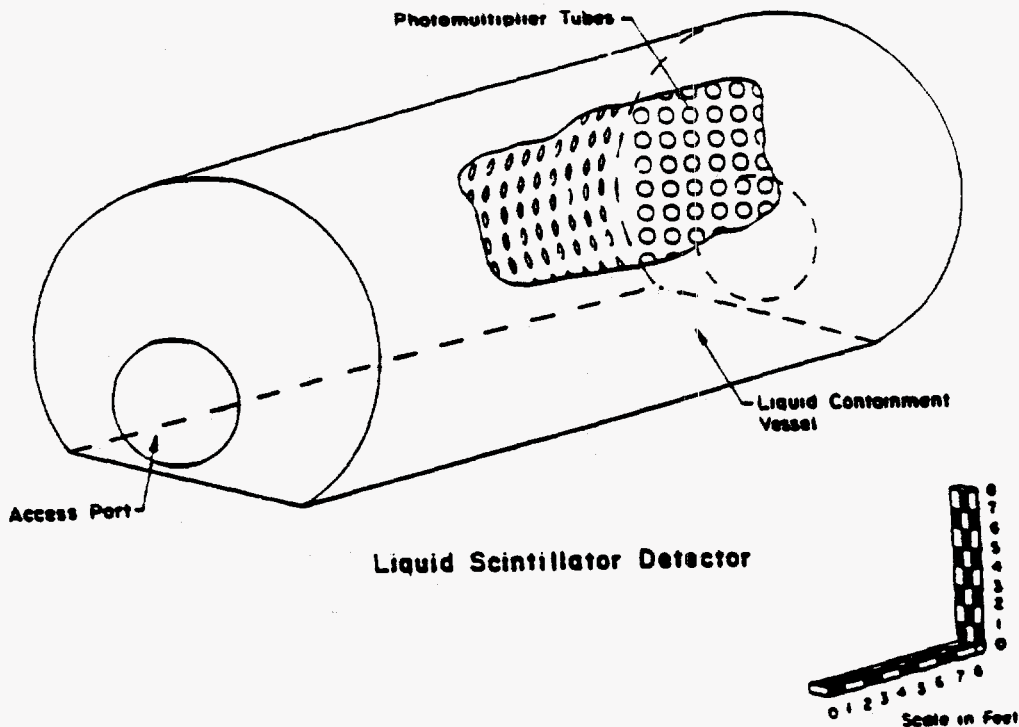


Figure 2.24: Schematic view of the LSND detector

addition of small quantities of scintillator to the mineral oil gives the additional benefit that the energy resolution is substantially improved and offers the possibility of detecting muons below Cherenkov threshold and low-energy neutrons - a crucial element in lowering the background to one of the oscillation signals in the detector. The performance that is expected in this experiment is dependent on the use of large-area, precise-timing phototubes that have been developed recently. All of these improvements in the imaging technique make it feasible to search for neutrino oscillations with high sensitivity at LAMPF.

The proposed detector is shown in Figure 2.24. It consists of a cylindrical tank of dilute mineral-oil-based liquid scintillator approximately 6 m in diameter by 9 m long with an active mass of 200 tons. The tank will reside inside the existing E645 veto shield, which is located 27 m downstream of the proton beam stop and is at an angle of approximately 17° to the beam direction. The tank will be made of 1 cm thick steel and have 1000 9" diameter, very low time jitter ($\sigma \sim 1$ ns) photomultiplier tubes mounted uniformly over the inside surface.

The 1000 9" photomultiplier tubes cover 28% of the surface area of the tank with sensitive photocathode. These tubes are manufactured by Hamamatsu and have excellent timing resolution, 2.3 ns FWHM for single photons and full-face illumination. They also have single photoelectron separation and typical noise rates < 10 kHz. Pre-production phototubes are being tested and evaluated within the collaboration.

We plan to use a dilute concentration of scintillator such that about 20% of the total light output will be Cherenkov light and 80% scintillation light. This concentration may vary after we perform further tests and optimizations. Mineral oil has advantages relative

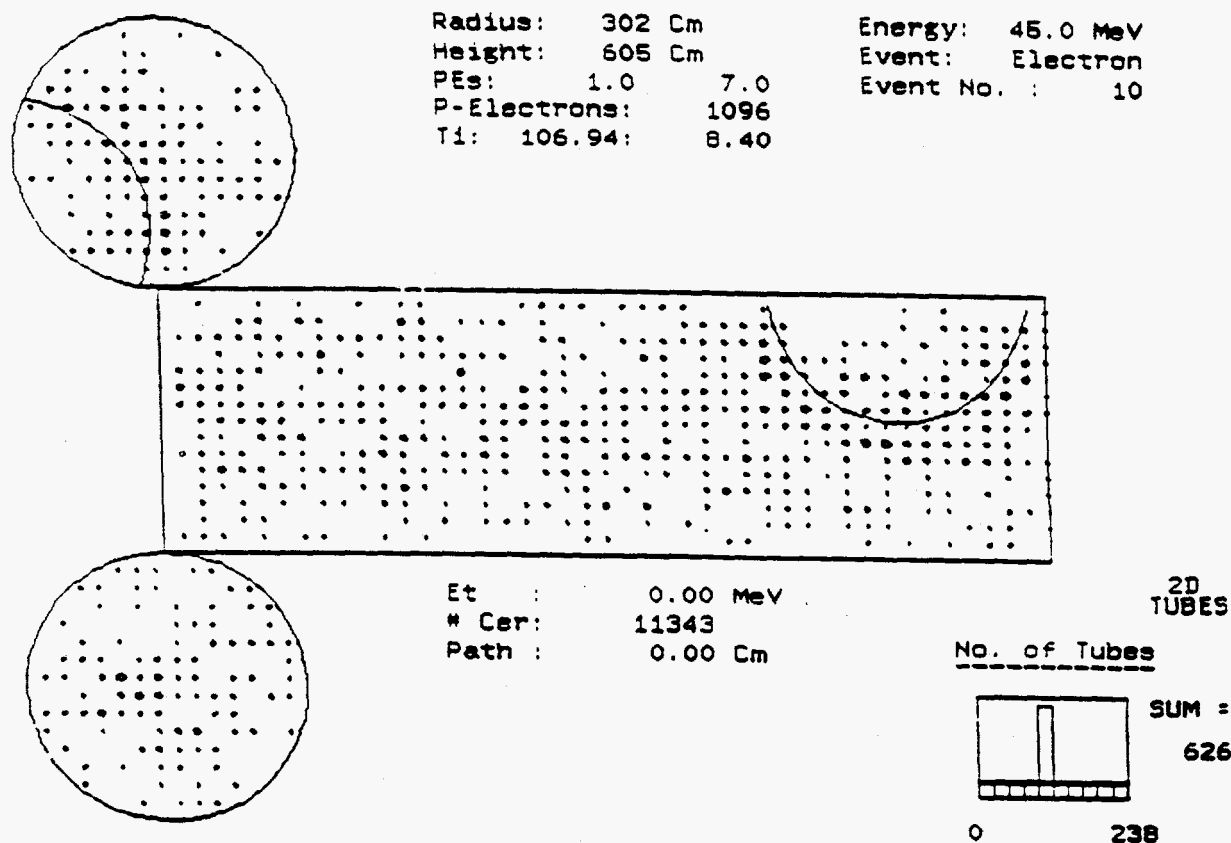


Figure 2.25: Monte Carlo event seen in the detector.

to water for the detection of Cherenkov light as it has a higher index of refraction, a lower density so that electrons travel farther before stopping, and a sharper Cherenkov ring due to the longer radiation length. The absorption and emission spectra of the scintillator

Figure 2.25 shows a typical 45 MeV electron event generated by the Monte Carlo. Each number corresponds to a hit photomultiplier tube and equals the number of photoelectrons. The detector cylinder has been unrolled to clearly show the phototube hit pattern. Note that the location of the Cherenkov ring can be seen by eye.

The front-end electronics and data acquisition system to handle the event triggers and above rates is being designed to record and selectively process the pulse histories (charge and time) of each of the 1000 photomultiplier tubes with minimal dead time and very high system reliability.

2.4.2 Event Rates

An estimate of LSND event rates is shown in Table 2.8 for events from pion decays at rest, and in Table 2.9 for neutrinos from pion decay in flight. All rates are per 130 days of running (one "LAMPF year").

| Process | Cross Section (cm ²) | Acceptance | Events | Comments |
|---|----------------------------------|------------|--------|--------------------------------|
| $\bar{\nu}_e \rightarrow e^+ n$ | 1.3×10^{-40} | 0.234 | 19,350 | max.-mixing, $E_e > 37$ MeV |
| $\nu_e {}^{12}\text{C} \rightarrow e {}^{12}\text{N}$ | 1.46×10^{-41} | 0.342 | 1588 | $E_e > 10$ MeV |
| $\nu_e {}^{13}\text{C} \rightarrow e {}^{13}\text{N}$ | 1.09×10^{-40} | 0.490 | 190 | $E_e > 10$ MeV |
| $\nu e^- \rightarrow \nu e^-$ | 4.0×10^{-43} | 0.331 | 340 | $E_e > 10$ MeV |
| $\nu C \rightarrow \nu C^*$ | 7.5×10^{-42} | 0.509 | 1215 | C^* emits 15.11 MeV γ |

Table 2.8: Event rates per 130 days for neutrinos from pion decay at rest.

| Process | Cross Section (cm ²) | Acceptance | Events | Comments |
|---------------------------------------|----------------------------------|------------|----------------|--------------------------------|
| $\pi^0 \rightarrow \nu \bar{\nu}$ | | 0.509 | $\approx 10^8$ | for B.R.=1 |
| $\eta \rightarrow \nu \bar{\nu}$ | | 0.509 | $\approx 10^4$ | for B.R.=1 |
| $\nu_\mu p \rightarrow \nu_\mu p$ | 4.5×10^{-40} | 0.234 | 1970 | $E_p > 20$ MeV |
| $\nu_e C \rightarrow e^- N$ | 3×10^{-39} | 0.509 | 14,310 | max.-mixing, $E_e > 60$ MeV |
| $\nu_\mu C \rightarrow \mu^- N$ | 6×10^{-40} | 0.283 | 910 | $E_\mu > 10$ MeV |
| $\bar{\nu}_\mu p \rightarrow \mu^+ n$ | 5×10^{-40} | 0.283 | 300 | $E_\mu > 10$ MeV |
| $\bar{\nu}_\mu C \rightarrow \mu^+ B$ | 1.5×10^{-40} | 0.283 | 45 | $E_\mu > 10$ MeV |
| $\nu_\mu C \rightarrow \nu_\mu C^*$ | 3.5×10^{-41} | 0.509 | 170 | C^* emits 15.11 MeV γ |
| $\nu_m u e^- \rightarrow \nu_m u e^-$ | 2.5×10^{-43} | 0.509 | 9 | $E_e > 10$ MeV |

Table 2.9: Event rates per 130 days for neutrinos from decay in flight.

2.4.3 The Physics

$\nu_\mu \rightarrow \nu_e$ Oscillations

A high-sensitivity search for $\nu_\mu \rightarrow \nu_e$ oscillations can be performed by using neutrinos with energies greater than ~ 80 MeV from pion decay in flight in the beam dump. If oscillations occur, then ν_μ neutrinos oscillate into ν_e neutrinos, which would be detected via the reaction $\nu_e C \rightarrow e^- N$. The event signature for these oscillations is a single high-energy electron with energy in the approximate range $60 < E_e < 180$ MeV. The lower-energy events in this range will be most useful for establishing an oscillation limit at low Δm^2 , while the higher-energy events will be most important at high Δm^2 .

Although only about 2.5% of the pions decay in flight before stopping in the A6 beam stop, the cross section for $\nu_e C \rightarrow e^- N$ rises rapidly with neutrino energy. A simulation of the A6 beam line has determined¹¹ the π^+ decay-in-flight neutrino flux at a distance of ~ 27 m from the beam stop to be $2.0 \times 10^{12} \nu_\mu/\text{cm}^2$ ($3.9 \times 10^{11} \bar{\nu}_\mu/\text{cm}^2$ from π^- decay in flight) for $E_\nu > 80$ MeV after 130 days of running at LAMPF (~ 3000 actual hours) or 8678 Coulombs. Using 5.9×10^{30} C nuclei, a $\nu_e C \rightarrow e^- N$ cross section¹³ of 2.8×10^{-39} cm^2 , and an acceptance of 0.513, we estimate the number of $\nu_e C \rightarrow e^- N$ events per 130 days for maximal neutrino mixing to be

$$(2.0 \times 10^{12})(2.8 \times 10^{-39})(0.513)(5.9 \times 10^{30}) = 16,950.$$

The $\nu_e C \rightarrow e^- N$ acceptance (0.513) is the product of the shield live time (86.0%), the 25 cm fiducial volume cut (66.3%), and the electron identification efficiency (90%), which results from rejecting possible proton events. The shield live time is the total live time and includes dead-time losses from the hardware trigger and the off-line analysis.

Our per-event sensitivity after two years of data collection is 2.9×10^{-5} , which is based on a total of 33,900 $\nu_e C \rightarrow e^- N$ events for maximal mixing. Using a background level of 3.8×10^{-4} , or 13 events, a 90% confidence level limit of 2.7×10^{-4} for $\nu_\mu \rightarrow \nu_e$ oscillations at $\Delta m^2 > 3 \text{ eV}^2$ can then be obtained. Note that the cosmic-ray background level can be precisely determined from the beam-off data, while the μ^+ decay-in-flight and $\pi^+ \rightarrow e^+ \nu_e$ background can be determined in two ways: from the Monte Carlo simulation and from fitting to the energy distribution, as the background energy distribution is different from the energy distribution of the oscillation signal. Figure 2.26 shows the limiting oscillation curve in the Δm^2 vs $\sin^2 2\theta$ parameter space, which is seen to be comparable to the $\bar{\nu}_\mu \rightarrow \bar{\nu}_e$ limiting oscillation curve discussed in the next section.

$\bar{\nu}_\mu \rightarrow \bar{\nu}_e$ Oscillations

A high-sensitivity search for $\bar{\nu}_\mu \rightarrow \bar{\nu}_e$ oscillations can be performed with neutrinos from muon decay at rest with energies greater than ~ 40 MeV. If oscillations occur, then $\bar{\nu}_\mu$ neutrinos oscillate into $\bar{\nu}_e$ neutrinos, which are detected via the charged-current reaction on a free proton, $\bar{\nu}_e p \rightarrow e^+ n$, followed by the capture of the recoil neutron on hydrogen. The event signature is an electron in the energy range $37 < E_e < 50$ MeV in coincidence with a 2.2 MeV γ from neutron absorption on a free proton within 1 m and 0.5 ms of the electron event. These position and time requirements may vary somewhat after data are obtained and a further optimization is performed.

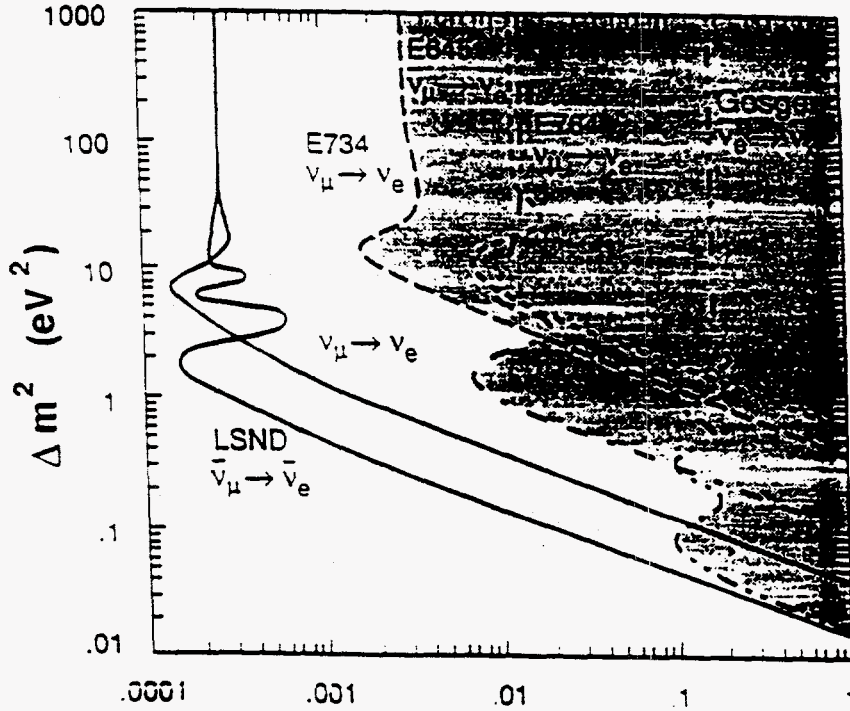


Figure 2.26: Limiting oscillation curve in the Δm^2 versus $\sin^2 2\theta$ parameter space for accelerator experiments.

A simulation of the A6 beam line has determined¹¹ the decay-at-rest neutrino flux at a distance of ~ 27 m from the beam stop to be $5.4 \times 10^{13} \nu_\mu / \text{cm}^2$ from pion decay at rest and an equal number of ν_e and $\bar{\nu}_\mu$ from muon decay at rest, after 130 days of running at LAMPF (~ 3000 actual hours) or 8678 Coulombs. Using 11.8×10^{30} free protons, a $\bar{\nu}_e p \rightarrow e^+ n$ cross section¹³ of $1.5 \times 10^{-40} \text{ cm}^2$, and an acceptance of 0.173, we can estimate the number of $\bar{\nu}_e p \rightarrow e^+ n$ events per year for maximal neutrino mixing to be

$$(5.4 \times 10^{13})(1.5 \times 10^{-40})(0.173)(11.8 \times 10^{30}) = 16,540.$$

The 0.173 $\bar{\nu}_e p \rightarrow e^+ n$ acceptance is the product of the shield live time (74.3%), the 25 cm fiducial volume cut (66.3%), the electron identification efficiency (90%), the fraction of events with $E_e > 37 \text{ MeV}$ (45.9%), and the recoil neutron detection efficiency (85.0%). The shield live time is the total live time and includes dead-time losses from the hardware trigger and the off-line analysis.

Our per-event sensitivity after two years of data collection is 3.0×10^{-5} , which is based on a total of 33,080 $\bar{\nu}_e p \rightarrow e^+ n$ events for maximal mixing. Using a background level of 3.9×10^{-4} , or 12.8 events in two years, a 90% confidence level limit of 2.7×10^{-4} for all $\bar{\nu}_\mu \rightarrow \bar{\nu}_e$ oscillations with $\Delta m^2 > 1 \text{ eV}^2$ can be obtained. For $\sin^2 2\theta = 1$, the 90% confidence level limit on Δm^2 is $1.7 \times 10^{-2} \text{ eV}^2$.

Note that the sensitivity estimates are reasonable because the cosmic-ray background level can be precisely determined from the beam-off data, while the μ^- decay-at-rest background can be determined from fitting to the combined energy distribution. Figure 2.26 shows the limiting oscillation curve in the Δm^2 vs $\sin^2 2\theta$ parameter space.

$\bar{\nu}_\mu \rightarrow \bar{\nu}_e$ Oscillations with PSR Neutrinos

A search for $\bar{\nu}_\mu \rightarrow \bar{\nu}_e$ oscillations at low Δm^2 can also be performed with neutrinos from the Proton Storage Ring (PSR). The event signature, an electron from the reaction $\bar{\nu}_e p \rightarrow e^+ n$ followed by the capture of the recoil neutron on hydrogen, is the same as discussed in the previous section, except that there is the additional constraint that the event time must correspond to within a few muon lifetimes with one of the short (270 ns) PSR spills. There is essentially no cosmic-ray, beam-neutron, or beam-neutrino background because the duty factor is so low ($\sim 10^{-4}$). This measurement will be done with the detector in the same location and concurrently with the measurements described above.

The event rate can be estimated by comparison with the last sections. As the PSR intensity is $\sim 100 \mu\text{A}$, the neutrino flux at a distance of ~ 209 m from the PSR beam stop is estimated to be $1.13 \times 10^{11} \nu_\mu / \text{cm}^2$ from pion decay at rest and an equal number of ν_e and $\bar{\nu}_\mu$ from muon decay at rest after 130 days of running at LAMPF (~ 3000 actual hours) or 8678 Coulombs. Using 11.8×10^{30} free protons, a $\bar{\nu}_e p \rightarrow e^+ n$ cross section¹³ of $1.5 \times 10^{-40} \text{ cm}^2$, and an acceptance of 0.233 we can estimate the number of $\bar{\nu}_e p \rightarrow e^+ n$ events per year for maximal neutrino mixing to be

$$(1.13 \times 10^{11})(1.5 \times 10^{-40})(0.233)(11.8 \times 10^{30}) = 46.$$

The 0.233 $\bar{\nu}_e p \rightarrow e^+ n$ acceptance is the product of the the 25 cm fiducial volume cut (66.3%), the electron identification efficiency (90%), the fraction of events with $E_e > 37$ MeV (45.9%), and the recoil neutron detection efficiency (85.0%). The acceptance does not include the 0.743 veto shield efficiency due to the low PSR duty factor.

Our per-event sensitivity after two years of data collection is 1.1×10^{-2} , which is based on a total of 92 $\bar{\nu}_e p \rightarrow e^+ n$ events for maximal mixing. As there is essentially no background, a 90% confidence level limit of 2.5×10^{-2} for $\bar{\nu}_\mu \rightarrow \bar{\nu}_e$ oscillations can be obtained at the peak sensitivity of $\Delta m^2 = 0.2 \text{ eV}^2$. For $\sin^2 2\theta = 1$, the 90% confidence level limit on Δm^2 is $3 \times 10^{-2} \text{ eV}^2$. Figure 2.26 shows the oscillation limit in the Δm^2 vs $\sin^2 2\theta$ parameter space. This $\bar{\nu}_\mu \rightarrow \bar{\nu}_e$ oscillation limit would be comparable to the limit obtained in the previous section for low values of Δm^2 .

Neutrino Oscillation Summary

LSND does two largely independent neutrino oscillation experiments with similar sensitivities that can be performed concurrently. Simply stated, one experiment looks for high-energy ν_e ($80 < E_\nu < 200$ MeV) produced by conversion to ν_e of the ν_μ from the decay-in-flight component of the beam-dump neutrino beam. Simultaneously, another experiment looks for low-energy $\bar{\nu}_e$ produced by conversion of $\bar{\nu}_\mu$ ($40 < E_\nu < 53$ MeV) from the decay-at-rest component of the same beam. In each experiment the incident beam, the event signature, and the backgrounds are different. Consequently, with similar sensitivities as shown in Figure 2.26, the two experiments (plus the PSR experiment) provide important redundancy in addition to significantly wider coverage of the $\Delta m^2 - \sin^2 2\theta$ space than all previous accelerator searches for $\nu_\mu \rightarrow \nu_e$ ($\bar{\nu}_\mu \rightarrow \bar{\nu}_e$) oscillations combined.

The experimental techniques involved in accomplishing these searches are not especially demanding. The use of dilute mineral-oil-based liquid scintillator to allow the ener-

getic electrons (positrons) to be detected by Cherenkov radiation and the neutron capture 2.2 MeV gamma ray (from $\bar{\nu}_e p \rightarrow e^+ n$) to be identified by scintillation light is novel. It is worth pursuing in its own right for other possible applications and can be empirically validated in a reasonable scale prototype well before large-scale construction begins.

From the experience gained by E645, several members of which are also members of the LSND collaboration, the backgrounds in the LAMPF neutrino area are well understood. It is unlikely that any appreciable surprise will come from that quarter.

It is possible that appreciable running time with the pulsed proton beam from the PSR may be acquired by LSND, again at the same time as the data-taking described above. This additional attack on the neutrino oscillation problem is less sensitive to low mixing strength at large Δm^2 than the high beam intensity experiments, but it has good Δm^2 sensitivity in the region of large mixing.

In short, neutrino oscillation searches proposed for LSND constitute a powerful program aimed at physics of topical interest and with every likelihood of successful achievement of that aim. Furthermore, the program makes use of and builds on the investment in and the experience gained from the previous neutrino oscillation experiments at LAMPF.

Other Physics

There are many other physics objectives that can be pursued with the liquid scintillator detector. Searching for $\bar{\nu}_\mu \rightarrow \bar{\nu}_e$ oscillations is equivalent to searching for the lepton number violating decay $\mu^+ \rightarrow e^+ \nu_\mu \bar{\nu}_e$. Limits on this decay are directly comparable to limits on neutrino oscillations, so that we should be sensitive to branching ratios as low as 10^{-4} . A branching ratio limit this low would be very interesting theoretically,¹⁹ and would complement present searches for muonium-antimuonium conversion.

The $\nu C \rightarrow \nu C^*$ (15.11 MeV γ) neutral-current reaction, one of the only neutrino-nuclear neutral-current reactions that can be easily observed, will be measured to approximately 10% accuracy and will be recognized by the detection of the 15.11 MeV γ emitted by the excited carbon nucleus when it decays to the ground state. Our energy resolution at 15 MeV is $< 10\%$, so that we should observe a peak in the 13.5-16.5 MeV range. A precision measurement of this process is especially important because it allows a calibration of the calculations used in current models of neutrino-nucleus interactions during supernova bursts. We are able to measure this reaction at two energies, at about 30 MeV using decay-at-rest neutrinos and at about 150 MeV using decay-in-flight neutrinos, and we are able to separate these two classes of events with the 200 MHz LAMPF beam structure as the decay-in-flight events will be synchronous with the proton spill RF structure.

The rare decays $\pi^0 \rightarrow \nu \bar{\nu}$ and $\eta \rightarrow \nu \bar{\nu}$, followed by $\nu_e C \rightarrow e^- N$, can be searched to sensitivities of about 10^{-8} and 10^{-4} , respectively, with very little background because the neutrinos from these decays are extremely energetic. These decays are forbidden for massless Weyl neutrinos and can proceed only if neutrino states of both chiralities exist or if lepton number is not conserved.²⁰ The current best limits for these decays are $\Gamma(\pi^0 \rightarrow \nu_e \bar{\nu}_e)/\Gamma(\pi^0 \rightarrow \text{all}) < 5.0 \times 10^{-7}$ and $\Gamma(\eta \rightarrow \nu_e \bar{\nu}_e)/\Gamma(\eta \rightarrow \text{all}) < 1.0 \times 10^{-3}$ from the LAMPF E645 experiment.²¹ The expected branching ratios of these decays in the standard model for reasonable neutrino masses are much lower than our sensitivities; however,

branching ratios as large as the current limit are possible in various phenomenological models.²⁰

We shall also measure the $\nu_e C$ and $\nu_\mu C$ charged-current scattering cross sections and the νe elastic scattering cross section to approximately 10–15% accuracy. These measurements would test present theories of neutrino-nucleus scattering and provide an estimate of $\sin^2\theta_W$, the fundamental parameter of the standard model of electroweak interactions. The electron angular distribution in the νe elastic scattering process is strongly peaked in the neutrino direction, while it is slightly peaked in the backward direction for the charged-current reaction. The $\nu_e C \rightarrow e^- N$ charged-current interaction is dominated by ^{12}C , as the fraction of ^{13}C nuclei is only about 1.1% of the total. Nevertheless, we shall be able to measure the ^{13}C component separately due to the larger $\nu_e^{13}C \rightarrow e^- N$ cross section and the higher electron energy.

Finally, we will obtain a large sample of neutrino-proton elastic-scattering events, where the neutrinos are from pion decay in flight. The cross section for $\nu p \rightarrow \nu p$ is proportional to $G_A^2 + F_1^2 + Q^2/4/m_p^2 F_2^2$ at low Q^2 . The term involving G_A is dominant, and a measurement of the cross section at low Q^2 affords a method of measuring G_A directly. The principal component of G_A is isovector, which is known from neutron decay at low Q^2 . Any additional contribution (an isoscalar term, for example) would affect the total cross section. We expect to make a preliminary search for recoil protons from neutrino-proton elastic scattering in the 20 to 60 MeV range. These protons will be coherent with the beam spill from LAMPF in contrast to proton recoil from cosmic-ray or beam neutrons. A preliminary estimate of this background gives a signal to noise as evidenced by the 200 MHz RF time structure of about 1.

2.4.4 Personnel

Construction of the LSND began in 1990-91 and continues in 1991-92. Data acquisition with the LAMPF beam should extend through 1992-1993 (setup and testing), and 1993-95 (physics data). UC Riverside is primarily responsible for the data acquisition computing hardware and software. This will draw heavily on the very successful OPAL data acquisition system. UCR is also involved in phototube testing and front-end readout design.

In 1991-92 a research assistant (William Strossman) will work on data acquisition and tube testing. A post-doc will be hired with university funds. In 1992-93 a second research assistant will be hired. W. Gorn and B. O'Neill will participate in the design of the data acquisition system. Since this system will borrow heavily from the existing OPAL data acquisition system, the design work requires relatively little time. G. VanDalen and B. Shen will devote approximately 15% of their research time to the LSND project.

2.5 Muon Experiment at the SPS

One of the most fundamental questions to be answered in the next decade is the physics origin of the electroweak symmetry breaking and how the particles acquire their masses. Within the minimum version of the Standard Model, spontaneous symmetry breaking through the Higgs mechanism leads to the existence of a spin zero particle, the Higgs boson H . The searches carried out at LEP have found no evidence for the Higgs up to a mass of 45 GeV. With LEP200 the search will have a sensitive range up to the mass of the Z^0 . Although there is no definitive theoretical prediction of the mass of the Higgs, it is expected to be below a few TeV. Therefore, the search for the Higgs boson will be the most important physics goal of the next generation of colliders.

We have begun participating in an approved experiment, RD5, at the CERN SPS to study muon triggering and momentum reconstruction in a strong magnetic field for a muon detector at a high energy collider such as LHC or SSC. The primary goal of this experiment is to study the feasibility of triggering on the production of Higgs bosons which decay into Z^0 's leading to four muons among the final state particles. We intend to study a number of questions which are crucial to the successful use of muon triggers in such a detector: the rate of muons from hadron punchthrough and decays, the efficiency of triggering using transverse momentum cuts, and the precision in momentum reconstruction required for identifying the Higgs. This short term program (scheduled for two to three years) will use the test beam at the CERN SPS. The results of this experiment will be of great benefit in the design of a detector at the next high energy hadron collider.

2.5.1 Physics

In final states with four muons, the produced Higgs can decay into two real Z^0 's if the Higgs mass is greater than twice the Z^0 mass. For the Higgs mass between 130 GeV and $2m_Z$, the Higgs decays into one real Z^0 and one virtual Z^0 . The main background consists of $Z^0 Z^0$ continuum:

$$pp \rightarrow \mu^+ \mu^- \mu^+ \mu^- X$$

and a non-resonant part for which at least one muon pair does not arise from a Z^0 . [25] In this case the dominant contributions are pair-produced top quarks and $Z^0 b\bar{b}$:

$$pp \rightarrow \tau^+ \tau^- X \text{ or } Z^0 b\bar{b} X \rightarrow \mu^+ \mu^- \mu^+ \mu^- X.$$

The invariant mass distributions of the four muons are shown in Figure 2.27 for the background in comparison with the Higgs signal for masses of 200, 400, and 700 GeV. A center of mass energy of 16 TeV, corresponding to that of the LHC, is assumed. The requirements of $p_T > 20$ GeV/c and pseudo-rapidity less than 2.5 for each muon and the requirement for muon pair masses within 16 GeV of the Z^0 reduce the non-resonant background well below the resonant $Z^0 Z^0$ background. The assumed momentum resolution of 1.5% achievable with 3 m of iron magnetized to 1.8 T is adequate to resolve the signal from the background except for the very low mass region.

Using the reconstructed muon momenta from the constraint that the muon pair mass be that of the Z^0 mass greatly improves the resolution in the low mass region as shown

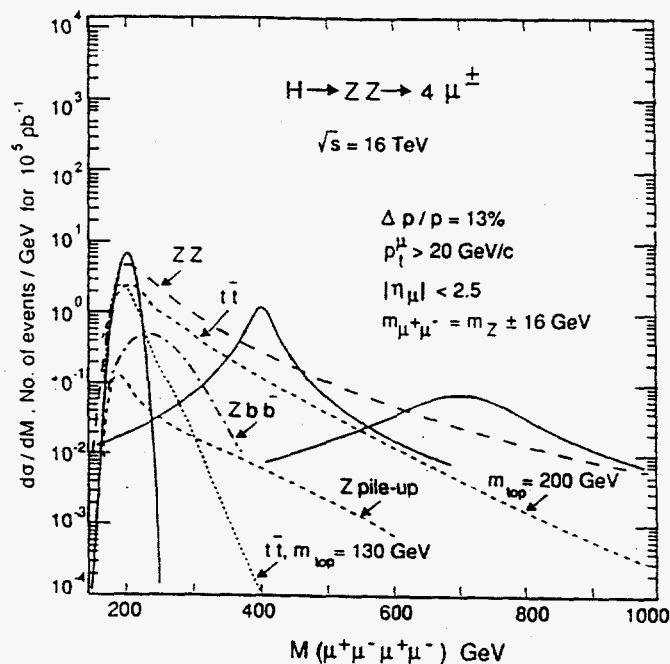


Figure 2.27: Higgs signal in the $H \rightarrow ZZ \rightarrow 4\mu^\pm$ channel, and $4\mu^\pm$ backgrounds, assuming 13% resolution.

in Figure 2.28 For mass regions below 200 GeV the Z^0 mass constraint can only be used once since only one of the Z^0 s is real. In order to maintain good acceptance the p_T cut has to be lowered, resulting in an increase in the background. As a result the dominant background comes from the pair-produced top quarks. If a tight mass cut can be placed on the muon pair this background can be greatly reduced. The reconstructed muon pair invariant mass distribution is shown for the momentum resolution of 15% and $0.2p_T(\text{TeV})$ for comparison in Figure 2.29. As can be seen, the excellent mass resolution at 100 GeV allows a narrow mass cut of 5 GeV and in turn a significant improvement in the signal to background ratio. Therefore good momentum resolution is an important consideration in detector design.

The acceptances of muons in rapidity and transverse momentum are also important design parameters for a collider detector. The acceptances of a Higgs boson decaying into four muons as a function of transverse momentum is shown in Figure 2.30, and as a function of rapidity in Figure 2.31. For high-mass Higgs particles which are centrally produced, the chosen rapidity interval of $|\eta| < 3$ and a p_T cut of 10 GeV/c presents little detection loss. For low-mass Higgs a larger acceptance in rapidity would be desirable. However, the muon trigger becomes increasingly difficult in the forward directions because of the rapidly increasing particle densities. There are also further demands on detector capabilities in the identification and momentum measurement of the muons at large rapidities.

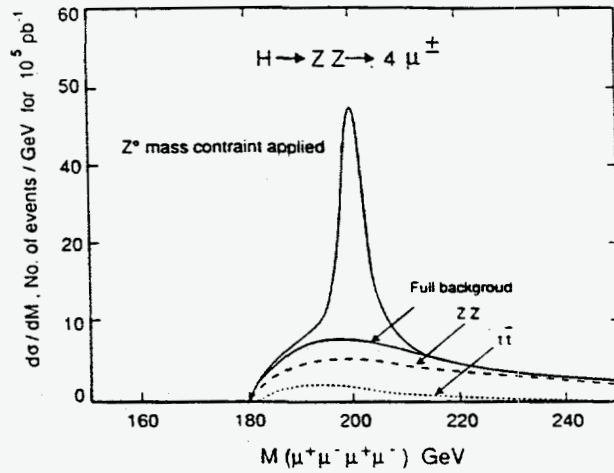


Figure 2.28: The four muon invariant mass distribution for a Higgs mass of $200 \text{ GeV}/c^2$, but with Z mass constraint. Background contributions are as indicated.

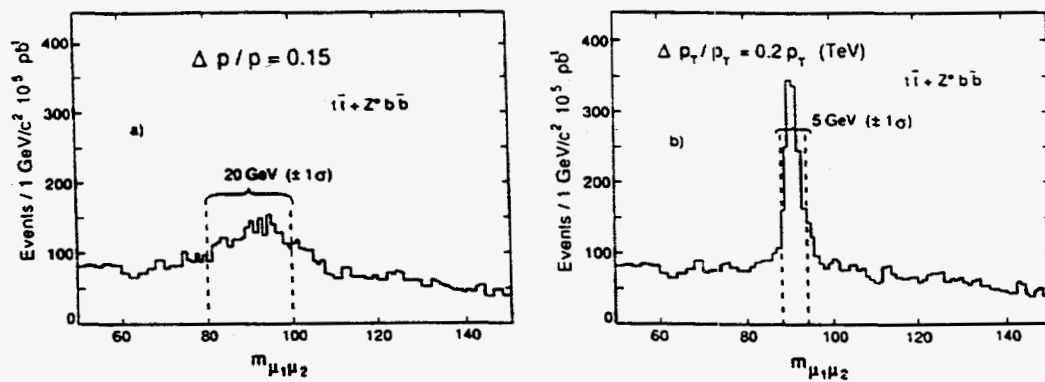


Figure 2.29: Reconstructed μ -pair invariant mass for a) 15%, and b) $0.2p_T(\text{TeV})$ momentum resolution.

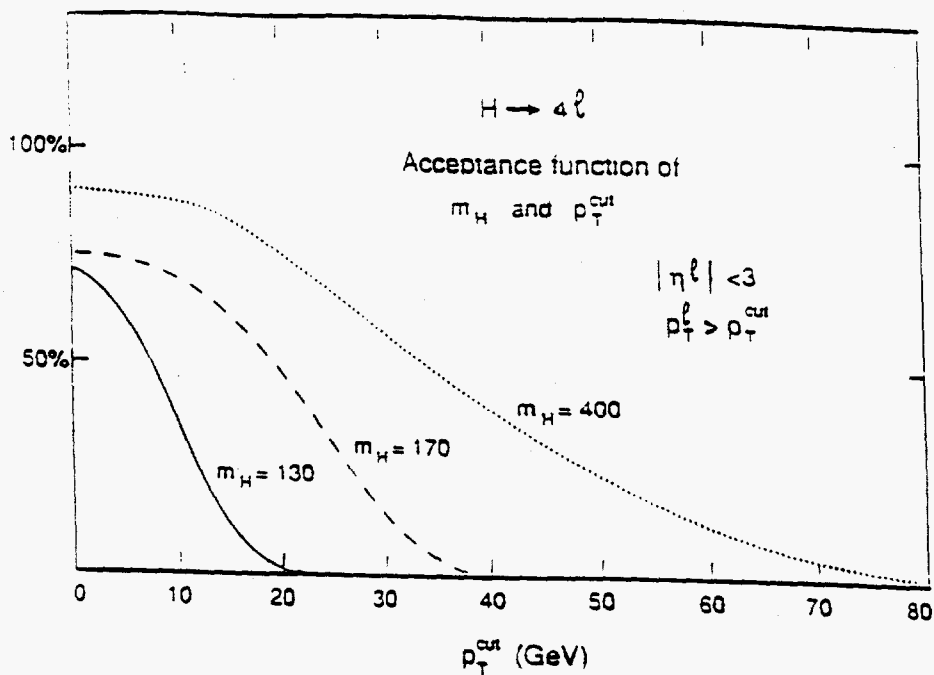


Figure 2.30: Efficiency to detect $H \rightarrow 4\mu^\pm$ for $|\eta| < 3$ as a function of p_T cut for various Higgs masses.

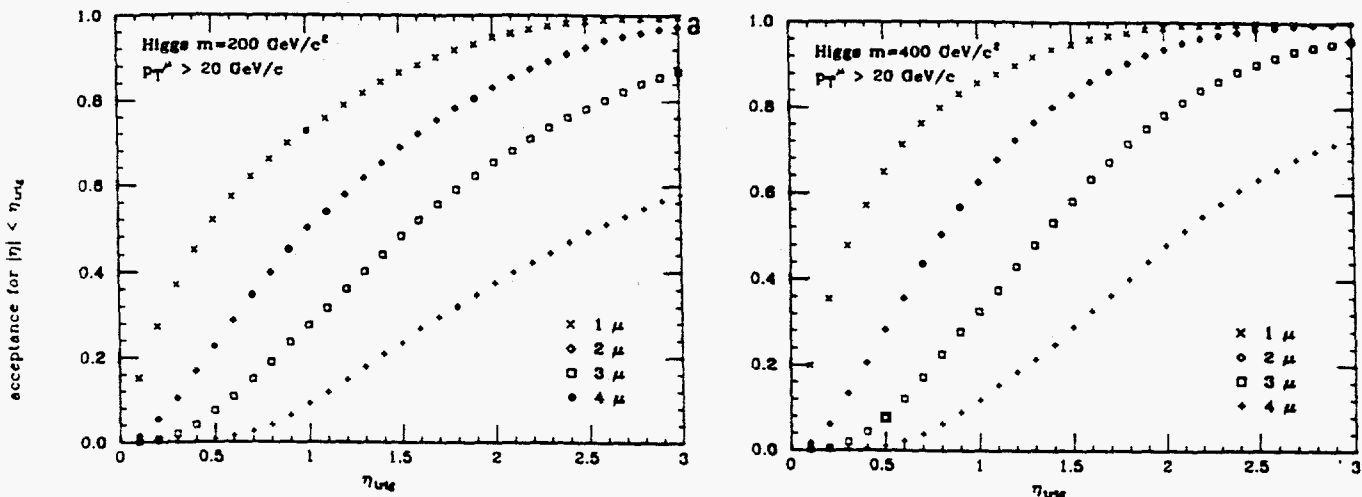


Figure 2.31: Acceptance for detecting the Higgs boson through the process $H^0 \rightarrow Z^0 Z^0 \rightarrow \mu^+ \mu^- \mu^+ \mu^-$ when n muons ($n = 1, 2, 3, 4$) are detected in the pseudorapidity region $|\eta| \leq \eta_{\text{trig}}$. The p_T cut applied for all muons is $20 \text{ GeV}/c$.

2.5.2 Experimental Program

Physics requirements for muon detection at a high energy hadron collider can be summarized as follows:

1. Muons must be identified over a large pseudorapidity range ($|\eta| < 3$), down to transverse momentum as low as $p_T = 5$ GeV/c,
2. Muon momentum should be measured up to about 3 TeV/c with resolution better than 10%.
3. Improved momentum resolution better matched to the natural resolution of the Z^0 peak is desirable for the detection of low-mass Higgs.

The main objective of this project is to demonstrate that an efficient trigger can be constructed utilizing the topological properties of tracks in a strong magnetic field to efficiently reject muons from secondary decays and hadronic punch-throughs. The principle is shown in Figure 2.32 which presents a segment of a possible compact muon solenoid detector, on which is superimposed a muon track. The angle α in the figure is related to the transverse momentum of the track. The effect of a cut on the angle on the various components of the single muon and dimuon rate is shown in Figure 2.33. Requiring a coincidence between "Station 1" and "Station 2" would discriminate against hadronic punch-throughs.

The apparatus to be used for the experiment is illustrated schematically in Figure 2.34. The similarity to the detector of Figure 2.32 is readily apparent. Several completed CERN experiments will be cannibalized to provide the equipment at low cost. In particular, the muon chambers at Stations 1 through 3 will come from the UA1 experiment. The possibility that additional hits at the Station 1 level could produce spurious coincidences with Station 2 leads to the desirability of having additional information to make a connection between these two positions. Devices developed at Rome and known as resistive plate chambers [26] (RPCs in Figure 2.34) could provide a fast detector element of sufficient precision for this purpose. The examination of the performance of these devices is another important objective of this experiment.

An additional objective of the project is the study of the momentum resolution that can be achieved in such a detector, taking into account the effects of catastrophic energy losses and of delta rays and additional hits from the tails of hadronic jets on pattern recognition and tracking. This will be done with muon beams of known beam energies. The efficiency of the proposed trigger for muons can of course be determined at the same time.

2.5.3 UCR Participation and Schedule

The Riverside group has agreed to participate in the implementation of the muon chambers. This involves dismounting the chambers, with their associated high voltage supplies and readout electronics, from the UA1 experiment and reassembling them in place at the SPS North Hall. Modifications will have to be made to the mechanical structure of the chambers and to the signal processing electronics. In this effort they will work with one

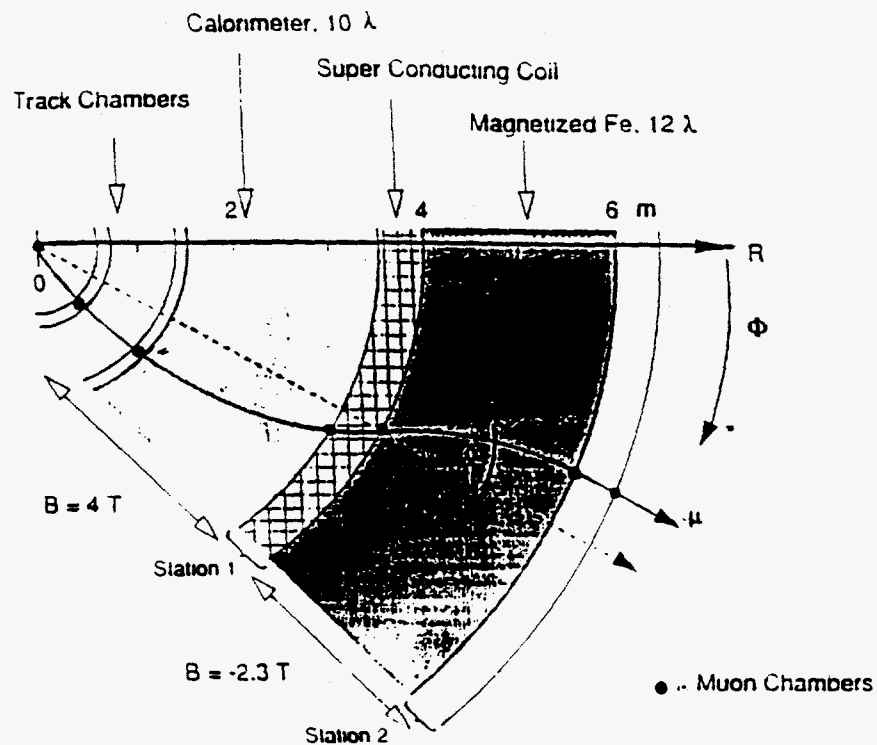


Figure 2.32: Transverse view of the Compact Muon Solenoid detector with superimposed particle trajectory.

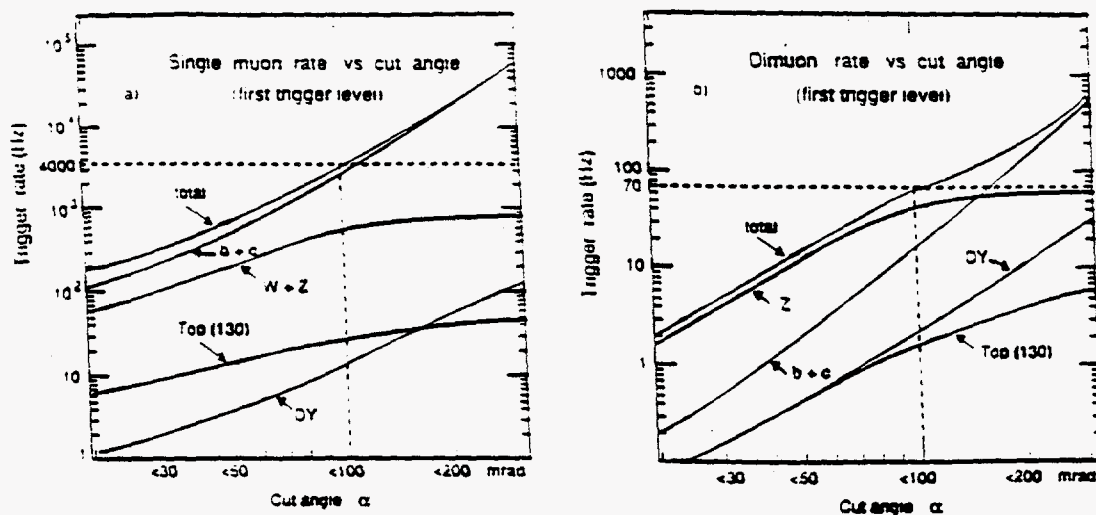


Figure 2.33: Expected first level trigger rates from muons as a function of the coil angular cut for a luminosity of $4 \times 10^{34} \text{ cm}^{-2} \text{ sec}^{-1}$: a) Single muons, b) Dimuons.

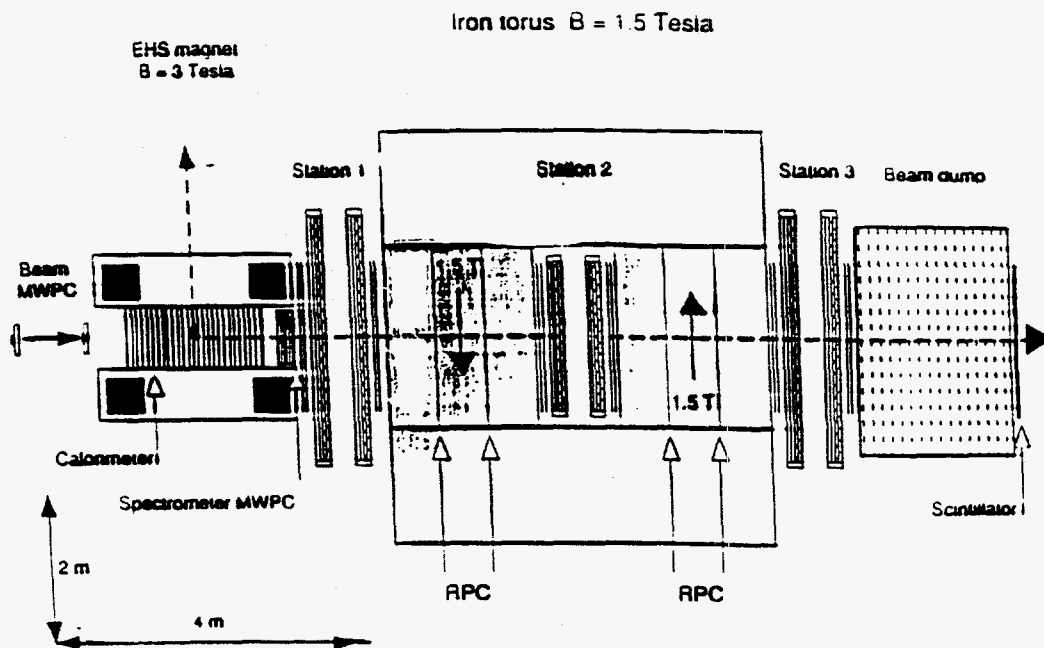


Figure 2.34: Plan view of the experimental setup proposed for the experiment RD5.

or more persons from the Aachen group which originally constructed the chambers, and possibly by members of one or two other groups in the Collaboration.

In addition the Riverside will see to the incorporation of surveying information into the simulation and reconstruction programs. It is expected that existing UA1 code can be adapted for the reconstruction subroutines themselves. Also Riverside will contribute electronics modules to interface the readout electronics to the data acquisition system, and workstations for use in online monitoring and offline data analysis.

The first beam test is scheduled for the period August 16 - September 10. The installation of components has progressed according to schedule. The beam time during 1991 will be used for the check-out of the subdetectors and the data readout system, as well as the acquisition of initial data. The EHS magnet will not be powered during 1991, as the cryogenic system is in use elsewhere and will be available only after 1991. The entire system will be operating for the second beam run in 1992. Further running in 1993 will be scheduled if additional data are required.

Members of the Riverside group involved in this experiment include W. Gorn, J.G. Layter, and B.C. Shen. In addition, a technician/research associate and a graduate student will participate in the project.

2.6 Replacing the VAX-8700 in OPAL Data Acquisition System

When the UCR group joined the OPAL collaboration in 1985, it was agreed that our group would contribute in two areas toward the OPAL detector: the VAX-8700 system in the data acquisition, and the segmented strip readout in the hadron calorimeter. It was further agreed that our group would assume the financial responsibility in providing the hardware for the VAX-8700 package and the manpower in the implementation of the hadron strip readout, with OPAL providing 350,000 SF toward the initial cost of the strips detector and electronics. An exceedingly competitive price of \$500,000 was offered by regional Digital Equipment Corp on the VAX-8700 package at more than a 50% discount. The University contributed \$100,000 toward the purchase and provided an interest free loan for the remaining \$400,000, which was provide by DOE over five installment payments.

The VAX-8700 and associated peripheral devices constitute the central component of the OPAL data acquisition system as shown in Fig.fig-exist. It has performed this important function well in providing OPAL with high efficiency data taking. As a result, OPAL managed to recorded the largest amount of data for luminosity delivered among the four LEP experiments. However, the VAX-8700 system is rapidly becoming inadquate because of the high data rate on the one hand and overly expensive to maintain on the other. Maintenance costs for the existing system are 13 KSF per month. The OPAL collaboration has conducted an extensive review and decided that the VAX-8700 system be replaced by an upgraded configuration at the end of the 1991 running period. The new configuration, based on a dual VAX-4300 system, as shown in Fig.fig-config is designed to be adequate for the remaining running of LEP and the upcoming operation of LEP-200 from 1994 to 1997 at a minimum cost for hardware and maintenance. Taking advantage of the initial warranty period, maintenance costs for the first year will be 3000 SF per month, rising to about 4500 SF per month thereafter.

Since the central component of the OPAL data acquisition system has been the responsibility and the only financial contribution of our group, we are obligated toward this upgrade. The cost of the new system is listed below.

UAX 8700

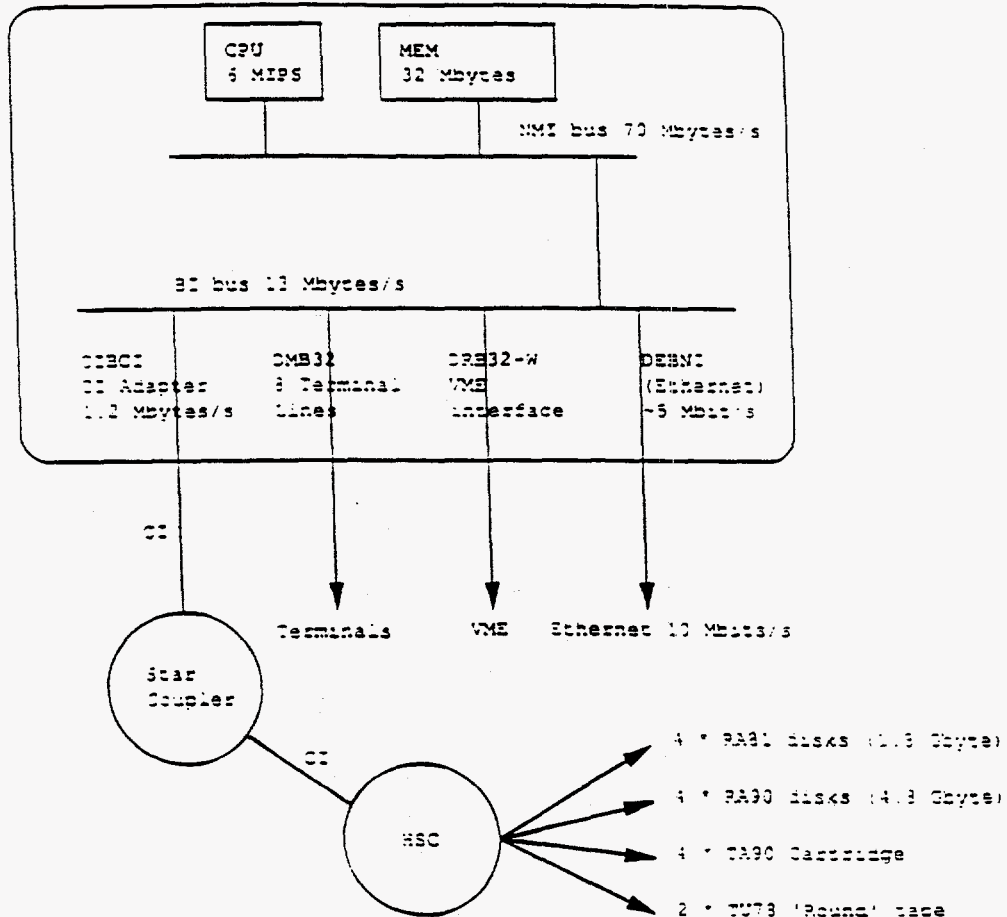


Figure 2.35: Existing On-Line VAX Configuration

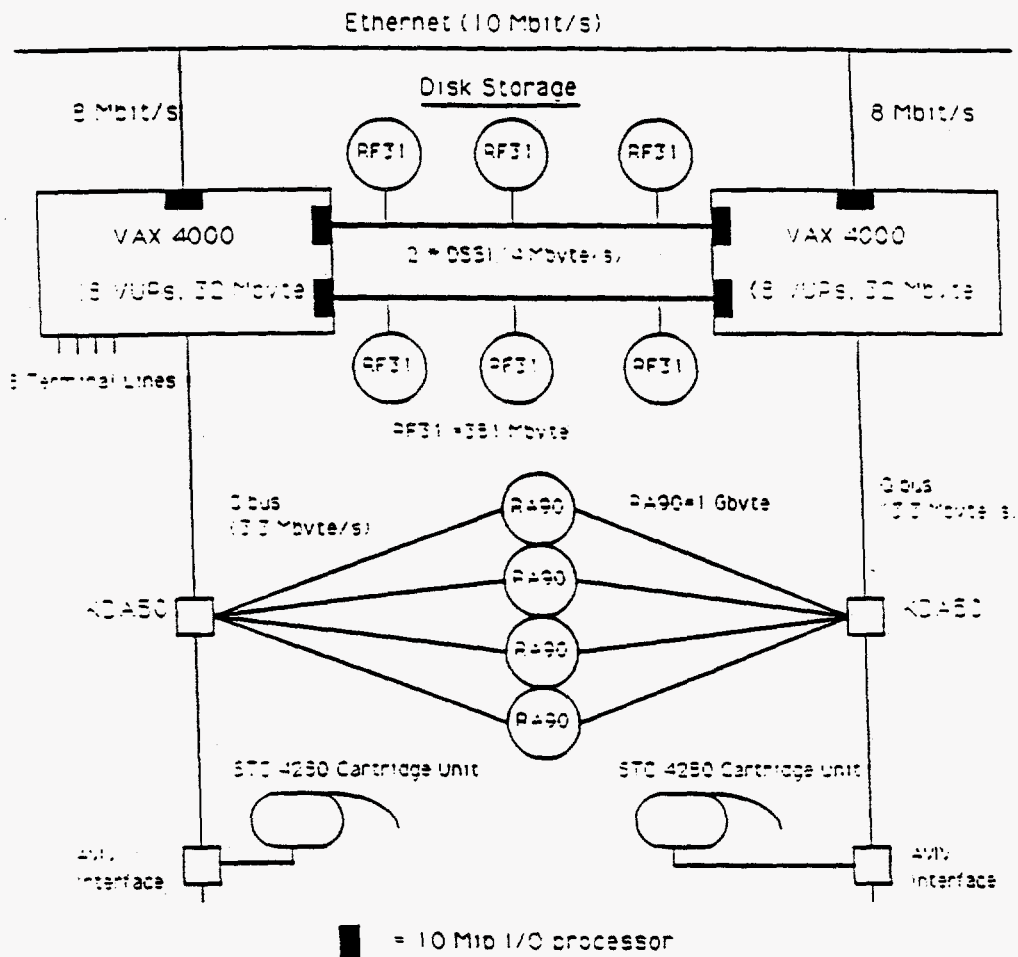


Figure 2.36: Proposed On-Line VAX Configuration

| Equipment | List Price (SF) |
|-------------------------------------|------------------------|
| Hardware | |
| 2 VAX 4300s, 32 MB, 40 user license | 424,000 |
| 8 Terminal lines | 3,770 |
| 6 RF31 disks (DSSI, 381 MB) | 72,000 |
| 2 KDA50 disk interfaces | 26,000 |
| 2 AVIV cartridge interfaces | 5,760 |
| TOTAL | 531,530 |
| TOTAL (after discounts) | 280,858 |
| Software | |
| VAXCluster license | 6,325 |
| 2 Volume Shadowing licenses | 58,580 |
| TOTAL | 64,905 |
| TOTAL (after discounts) | 12,981 |

Taking advantage of the discount agreement with DEC under an existing joint development program between OPAL and DEC, we were able to obtain better than 50% discount on hardware and 80% on software. The total cost, after discount, amounts to about 294,000 SF. It is anticipated that we may receive a credit of about 50,000 SF for the VAX-8700 in this upgrade. This leaves us with a financial obligation of 244,000 SF, equivalent to about \$160,000.

The Riverside group has been one of the most respected within OPAL and at LEP. It is important that we continue to have our hardware in the OPAL detector. We, therefore, request the funding of \$160,000 for the replacement of the VAX-8700 system. With this modest investment, we will be able to maintain our presence and to continue our strong physics program at LEP. It is possible that CERN may be willing to provide funds as a loan for the purchase of the hardware and allow us to pay in two or three installments. From our standpoint, we would rather invest the equivalent amount in offline computer equipment for data analysis since our group is severely limited in this area for our physics program on site at CERN. These issues are currently under discussion within OPAL and with CERN.

2.7 Budget Justification

Before discussing the proposed budget for the 92-93 contract year, it may be useful to review the operation of the current contract year in relation to the funding level. Task A2 was granted a total of \$560,000 for the contract period February 1, 1991 - January 31, 1992. Of this amount, \$50,000 was for the last payment of the VAX-8700 and \$60,000 was for our share of the yearly operations cost of OPAL. After removing \$53,617 in overhead charges by the University, we have a net of \$396,383 available to carry out our program. We would not have been able to manage if we did not receive generous support from the University. The University provided one quarter of full salary for Shen to supplement his sabbatical for a year's stay at CERN, partial salary for Layter, full salary for a research associate, and summer salaries for VanDalen and our new assistant professor J. William Gary. In addition, we received some support from the Academic Senate for research and travel. This is equivalent to approximately \$143,000 of extramural funds.

For the coming contract year, we have a new assistant professor Gary, who joined the UCR faculty on July 1, 1991. We are requesting the nominal 2 month summer salary in 1992. The University agreed to provide Gary, as part of the start-up support, 50% of a postdoc in matching funds. Therefore we are requesting funds for 50% of a postdoc. There are no other changes in staffing at the Ph.D. level.

Four of our graduate students on OPAL will have completed their Ph.D. requirements during the current contract period. Because of lack of funds, we will replace only two of the four. However, the University is providing funds in graduate student support for Gary, which will help to bring the number of graduate students close to the level for the current year.

Our share of the common operations cost of OPAL is 76,000 SF for 1992, or about \$56,000. We need some minor repairs/replacements of the electronics for the hadron strip readout to cope with increased rates. We request a total of \$60,000 for these under the item OPAL Operational Upgrades.

As mentioned in Section 2.6, the VAX-8700 will be replaced by a dual VAX-4300 system at the end of the 1991 run. We have included in our budget a request in the amount \$160,000 for the purchase. We are negotiating with CERN to determine whether it is possible to arrange payments in two to three installments.

Part of our operation requires the handling of funds through the CERN Finance Division. We have been informed that there will be a 15% overhead charge beginning July 1, 1991 and a 30% overhead charge beginning 1992. Our proposed budget does not include this item since we were told that CERN was negotiating directly with funding agencies.

2.8 Activities for the Coming Year

As a result of the machine development work, LEP is operating with improved optics with luminosity approaching $10^{31} \text{ cm}^{-2} \text{ s}^{-1}$. We expect to have collected about 500,000 hadronic decays of the Z by the end of the 91 run.

The mass and widths of the Z will be determined with improved precision both in statistics and in systematics. The forward-backward asymmetries of lepton pairs and quark pairs and the polarization of tau will be measured with unprecedented precision. Combining these measurements we will determine $\sin^2 \theta_W$ to an accuracy of 0.002.

The search for new particles will continue. We will establish higher mass limits for the Higgs, supersymmetric particles, and new leptons. The final states containing two charged particles with a pair of leptons will be studied in relation to the observed rates by ALEPH. With the high statistics data sample we will improve our measurements on rare decays and forbidden decays, such as those violating lepton flavor conservation. With the installation of a silicon vertex detector there will be major activities in the area of lifetime measurements and in the study of heavy quarks using tagging. We expect to participate in these efforts.

Although little affected by the Z^0 resonance, two-photon physics benefits from the high center-of-mass energy of LEP and the high luminosities. Single-tagged events are presently being recorded, along with a reasonable sample of high-visible-energy untagged events. Within the next year, OPAL should be able to measure the photon structure function F_2 at Q^2 values inaccessible to previous e^+e^- experiments. Our group, having done a great deal of two photon physics at PEP, will participate in this measurement.

J. W. Gary has an established reputation in the area of QCD. He has made major contributions in OPAL as a member of Heidelberg until joining UCR faculty in July 1991. The University is providing support for a graduate student and 50% of a postdoc for him to carry out research for the next two years. He has pioneered the studies of various aspects of QCD using tagging of the jets. We expect that this area will become a major part of our program.

The LSND neutrino oscillation and neutrino scattering experiment will significantly extend the range of coverage by accelerator based experiments, and introduces an era of high statistics electroweak physics with the unique facilities at LAMPF. The next year will see major detector construction followed by first operation in early 1993.

Looking into future physics opportunities we have begun participating in an experiment at the CERN SPS to study muon triggering and momentum reconstruction for a detector at a high energy hadron collider. The experiment RD5 is being installed in the North Area of the SPS, and the first beam test is scheduled for August and September 1991.

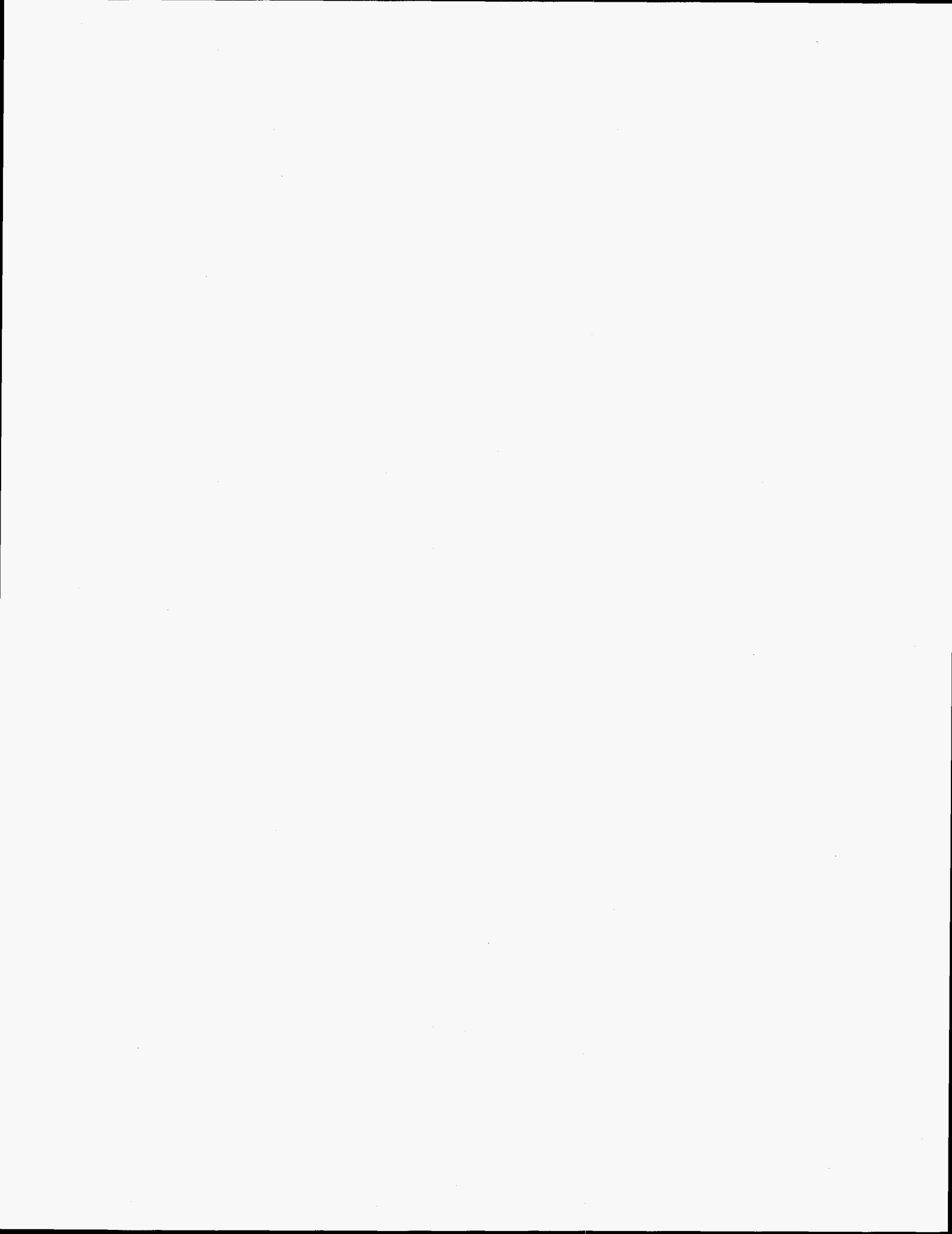
Bibliography

- [1] S. Myers, "LEP Status Report to LEPC," November, 1990.
- [2] "LEP Absolute Energy in 1990," LEP Performance Note 12.
- [3] K. Ahmet, *et al.*, "The OPAL Detector at LEP," CERN-PPE/90-114, to appear in Nucl. Instrum. and Methods.
- [4] M. Arignon, *et al.*, "The Trigger System of the OPAL Experiment at LEP," CERN-PPE/91-32, to appear in Nucl. Instrum. and Methods.
- [5] S. Jadach, *et al.*, Phys. Lett. **B253** (1991) 469; and "Higher Order QED Corrections to Bhabha Scattering at Low Angles," CERN-TH:5995/91 (February, 1991).
- [6] M.Z. Akrawy, *et al.*, CERN-PPE/91-67, submitted to Z. Phys. C.
- [7] M.Z. Akrawy, *et al.*, Phys. Lett. **B240** (1990) 497-512
- [8] M.Z. Akrawy, *et al.*, Z. Phys. **C49** (1991) 375.
- [9] Z. Kunszt and P. Nason (convenors) in "Z Physics at LEP I," (eds. G. Altarelli, R. Kleiss, and C. Verzegnassi), CERN 89-08.
- [10] R.K. Ellis, D.A. Ross, and A.E. Terrano, Nucl. Phys. **B178** (1981) 421.
- [11] M.K. Akrawy *et al.*, CERN-PPE/91-31, to be published in Phys. Lett. B.
- [12] M.K. Akrawy *et al.*, CERN-PPE/91-37, to be published in Phys. Lett. B.
- [13] For recent reviews see, for example, L. van Hove, Mod. Phys. Lett. **A4** (1989) 1867; B. Buschbeck and P. Lipa, Mod. Phys. Lett. **A4** (1989) 1871; R. Peschanski, CERN-TH5891/90, to be published in J. Mod. Phys.
- [14] A. Bialas and R. Peschanski, Nucl. Phys. **B273** (1986) 703; A. Bialas and R. Peschanski, Phys. Lett. **B207** (1988) 59; A. Bialas and R. Peschanski, Nucl. Phys. **B308** (1988) 857.
- [15] G. Marchesini and B. Webber, Nucl. Phys. **B310** (1988) 461; G. Marchesini and B. Webber, Cavendish-HEP-88/7.

- [16] T. Sjöstrand, *Comp. Phys. Comm.* **39** (1986) 347; M. Bengtsson and T. Sjöstrand, *Comp. Phys. Comm.* **43** (1987) 367; M. Bengtsson and T. Sjöstrand, *Nucl. Phys.* **B289** (1987) 810.
- [17] G. Kramer and B. Lampe, *Z. Phys.* **C39** (1988) 101.
- [18] L. Lönnblad, *ARIADNE 3.2*.
- [19] E. Ma and J. Okada, *Phys. Rev. Letters* **41**, 287 (1987)
- [20] M.K. Akrawy, *et al.*, *Phys. Lett.* **B241** (1990) 133.
- [21] M.K. Akrawy, *et al.*, *Phys. Lett.* **B240** (1990) 261.
- [22] Particle Properties, *Phys. Lett.* **B239** (1990).
- [23] M.K. Akrawy, *et al.*, CERN-PPE/91-XX, submitted to *Phys. Lett. B*.
- [24] M.K. Akrawy, *et al.*, *Phys. Lett.* **B254** (1991) 293.
- [25] P. Duinker and K. Eggert, *ECFA 90-133*, Vol. 1 (1990) 452.
- [26] R. Santonico and R. Cardarelli, *Nucl. Instrum. and Methods* **187** (1981) 377.
- [27] T. Dombeck, *et al.*, *Phys. Lett.* **B194** (1987) 591.
- [28] X. Q. Lu, *et al.*. LSND Proposal, Los Alamos Meson Physics Facility, 1989.

TASK B:

THEORY



TASK B: THEORY

a. Introduction

The High Energy Physics Theory Program at UC Riverside has had another productive year. Since July 1990, there have been 23 completed research papers (UCRHEP-T58 to UCRHEP-T80). They are listed under Publications (Section c) together with six other papers which were listed in last year's report as yet to be published but are now published. Of the 22 papers with definite publication information, seven are in letter journals: three in Phys.Rev.Lett., one in Phys.Lett.B, and three in Mod.Phys.Lett.A; and four others are in the Rapid Communications section of Phys.Rev.D. This is certainly indicative of our quality as well as productivity.

The Theory Group has consisted mainly of E. Ma (Professor), J. Wudka (Assistant Professor), J. Pantaleone (Postgraduate Researcher), S. Umasankar (Postgraduate Researcher until July 1991), T. V. Duong and K. McIlhany (Graduate Student Research Assistants). Dr. S. Umasankar came in February 1991 but will leave to take up a faculty position at the Institute of Mathematical Sciences, Madras, India, beginning August 1991. A new postgraduate researcher, Dr. H. Kikuchi, now at Kyoto University, will join us in September 1991.

In Section b the research activities of the Theory Group since July 1990 are discussed. In Section c there is a list of completed or published papers since July 1990. In Section d travel activities of the group are described and visitors to Riverside noted. In Section e there is a list of personnel and there are statements concerning their needs. In Section f the future research plans of Ma and Wudka are outlined. Finally the vitae of Dr. Kikuchi are appended.

b. Research Program

Since July 1990, E. Ma has completed ten papers for publication. They are described briefly below.

In a talk given at the 25th International Conference on High Energy Physics in Singapore last August (Paper #11), the possibility is raised that the top quark simply does not exist. However, it must then be replaced by some other new physics and the latter has to show up below an energy scale of about 400 GeV.

As a continuation of an earlier work by E. Ma and D. Ng (Paper #4), E. Ma and K. McIlhany (Paper

#12) worked out the details of the proposed supersymmetric extension of the standard model where all quark masses and mixing angles except m_t are derived as radiative effects induced by the gluino mass. A new valid approximate relationship $m_s^2/m_b^2 \approx -V_{ub}V_{cb}/V_{us}$ is obtained.

Motivated by the successful formulas $|V_{us}| \approx (m_d/m_s)^{1/2}$ and $m_s^2/m_b^2 \approx -V_{ub}V_{cb}/V_{us}$, it is proposed (Paper #15) that the standard model be supplemented by an $S_3 \times Z_3$ discrete symmetry, from which the second relationship can be derived and the first relationship is modified to read $|V_{us}| \approx (m_d/m_s)^{1/2} (1 + m_t^2/m_b^2 |V_{cb}|)^{-1/4}$. Subsequently, with the two recent reports of new evidence for the 17 keV neutrino (B. Sur et al., Phys.Rev.Lett.66, 2444 (1991); A. Hime and N. A. Jelley, Phys.Lett.B257, 441 (1991)), the $S_3 \times Z_3$ model is extended to include leptons. Whereas the structure of the Dirac mass matrices should have the forms already found for the quarks, the Majorana mass matrix for the singlet right-handed neutrinos is not yet specified. Using the Glashow prescription for the 17 keV neutrino (Phys.Lett.B256, 218 (1991)), two models have been constructed. In Paper #17, which is a straight forward extension of #15, it is found that the 17 keV neutrino can be accommodated but with a coupling to the electron of only up to 6%, much below the present experimental indication of about 9%. Its decay lifetime is about 10^4 years. In Paper #23, a less obvious extension is found where the τ lepton belongs to the second family rather than the third. There is now no problem in obtaining $V_{e\tau} = 0.09$ and the 17 keV neutrino decays rapidly with a lifetime of 3×10^{-3} s. In both cases, a solution to the solar neutrino problem in terms of the Mikheyev-Smirnov-Wolfenstein effect is possible.

In Paper #28, the results of Papers #15, 17, and 23 are summarized in a special lecture at the Second Winter School on Cosmology and Elementary Particles in Puerto Rico and will appear in the Proceedings. In Paper #29, the $S_3 \times Z_3$ model for quarks is made more flexible by the addition of one more scalar doublet. As a result, V_{ub}/V_{cb} is allowed a range of values in very good agreement with data and enough CP nonconservation exists in the mixing matrix to account for the parameter ϵ in the $K-\bar{K}$ system.

In paper #24, the problem of $Y(4S)$ decay into J/ψ mesons which cannot come from B decays is reviewed. It appears that there is no explanation within the standard model and new physics may be required. In Paper #25, E. Ma reported on the activities of Working Group III at the Second Workshop on High Energy Physics Phenomenology (WHEPP II), Calcutta, India. Among the topics discussed are a possible 17 keV neutrino, mechanisms for generating a large neutrino magnetic moment, exotic fermions and bosons, models with

two Higgs doublets, loop-induced vertices, and CP nonconservation.

Finally in Paper #26, E. Ma proposed a simple model of the 17 keV neutrino which satisfies all the laboratory, astrophysical, and cosmological constraints discussed recently by Caldwell and Langacker. It is mainly ν_μ , with $\bar{\nu}_\mu$ as its pseudo-Dirac partner, whereas ν_e is mainly a light pseudo-Dirac neutrino with an inert partner. The decay lifetime of the 17 keV neutrino is estimated to be 10s or longer. The solar neutrino problem is solved here by the long-wavelength vacuum-oscillation scenario with ν_e converting to $\bar{\nu}_{IR}$.

J. Wudka has investigated the effect of gravity on the propagation of neutrinos in matter. This is discussed in Papers #20 and #22. It is seen that gravitational effects can induce left-right transitions by the same process which gives the Thomas-Fermi precession of gyroscopes. Within the WKB approximation, the modifications due to gravity on neutrino oscillations are studied. For sufficiently strong fields, the gravitationally induced left-right transitions are important, and will significantly modify the persistence probability for a neutrino to retain its original flavor and helicity.

In Paper #21, Wudka studied the construction of the adiabatic connection in the case where the symmetry of a Hamiltonian is broken explicitly by a slowly varying perturbation. It is proven that the adiabatic connection is completely determined by the group structure, up to a set of reduced matrix elements.

J. Pantaleone has continued to focus his research on solar neutrinos. The next generation of solar neutrino detectors may be able to directly observe the low energy neutrinos from the reaction $e + {}^7\text{Be} \rightarrow {}^7\text{Li} + n$. The flux of these neutrinos is many orders of magnitude larger than that of the presently observed ${}^8\text{B}$ reaction and thus high statistics experiments are feasible (e.g., BOREXINO). Such a detector could provide several, new, DIRECT probes of neutrino properties, unlike the present situation where conclusions depend on solar model calculations. The possible probes suggested in Paper #5 are:

- 1) Night vs day flux comparisons probe a very large region of the MSW solution to the solar neutrino problem.
- 2) Energy dependent flux measurements can lower the experimental bound on the neutrino magnetic moment by an order of magnitude.
- 3) Time variations in the neutrino flux on scales of order one week to one year can occur from actual flavor oscillations of solar neutrinos.

The details of 3) have been examined. The effects of background matter have been shown to enhance the observability of these oscillations (Paper #8). Also, for three flavors, these oscillations may be present in addition to the MSW solution to the solar neutrino problem (Paper #13). The oscillation damping from the energy spread of the reaction has been calculated for the 7Be and pep neutrino lines (Paper #14).

The long standing solar neutrino problem, i.e., the disagreement between the ^{37}Cl neutrino flux measurements and the predicted flux from solar model calculations, has been reinforced and extended by recent flux measurements at Kamiokande-II and SAGE. These measurements are consistent with either the "nonadiabatic" or "large angle" Mikheyev-Smirnov-Wolfenstein solutions (Paper #9). In addition, the data is also consistent with a host of other previously proposed solutions (Paper #10): maximal vacuum mixing of three flavors, two flavor vacuum oscillations, and/or neutrino decay. These different scenarios are consistent with all present results but can be resolved from each other by continuing and planned neutrino measurements. In particular, a new model for neutrino decay has been examined (Paper #16) which can explain the solar neutrino problem and can readily incorporate the recent experimental results for a 17 keV neutrino mass.

Graduate student T. V. Duong participated in Papers #23 and #29. Graduate student K. McIlhany participated in Paper #12.

c. Publications

The following list contains work published or completed by the Riverside Theory Group since July 1990.

1. UCRHEP-T51: "Muon-Electron Transitions in Models of Radiative Lepton Masses," E. Ma, D. Ng, and G. G. Wong, *Z. Phys.* **C47**, 431 (1990).
2. UCRHEP-T52: "Solar Neutrino Observations and Neutrino Oscillations," T. K. Kuo and J. Pantaleone, *Phys.Rev.D* **41**, 3842 (1990).
3. UCRHEP-T54: "Radiative Generation of Quark and Lepton Masses," E. Ma, in Proc. of the Rice Meeting, edited by B. Bonner and H. Miettinen (World Scientific, Singapore), 861 (1990).
4. UCRHEP-T55: "CP Nonconservation in Supersymmetry with Radiative Quark Masses," E. Ma and D. Ng, *Phys.Rev.Lett.* **65**, 2499 (1990).
5. UCRHEP-T56: "Direct Probes of Neutrino Properties Using Solar-Neutrino Lines," S. Pakvasa

- and J. Pantaleone, Phys.Rev.Lett.65, 2479 (1990).
6. UCRHEP-T57: "Quark Mass Problem," E. Ma, in Proc. of 13th Warsaw Symposium on Elementary Particle Physics, edited by Z. Ajduk et al., (World Scientific, Singapore), 226 (1991).
 7. UCRHEP-T58: "u- and d-Quark Masses in Nambu's BCS Model," B. R. Desai, Phys.Rev.Lett.66, 2187 (1991).
 8. UCRHEP-T59: "Matter Effects on Observable Vacuum Oscillations of Solar Neutrinos," J. Pantaleone, Phys.Lett.B251, 618 (1990).
 9. UCRHEP-T60: "Recent Solar Neutrino Observations and Resonant Neutrino Mixing," T. K. Kuo and J. Pantaleone, Mod.Phys.Lett.A6, 15 (1991).
 10. UCRHEP-T61: "Solar-Neutrino Problem: Some Old Solutions Reexamined," A. Acker, S. Pakvasa, and J. Pantaleone, Phys.Rev.D43, R1754 (1991).
 11. UCRHEP-T62: "What If There is Really No Top?," E. Ma, in Proc. of 25th International Conference on High Energy Physics, Singapore, 1990 (in press).
 12. UCRHEP-T63: "Gluino Induced Quark Mass Matrices," E. Ma and K. McIlhany, Mod.Phys.Lett.A6, 1089 (1991).
 13. UCRHEP-T64: "Three Neutrino Flavors: Oscillations, Mixing, and the Solar-Neutrino Problem," J. Pantaleone, Phys.Rev.D43, R641 (1991).
 14. UCRHEP-T65: "Suppression of Solar Line Neutrino Oscillations," J. Pantaleone, Phys.Rev.D43, 2436 (1991).
 15. UCRHEP-T66: "Two Derivable Relationships Between Quark Masses and Mixing Angles," E. Ma, Phys.Rev.D43, R2761 (1991).
 16. UCRHEP-T67: "Decaying Dirac Neutrinos," A. Acker, S. Pakvasa, and J. Pantaleone, submitted to Phys.Rev.Lett.
 17. UCRHEP-T68: " $S_3 \times Z_3$ Model of Lepton Mass Matrices," E. Ma, Phys. Rev.D. (Rapid Communications, in press).
 18. UCRHEP-T69: Non-MSW Solutions to the Solar Neutrino Problem," J. Pantaleone, in Proc. of Trends in Astroparticle Physics, Santa Monica, California, November 1990 (to be published).

19. UCRHEP-T70: "How Propagation Through Matter Enhances the Observability of Solar Neutrino Oscillations in Vacuum," J. Pantaleone, Mod.Phys.Lett.A (to be published).
20. UCRHEP-T71: "Weak Neutrinos in Strong Gravity," J. Wudka, in Proc. of the 4th Mexican School of Particles and Fields, Oaxtepec, Mexico, December 1990 (to be published).
21. UCRHEP-T72: "Adiabatic Phases and Group Theory," J. Wudka, submitted to Journal of Physics.
22. UCRHEP-T73: "Gravitational Effects on Neutrino Oscillations," J. Wudka, submitted to Phys.Lett.B.
23. UCRHEP-T74: "Variants of the $S_3 \times Z_3$ Model for the 17 keV Neutrino," T. V. Duong and E. Ma, submitted to Phys.Lett.B.
24. UCRHEP-T75: "What Causes the J/ψ Anomaly at the $Y(4S)$?", E. Ma, in Proc. of the Workshop on Rare and Exclusive B and K Decays and Novel Flavor Factories, Santa Monica, California, February, 1991 (to be published).
25. UCRHEP-T76: "Report from Working Group III: Quest for New Physics," E. Ma, in Proc. of the Second Workshop on High Energy Physics Phenomenology, Calcutta, India, January 1991 (to be published).
26. UCRHEP-T77: "Custom-Designed Model of the 17 keV Neutrino," E. Ma, submitted to Phys.Rev.Lett.
27. UCRHEP-T78: "Dirac Neutrino Helicity Flip in Dense Media," J. Pantaleone, submitted to Phys.Lett.B.
28. UCRHEP-T79: "Unified Description of Quark and Lepton Mass Matrices," E. Ma, in Proc. of the Second Winter School on Cosmology and Elementary Particles, Rio Piedras, Puerto Rico, April 1991 (to be published).
29. UCRHEP-T80: "Restrictions on the Quark Charged-Current Mixing Matrix in the $S_3 \times Z_3$ Model," T. V. Duong and E. Ma, submitted to Phys.Rev.D.

d. Travel and Consultants

E. Ma attended the 25th International Conference on High Energy Physics (Singapore) in August 1990. He was the organizer and chair of the parallel session "Extended Standard Model" and gave a talk. In October 1990, he attended the Workshop on Waiting for the Top Quark at DESY, Hamburg and gave a talk. He then went on to the University of Oslo at the invitation of Dr. J. Eeg and gave a seminar. In November 1990, he gave seminars at the University of Maryland, College Park, the University of Wisconsin, Madison and the University of California, Irvine. In January 1991, he participated in the Second Workshop on High Energy Physics Phenomenology in Calcutta, India. He gave a review talk on radiative quark and lepton masses and presented the summary report of one of the four working groups. This trip was supported mainly by a special NSF grant for the U. S. participants. In February, he talked at the Workshop on Rare and Exclusive B and K Decays and Novel Flavor Factories, Santa Monica. In April, he gave a special lecture at the Second Winter School on Cosmology and Elementary Particles in Puerto Rico and gave a seminar at the University of North Carolina, Chapel Hill. In June, he gave seminars at CERN, Geneva, and PSI, Villigen, Switzerland, and attended the Physics in Collision Conference at Colmar, France.

J. Wudka gave a lecture at the 4th Mexican School of Particles and Fields, Oaxtepec, Mexico in December 1990. In February 1991, he participated in an intensive workshop on Precise Electroweak Measurements at the Institute of Theoretical Physics, Santa Barbara, and gave a talk there. In May, he gave seminars at the University of California, Los Angeles, and the Stanford Linear Accelerator Center.

J. Pantaleone attended the Conference on Astroparticle Physics at Santa Monica, California in November 1990 and gave a talk. From January to April 1991, he gave seminars at California State University, Los Angeles, University of Central Florida, Orlando, University of North Carolina, Chapel Hill, Duke University, Durham, North Carolina, University of Texas at Arlington, Southern Methodist University, Dallas, Texas, Alma College, Alma, Michigan, and Southeastern Louisiana University, Hammond.

Visitors who gave high-energy theory seminars/colloquia include A. Filippov (JINR, Dubna), G. Gelmini (UCLA), J. Goity (PSI, Villigen), E. Gotsman (Tel Aviv University), T. Huang (IHEP, Beijing), S. Love (Purdue University), T. Rizzo (University of Wisconsin), L. Roszkowski (CERN), and M. Srednicki (UC Santa Barbara).

e. Personnel and Needs

Two faculty members are covered by this proposal: E. Ma (Professor) and J. Wudka (Assistant Professor), for whom 2.5 months of summer salary are requested. J. Pantaleone will continue to be Postgraduate Researcher but only at 50% time and only until August 1992. H. Kikuchi will join Riverside as a new Postgraduate Researcher (100%) beginning September 1991. His curriculum vita is attached. T. V. Duong and K. McIlhany will be graduate research Assistants.

Two foreign trips are planned, at about \$3,000 each, to conferences such as the International Conference on High Energy Physics and the International Conference on Neutrino Physics and Astrophysics. Four domestic trips are planned, at about \$1,500 each, to conferences such as APS meetings and various other workshops and summer institutes yet to be announced. About \$2,000 is requested for visitors. A total of \$8,000 is needed for supplies and expenses.

f. Future Research Plans

In the immediate future, E. Ma plans to work on two projects. With J. Pantaleone and S. Umasankar, he is pursuing a possible solution to the problem of the J/ψ anomaly at the $Y(4S)$ discussed in Paper #24. The idea is to postulate a new scalar particle x which is a neutral color octet with a mass of about 5 GeV. If xxg is a significant component of the $Y(4S)$, then the decay $xx \rightarrow gg$ results in two energetic gluons, either one of which can convert into a fast moving $c\bar{c}$ pair and end up as J/ψ . Since x is neutral, photon emission is suppressed and the CUSB limit (Phys.Rev.Lett.65, 2749 (1990)) is avoided. A more radical scenario is to have xx decay into gy , where y is a scalar color singlet of say, 6 GeV which predominantly decays into $c\bar{c}$. Of course, y must have a reduced coupling to the Z boson so that it is not produced in Z decay at LEP. This could happen if the standard Higgs boson mixes with an SU(2) singlet scalar which appears naturally together with x in chiral color models (Pati and Salam, Phys.Lett.58B, 333 (1975); Frampton and Glashow, Phys.Lett.B190, 157 (1987)) as the symmetry $SU(3)_L \times SU(3)_R$ is broken down to $SU(3)_C$. If xxg exists, then xx should also exist at a lower mass. Now xx should have $J^{PC} = 0^{++}$ and it is not directly produced in e^+e^- collisions. However, the $Y(3S)$ resonance may decay into it plus two pions. If there is not quite enough phase space for this to happen, the virtual xx state may become the $Y(1S)$ or the $Y(2S)$ and the dipion spectrum may be enhanced for low invariant mass. This is a

possible explanation of the anomalous spectrum observed in $Y(3S) \rightarrow \pi^+ \pi^- Y(1S, 2S)$ by the CLEO Collaboration, Phys.Rev.D43, 1448 (1991). Many details are of course yet to be worked out.

Another project is to consider the $S_3 \times Z_3$ models in their entirety. These models (Papers #15, 17, 23, and 29) have an extended scalar structure: 4 or 5 doublets (and 3 singlets). However, their interactions with the quarks and leptons and with one another are restricted by the assumed discrete symmetry. Consequently, whereas flavor-changing neutral currents exist at tree level, they are in general proportional to fermion masses and are thus suppressed. The exception is when a third family is involved. Hence a full phenomenological analysis is needed to assess the possible indirect effect on interactions involving the b quark and τ lepton, such as in their rare decays. The scalar sector is also a source of possible CP nonconservation and that has to be worked out as well. The two graduate students (Duong and McIlhany) will be pursuing this project together with Ma and Dr. A. Joshipura of the Physical Research Laboratory, Ahmedabad, India.

The proposed research activities of J. Wudka for the near future are detailed below:

Physics beyond the standard model. There is a thrust in the community to devise a reasonable scheme for describing the effects of physics beyond the standard model for situations where no new particles are discovered. In the scenario the underlying physics will manifest itself only through radiative corrections, or small modifications to the standard model predictions. It has been advocated that the time honored method of effective lagrangians is, in fact, the most economical and general way to proceed under these circumstances [Ref 1].

The basic idea, proposed in collaboration with Prof. M. Einhorn, C. Arzt and Dr. M. Golden, is to parametrize all interactions consistent with the symmetries of the standard model using composite operators. These operators are then segregated according to their properties under approximate symmetries of the standard model, notably the custodial symmetry. This last class of operators will, if present, have the most noticeable effects.

This approach is separated according to the following two possibilities for the scalar sector: either a Higgs particle is found, in which case it must be included in the effective lagrangian description of the effects of underlying physics; or else it is not. In this last case the standard model scalar sector is described by a non-linear σ model, and the composite operators represent effective interactions between the already known particles

and the top quark.

Heavy scalar effects. As a generalization of Veltman's screening theorem [Ref 2], and as an extension of its explanation in terms of the symmetries and renormalizability of the standard model [Ref. 3], J. Wudka, in collaboration with Prof. M. Einhorn (U.C. Santa Barbara, ITP) are currently completing a study of the effects of heavy scalars in spontaneously broken gauge theories. In this work the general circumstances under which the radiative effects from heavy scalars are screened from low energy observables is presented. In particular the possibility of screening these effects in the gauge boson masses is traced back to the symmetries and renormalizability of the models, thus generalizing the results of the standard model. Moreover, it is pointed out that the results obtained can be used in model building in case the experimental evidence for scalar particles continues to be negative, while no phenomenologically acceptable alternative to breaking symmetries spontaneously using scalar fields is available. Partial results have been already presented in invited talks [Ref.4].

Neutrino physics. It has been recently pointed out [Ref. 5] that the gravitational effects on neutrino physics can induce resonant oscillations near compact and rapidly rotating objects. These resonances correspond to the well known MSW effect [Ref. 6], or, in the case of very massive objects, the left-right transitions akin to those induced by a magnetic field via a magnetic moment coupling (though in this case the coupling parameter is the neutrino mass). The possibility for these effects to be perpetuated in realistic stellar models is currently under investigation.

In a related topic, and in collaboration with J. Vidal, a detailed study of solar neutrino oscillations induced by the solar magnetic field is currently under way. The proposal, made in Ref. 7, that the nature of the solar magnetic field, which arranges itself into flux tubes with small diameters and large fields, is to be examined using numerical simulations. In this respect the corrections induced by the rapid fluctuations present in the magnetic field and in the matter density must be included in the calculation. The expectation is that all these effects will allow for left-right transitions to be significant for magnetic moments one or two orders of magnitude below the currently accepted values.

Unitarity and higher spins. A collaboration is under way with Dr. Robert Vega (SLAC) where we intend to study the restrictions imposed by tree level unitarity on theories with fundamental particles of $\text{spin} > 1$. This work will generalize the results of Ref. 8, in particular it will be determined whether supersymmetry is the only

theoretically viable framework which allows for unitary tree level reactions and such high spins to be present.

Heavy scalars and triviality. In collaboration with M. Velkovsky, a graduate student at UCR, J. Wudka has started a study of the triviality in gauge theories using the large N expansion. We concentrate on a theory consisting of the standard model, with fermions deleted, and with an N -tuple in the scalar sector, with N chosen so as to preserve $\rho = 1$ at tree level. One can then calculate leading corrections in $1/N$ to the Higgs mass and width; the expectation is that one can determine an upper bound for the Higgs mass together with the leading radiative corrections to the ρ parameter. This problem will be a very good learning experience for Mr. Velkovsky and will provide insights into the behavior of gauge theories with very heavy scalars.

REFERENCES

1. J. Wudka, invited talk at the Topical Conference on Precise Electroweak Measurements, Santa Barbara, CA, Feb. 21-23, 1991. H. Georgi, Harvard University preprint HUTP-90/A077. R. Holdom, University of Toronto preprints UTPT-90-22 and UTPT-90-23.
2. M. Veltman Acta Phys. Pol. B8, 475 (1977).
3. M. B. Einhorn and J. Wudka, Phys.Rev.D39, 2758 (1989).
4. J. Wudka, invited seminars at University of California, Los Angeles and Stanford Linear Accelerator, May 10 and 16, 1991.
5. J. Wudka, talk presented at the IV Mexican School of Particles and Fields, Oaxtepec Morelos, Mexico, Dec. 3-14, 1990; and University of California at Riverside preprints UCRHEP-73 and UCRHEP-71.
6. S. P. Mikheev and A. Yu. Smirnov, Sov. J. Nucl.Phys.42, 913 (1985). L. Wolfenstein Phys.Rev.D17, 2369 (1978).
7. J. Wudka and J. Vidal, Phys.Lett.B249, 473 (1990).
8. M. Cornwall et.al., Phys.Rev.Lett.30, 1268 (1973); Phys.Rev.D10, 1145, (1974). Lewellyn Smith, Phys.Lett.B46, 1268, (1973).

Curriculum Vitae

1. *Name:* Hisashi Kikuchi
Present Address: Department of Physics
College of Liberal Arts and Sciences
Kyoto University
Kyoto 606, Japan
Telephone: (075)-753-6777
2. *Place of Birth:* Sendai, Japan
Date of Birth: April 8, 1959
Sex: Male
Marital Status: Married
Citizenship: Japanese
3. *Educational Background:*
B.Sc. March 1983 Tohoku University
M.Sc. March 1986 Tohoku University
Ph.D. March 1989 Tohoku University
4. *Ph. D.:*
Institution: Tohoku University
Date: March 24, 1989
Thesis Advisor: Professor Tomoya Akiba
Thesis Topic: The effect of sphaleron
on baryon number violating processes
5. *Positions after Ph.D.:*
April 1989-present
Fellowships of the Japan Society
for the Promotion of Science
for Japanese Junior Scientists
at Kyoto University, Japan
November 1989-January 1990

Visiting Researcher
at Theoretical Physics Institute,
University of Minnesota, U.S.A.

6. *Membership:* Member of Physical Society of Japan

7. *Current Research Interests:*

Applications of the anomalous baryon and lepton number violation to phenomenology at SSC and to cosmology.

Dynamical aspects of field theories such as the dynamical symmetry breaking, many-body-effects at finite temperature, and/or nonperturbative analysis in strong coupling region.

Publication List

Hisashi Kikuchi

1. Asymptotic Constraint for Chiral Condensation of Coulomb Gauge QCD (with T. Akiba), *Z. Phys.* C33 (1987) 377-383.
2. Finite-Temperature Effect on Broken $U_A(1)$ Symmetry and the η' Mass (with T. Akiba), *Phys.Lett.* B200(1988) 543-546.
3. Static Minimum-Energy Path from a Vacuum to a Sphaleron in the Weinberg-Salam Model (with T. Akiba and T. Yanagida), *Phys.Rev.* D38 (1988) 1937-1941.
4. Free Energy of the Sphaleron in the Weinberg-Salam Model (with T. Akiba and T. Yanagida), *Phys.Rev.* D40 (1989) 588-600.
5. Relaxation of Baryon Number in the Standard Electroweak Model (with T. Akiba and T. Yanagida), *Prog. Theor. Phys.* Vol.83 (1990) 671-676.
6. Unitarity Restoration in the Multi-Instanton Process (with H. Aoyama), *Phys.Lett.* B247 (1990) 75-80.
7. Multi-Instanton Induced Baryon and Lepton Number Violation in the Electroweak Theory (with H. Aoyama), *Phys.Rev.* D43 (1991) 1999-2002.
8. Interacting Instanton for TeV Physics (with H. Aoyama), Kyoto University preprint KUCP-25, September 1990.
9. A New Valley Method for Instanton Deformation (with H. Aoyama), SLAC-PUB-5551, April 1991.

II.

COMPUTING

A proposal to upgrade our computing infrastructure has been separately submitted to DOE[1]. The upgrades and changes requested are essential to support the research program described here. Since a final decision regarding approval/funding is pending we have not requested funds for any of this equipment here. Should support be declined we will submit a supplementary proposal requesting equipment money later in the year. The reasons for these changes and an overview of the current facilities is summarized below.

The present VAXCluster consists of a central boot server (VAX 3500), and 12 satellite VAXStations. Disk capacity exceeds 9 GB, and magnetic tape drives in both 9-track and 8 mm format are available. Both DZERO and OPAL have adopted the 8mm digital video tape as a standard for data and DST distribution. These units can be attached directly to the VAX stations allowing processing to and from tape, and backup of data on the local disks of the stations.

The present disk capacity does not meet the demands of several operating experiments concurrently. There are inadequate facilities for staging data samples to disk, and too few tape drives to provide the data. Without enhancement to disk and tape systems, the substantial computing capacity of the system cannot be fully exploited.

The present nine VAXStation 31x0's all have 12 MB of local memory. Effective use of these processors for batch work, without significant degradation of interactive capability calls for additional memory 12MB of memory on each station.

To fully utilize the display and graphics software being developed for OPAL and D-Zero we need to add a color graphics capability to our system. This will be of special use over the coming year or so in the search for rare event topologies and the study of the physics and detector-induced backgrounds. The optimal solution is to add a limited number of color VaxStations to the UCR cluster which can then be shared by D-Zero and OPAL.

Lastly, with the ever increasing demands of physics analysis and monte carlo studies we need to plan for a substantial increase in the cpu capacity of the cluster. With OPAL and D-Zero work in progress and SDC and possibly LHC work starting in the near future the current facilities are inadequate to provide the needed resources. Because of cost considerations this type of upgrade could be best achieved by introducing UNIX processors rather than adding a significant amount of additional VAX/VMS power.

References

- [1] G.J. VanDalen, S.J. Wimpenny, " Computing Infrastructure in High Energy Physics", DOE Proposal no. 17265.